

NATURAL RADIOACTIVE SERIES DATING

OF PLEISTOCENE OCEANIC MATERIALS.

T H E S I S

submitted for the Degree of

DOCTOR OF PHILOSOPHY

at the

UNIVERSITY OF GLASGOW

by

JOHN THOMSON.

September, 1971.

ProQuest Number: 11011983

All rights reserved

INFORMATION TO ALL USERS

The quality of this reproduction is dependent upon the quality of the copy submitted.

In the unlikely event that the author did not send a complete manuscript and there are missing pages, these will be noted. Also, if material had to be removed, a note will indicate the deletion.



ProQuest 11011983

Published by ProQuest LLC (2018). Copyright of the Dissertation is held by the Author.

All rights reserved.

This work is protected against unauthorized copying under Title 17, United States Code
Microform Edition © ProQuest LLC.

ProQuest LLC.
789 East Eisenhower Parkway
P.O. Box 1346
Ann Arbor, MI 48106 – 1346

SUMMARY.

Long sediment cores from the deep ocean can provide a continuous record of sedimentation from the present back in time, in contrast to the fragmentary record available from the continents. From such cores, micropaleontological analysis has established "paleoclimatic" and "paleotemperature" curves for the Pleistocene epoch, the most recent period of geological time. Elevated fossil coral reefs provide useful cross-correlations for the deep sea stratigraphy, because they may represent warm periods and corresponding high sea stands. Natural series disequilibrium dating is one of the few chronological methods available to define an absolute time scale for the marine record over the past 500,000 years.

Most previous dating work has been performed on cores taken from the Caribbean Sea, because of the uniformity of sedimentation in that area. In this study, a time scale is estimated back to 400,000 years B.P. for a long globigerina ooze core from the equatorial Atlantic Ocean. Experimental data from the core indicate that the clay component of sedimentation has been uniform over this period in respect of the natural series parents U^{238} and Th^{232} . While there is evidence that Ra^{226} migrates in the core, and that U^{234} possibly does, the Th^{230}/U^{234} activity ratio shows a regular logarithmic decrease with depth.

Sedimentation rates of 2.20 ± 0.16 cm./ 10^3 yr. and 2.32 ± 0.17 cm./ 10^3 yr. are obtained from the ($\text{Th}_{\text{excess}}^{230}$) and ($\text{Th}_{\text{excess}}^{230}/\text{Th}^{232}$) methods respectively over the depth interval 25-927 cm. These rates yield ages of 136,000 and 129,000 yr. B.P., and 423,000 and 401,000 yr. B.P. for the important W/X and U/V paleoclimatic boundaries. This is in good agreement with one of the two chronologies presently proposed. ($\text{Pa}_{\text{excess}}^{231}$) rates of sedimentation over the depth interval 5-185 cm. are consistently higher than ($\text{Th}_{\text{excess}}^{230}$) rates over the same range. While the components of sedimentation fluctuate in this depth interval, calculation shows that ($\text{Pa}_{\text{excess}}^{231}$) is consistently lacking in the core.

Ages obtained by the $\text{Th}^{230}/\text{U}^{234}$ method for unrecrystallised fossil corals from the Upper Terrace of Aldabra Atoll lie in the range $127,000 \pm 9,000$ yr. B.P., which is synchronous with the last high sea stand. Stratigraphic evidence suggests that the entire present atoll was formed at that time, implying that the fauna and flora have been established in less than 120,000 years.

CONTENTS.

Page.

CHAPTER 1 : INTRODUCTION.

| | | |
|-----|--|-----|
| 1.1 | Ocean Sedimentation. | 1. |
| 1.2 | Preservation of the Stratigraphic Record in Pelagic Cores | 6. |
| 1.3 | The Pleistocene Record from Deep Sea Stratigraphy . | 8. |
| 1.4 | Natural Series Dating of Sediments | 18. |
| 1.5 | Dating of the Climatic Curve Sequences | 34. |
| 1.6 | Thesis Objectives | 37. |

CHAPTER 2 : EXPERIMENTAL PROCEDURE.

| | | |
|-----|---|-----|
| 2.1 | Introduction. | |
| | a) Selection Criteria and Sample Description : | |
| | V16-200 | 38. |
| | b) Selection Criteria and Sample Description: | |
| | Corals | 40. |
| | c) Selection and Outline of Analytical Chemical Investigations | 43. |
| 2.2 | Sample Preparation and Subsidiary Chemical Analyses. | |
| | a) Sample Preparation : V16-200. | 49. |
| | b) Sample Preparation : Corals. | 49. |

| | | | |
|----|---------------------|-----------|-----|
| c) | Salt Analyses. | | 50. |
| d) | Carbonate Analyses. | | 51. |

2.3 Radiochemical Separations for Natural Series Isotopes.

| | | | |
|----|---|-----------|-----|
| a) | Dissolution of Samples : V16-200 | | 53. |
| b) | Dissolution of Samples : Corals | | 56. |
| c) | Preliminary Enrichment | | 57. |
| d) | Uranium Separation. | | 58. |
| e) | Thorium Separation. | | 60. |
| f) | Protactinium Separation | | 61. |
| g) | Radon Separation. | | 64. |
| h) | Chemical Apparatus, Reagents and Carriers | | 67. |

2.4 Nuclear Counting Techniques.

| | | | |
|----|---|-----------|-----|
| a) | Alpha Source Preparation | | 69. |
| b) | Alpha Spectrometry : Theory | | 70. |
| c) | Alpha Spectrometry : Spectrometer System | | 73. |
| d) | Low Alpha Background Proportional Counter | | 79. |
| c) | Radon Counters. | | 89. |

2.5 Standards and Spikes for Radiochemical Analysis.

| | | | |
|----|------------------------------|-----------|------|
| a) | U^{232} - Th^{228} Spike | | 98. |
| b) | Pa^{233} Spike. | | 99. |
| c) | Ra^{226} Standards. | | 100. |

2.6 Treatment of Data.

| | |
|---------------------------------|------|
| a) Uranium and Thorium Spectra. | 101. |
| b) Protactinium Data. | 102. |
| c) Radium Data. | 103. |

2.7 Errors and Reproducibility.

| | |
|---------------------------------------|------|
| a) Analytical Errors. | 105. |
| b) Counting Uncertainties and Errors. | 108. |
| c) Reproducibility. | 111. |

CHAPTER 3 : RESULTS AND EVALUATION : V16-200.

3.1 Data Presentation. 114.

3.2 Natural Series Element Concentrations and Activity Ratios.

| | |
|---|------|
| a) Uranium and Thorium Concentrations. | 119. |
| b) U^{234}/U^{238} Activity Ratios. | 123. |
| c) (Th^{230}_{excess}) Specific Activities and Th^{230}/U^{234} Activity Ratios. | 127. |
| d) Ra^{226} Specific Activities and Ra^{226}/Th^{230} Activity Ratios. | 131. |

CHAPTER 4 : DATING OF CORE V16-200.

4.1 Introduction. 140.

| | | |
|-----|--|------|
| 4.2 | (Th ²³⁰ _{excess}) Sedimentation Rates. | 143. |
| 4.3 | (Pa ²³¹ _{excess}) Sedimentation Rates. | 151. |
| 4.4 | Comparison of Theoretical and Experimental (Th ²³⁰ _{excess}) and (Pa ²³¹ _{excess}) Specific Activities. | 155. |
| 4.5 | Dating of Climatic Changes from Core V16-200 . | 161. |

CHAPTER 5 : GEOCHRONOLOGY OF ALDABRA ATOLL.

| | | |
|-----|--|------|
| 5.1 | Introduction. | 170. |
| 5.2 | Results and Calculation . | 173. |
| 5.3 | Implications to the Development of Aldabra . | 179. |

| | | |
|-------------------|--|------|
| <u>APPENDIX 1</u> | : V16-200. Magascopic Description of a Split Core. (Lamont-Doherty Laboratory). | 182. |
|-------------------|--|------|

| | | |
|-------------------|--------------------------------|------|
| <u>APPENDIX 2</u> | : Typical Sample Calculations. | 188. |
|-------------------|--------------------------------|------|

| | | |
|-------------------|---------------------------------------|------|
| <u>APPENDIX 3</u> | : "Best-fit line" Computer Programme. | 192. |
|-------------------|---------------------------------------|------|

| | | |
|--------------------------|--|------|
| <u>REFERENCES CITED.</u> | | 194. |
|--------------------------|--|------|

| | | |
|--------------------------|--|------|
| <u>ACKNOWLEDGEMENTS.</u> | | 205. |
|--------------------------|--|------|

LIST OF FIGURES.

| | <u>Page.</u> |
|--|--------------|
| 1. Ericson's Paleoclimatic Curve. | 12. |
| 2. Emiliani's Paleotemperature Curve. | 14. |
| 3. Natural Series Nuclides Suitable for Dating Applications. . | 19. |
| 4. Paleomagnetic Reversal Timescale. | 31. |
| 5. Separation Flow Chart. | 46. |
| 6. Alpha Line Spectra. | 47. |
| 7. Parr 4745 Acid Digestion Bomb. | 55. |
| 8. Radon Separation Apparatus. | 65. |
| 9. Vacuum Chamber for Surface Barrier Detector. | 75. |
| 10. Block Diagram of Alpha Spectrometer. | 76. |
| 11. Alpha Backgrounds of 20th Century Detector. | 80. |
| 12. Thorium Alpha Spectrum from a Sediment Sample. | 81. |
| 13. Uranium Alpha Spectrum from a Sediment Sample. | 82. |
| 14. Uranium Alpha Spectrum from a Coral Sample. | 83. |
| 15. Thorium Alpha Spectrum from a Coral Sample. | 84. |
| 16. Energy to Channel Linearity of the Alpha Spectrometer. . | 85. |
| 17. N.M.C. Counter a) Alpha Plateau, b) Beta Plateau. | 87. |
| 18. Protactinium Alpha Spectrum from a Sediment Sample. . . . | 90. |
| 19. Radon Counting Vessel. | 91. |
| 20. Rn ²²² and Daughter Nuclides. | 92. |

| | | |
|-----|---|------|
| 21. | Radon Counter Plateau. | 94. |
| 22. | Uranium and Thorium Concentrations <u>versus</u> Depth : VI6-200. | 120. |
| 23. | "CaCo ₃ + NaCl" Weight Percentage <u>versus</u> Depth : VI6-200. | 121. |
| 24. | Log. (Th ²³⁰ /U ²³⁴) Activity Ratio <u>versus</u> Depth : VI6-200. | 130. |
| 25. | Ra ²²⁶ Specific Activity <u>versus</u> Depth : VI6-200. | 132. |
| Ra | Ra ²²⁶ /Th ²³⁰ Activity Ratio <u>versus</u> Depth : VI6-200. | 134. |
| 27. | Radium Diffusion : ln.(R _s - R _x) <u>versus</u> Depth : VI6-200. | 138. |
| 28. | Log. (Th ²³⁰ _{excess}) Specific Activity in Total Sediment : VI6-200. | 145. |
| 29. | Log. (Th ²³⁰ _{excess}) Specific Activity on a "Carbonate-free" Basis : VI6-200. | 146. |
| 30. | (Th ²³⁰ _{excess} /Th ²³²) Activity Ratio in Total Sediment : VI6-200. | 147. |
| 31. | a) Th ²³⁰ and Pa ²³¹ Specific Activities in the Total Sediment : VI6-200. | 152. |
| | b) Th ²³⁰ and Pa ²³¹ Specific Activities on a "Carbonate-free" Basis. : VI6-200. | 152. |
| 32. | Comparison of Paleoclimatic Curves and Timescale. | 162. |
| 33. | Map of Aldabra Atoll Showing Sample Locations. | 171. |

LIST OF TABLES.

| | <u>Page.</u> |
|---|--------------|
| 1. Radon Detector Separation and Counting Efficiencies. | 96. |
| 2. Radon Detector Background and Blank Count Rates. | 97. |
| 3. Protactinium Blank Analysis. | 107. |
| 4. Uranium and Thorium Blank Analysis. | 107. |
| 5. Analytical Results on "Standard" Materials. | 109. |
| 6. Results of Duplicate Analyses. | 112. |
| 7a. Analytical Data on Core V16-200. | 115, 116. |
| 7b. Analytical Data on Core V16-200 (continued) | 117, 118. |
| 8. Sedimentation Rates determined for Core V16-200. | 150. |
| 9. Boundary Ages determined for Core V16-200. | 150. |
| 10. Comparison of Zone Boundaries in Cores V16-200 and V12-122. | 167. |
| 11. Sedimentation Rates determined for Core V12-122. | 167. |
| 12. Comparison of Mean Sedimentation Rates required from Cores V16-200 and V12-122 to fit Broecker's Timescale. | 168. |
| 13. Analytical Data on Coral Samples | 174. |
| 14. Coral Activity Ratios and Ages. | 175. |

CHAPTER 1INTRODUCTION1.1 Ocean Sedimentation.

Geologists have long appreciated that ocean sediments provide a unique record of the past. Sediment sections, if they can be recovered in an undisturbed condition, may indicate sedimentary changes which reflect local or global conditions. The possibility of obtaining continuous sections from the present back in time is particularly valuable in studies of the Pleistocene period, the most recent geological epoch. This period is of interest because of the rapid evolution of man. Extreme alternations of climate during the Pleistocene have resulted in a discontinuous and fragmentary continental record. Thus normal stratigraphic correlations are difficult or tenuous.

The most valuable sediment types for Pleistocene investigation generally come from the deep sea, and are sometimes referred to as pelagic sediments. Arrhenius (1963) has defined pelagic sediments on the basis of a maximum terrigenous deposition rate of the order of millimetres per thousand years for all basins. This rate compares with overall pelagic sedimentation rates ranging from about 1 mm./ 10^3 yr. in the deep waters of the South Pacific Ocean to several cm./ 10^3 yr.

in areas of high biological activity, such as the Caribbean Sea. The definition excludes areas such as the continental shelves where sedimentation is disturbed by slumping due to turbidity currents. This latter process is considered responsible for the relative smoothness of the abyssal sediment cover of the ocean floor relative to the rugged topography of the underlying rock (Ericson and Wollin, 1967).

The components of a sediment may be classified into three groups according to origin: terrigenous, biogenic and authigenic. All detritus derived from land comprises the terrigenous component, and in the case of pelagic sediments this includes material transported by winds and ice rafting besides fine material introduced to the oceans by continental runoff. The biogenic component comprises the remains of marine organisms, principally planktonic carbonates and silicates, which result from the accumulation of the dead organisms. A bacterial decomposition of the softer parts occurs in the prevalent oxidising conditions of the deep ocean. The authigenic contribution to pelagic sedimentation is marked only in areas of very low deposition, and consists of materials precipitated directly from solution. This class includes manganese nodules and zeolites such as phillipsite which are thought to be associated with submarine volcanic activity (Arrhenius and Bonatti, 1965). Both of these are very common on some parts of the ocean floor, especially in the Pacific.

Fluctuations in sedimentation rate arise mainly from variations in the deposition rates of terrigenous and biogenic components.

In early work, deep sea sediments were classified according to gross visual characteristics. Terms such as "red clay", "globigerina ooze", and "siliceous ooze" are still used although the components are recognised as more complex and varied than is indicated. Red clay, for example, is normally brown, and the term is used to include sediments which are primarily authigenic in origin, or which contain large fractions of other silicate minerals. The term globigerina ooze is applied to sediments which contain the calcium carbonate tests of coccoliths and pteropods as well as foraminiferal species other than Globigerina. Siliceous oozes are more accurately named, and contain the silica remains of diatoms and radiolarians.

The type of sediment being laid down in any locality at any time will be a complex function of such factors as distance from land, water depth, currents, windbelts and biological activity. This latter factor is in turn related to water temperature and nutrition.

The biogenic contribution to sedimentation depends on the productivity of the plankton and also the extent of dissolution of their hard parts as they settle through the ocean. As a general rule,

calcareous remains are the principal component of sediments at low latitudes under warm surface water, whereas at high latitudes below cold water a siliceous component predominates. However, the fraction of calcium carbonate in sediments falls off rapidly from depths of about 4,500 metres to virtually zero at depths in excess of 5,500 metres. This "compensation depth" is believed to arise from dissolution of the calcium carbonate tests in deep water either during settling or on the ocean floor (Broecker, 1971).

Most calcareous sediments are calcitic because aragonitic shells such as those of pteropods and some foraminifera are not preserved below about 3,500 metres. (The mean ocean depth is 3,800 metres.) The siliceous or opaline tests of radiolarians and diatoms are also very soluble in sea water, and a high productivity and large size is necessary for their preservation in deposits. At the present time, suitable conditions for preservation exist in the Antarctic Ocean and the Equatorial and Northern Pacific, and no "compensation depth" for silica has been found (Riedel, 1959).

The clay deposition rate in any sedimentary basin depends on injection of terrigenous detritus into the ocean circulation system from the continents via the various mechanisms. In addition, there may be a contribution from submarine volcanism in certain areas such as the South Pacific (Griffin and Goldberg, 1963). Once in the ocean system, the fine minerals will be homogenised and dispersed according

to current direction and strength. Ocean bottom currents are important since they may resuspend and further transport fine material already deposited. Sackett and Arrhenius (1962) have measured the mineral suspensoid concentration in the North Pacific, and calculate average residence times for this component from 100 to 600 years, dependent on size.

Arrhenius (1963) has presented a chart of the present areal distributions of the different classes of sediment. Ericson and Wollin (1967) have estimated that the areas occupied by calcareous, brown clay and siliceous sediments are 50, 40 and 12 million square miles respectively. The distributions of clay minerals in the world's oceans have been collated by Griffin et al. (1969) and for the Atlantic by Biscaye (1965).

1.2. Preservation of the Stratigraphic Record in Pelagic Cores.

As will be discussed in Section 1.3, the sympathetic variation of the sedimentary processes outlined in Section 1.1 with climatic fluctuations can have a marked effect on the sediment column formed. Once it is accepted that sedimentation may vary in time with climatic conditions, there arises the question of how well this sedimentary record is preserved and how well it may be retrieved for study.

The degree of preservation of the sediment will be progressively altered with depth of burial by diagenesis. In addition, an earlier loss of detail can result from reworking of the sediment by benthic organisms. These organisms appear to exist even at the greatest depths, wherever free oxygen is available. Studies of mixing across unconformities in cores (Arrhenius, 1963) indicate a mean mixing depth of 4 to 5 cm., a conclusion broadly supported by subsequent work (Berger and Heath, 1968; Glass, 1969). In core sections below the depth of active mixing, the quantity of younger material mixed downwards should be balanced by the quantity of older material mixed upwards, provided that mixing has occurred at an approximately constant rate. Fortunately, the larger and heavier components of sedimentation are less disturbed than lighter materials, and the former are often the most useful in micropaleontological work.

At present the retrieval of sediments for laboratory study is accomplished with two types of deep sea coring device. One is a variation of the open barrel gravity corer (Emery and Dietz, 1941), the other a modification of the Kullenberg (1947) piston corer. Both types of corer are allowed to fall freely over the last few metres of their fall, to be driven into the sediment by a heavy lead weight. There is thus a possibility of loss of material from core tops by the impact of the corer head, because the uppermost layers of sediment may contain up to 65% by volume of water. Friction caused by sediment rushing into the corer barrel results in open barrel cores being shorter (3 to 5 metres, dependent on sediment type) than piston cores (5 to 25 metres). Cores taken from the same station by the different types of device do not give identical strata lengths over the common section. At present there is no consensus of opinion as to which type provides the most representative core (Emery and Hulseman, 1964; Ross and Riedel, 1967), but, because of their length, piston cores are most commonly used for stratigraphic studies. The time span covered by piston cores ranges from a few hundred thousand to two or three million years.

1.3. The Pleistocene Record from Deep Sea Stratigraphy.

The Pleistocene is regarded by many geologists as the most recent epoch of geological time. It has been characterised globally by emergent continents, high mountain ranges, deep ocean basins and active volcanoes. In addition, marked climatic changes have occurred, with the successive advance and retreat of ice sheets over large areas of the continents. Indeed, the Pliocene-Pleistocene boundary has been defined arbitrarily on the basis of cold water fauna (the Calabrian fauna) overlying warm water Pliocene fauna found in various parts of Italy, which implies a climatic deterioration at the beginning of the Pleistocene (Emiliani and Flint, 1963).

Various features of continuous pelagic cores have been studied to decipher the sedimentary record. Mainly biogenic components have been investigated, because changes in terrigenous component sedimentation are less well marked or understood (Goldberg et al., 1964; Biscaye, 1965; Murray, 1970). Arrhenius (1952) determined the calcium carbonate content as a function of depth in several cores from the Eastern Equatorial Pacific at 137°W. Repeated oscillations were found, from which he concluded that high calcium carbonate deposition occurred during glacial periods because of climatically controlled productivity and dissolution changes. On the other hand, Turekian (1965) has shown that higher calcium carbonate percentages

occur during warm periods in some regions of the Atlantic Ocean. Related to this approach, attempts have also been made to correlate the fraction of coarse material (arbitrarily greater than 64 or 74 μm .) in sediments with climatic variations. This fraction consists exclusively of foraminiferal tests or their fragments, and a rise in their abundance should reflect an increased productivity and higher temperatures (Emiliani, 1955; Rosholt et al., 1962). Although good agreement has been achieved in some cases, Ericson et al. (1961) have indicated the shortcomings of this method when used alone.

The foregoing parameters are now regarded as having a lesser value than approaches which use the abundances of various foraminiferal species as climatic indicators. Schott (1935) deduced, from a study of the short cores taken on the 1924 Meteor expedition, that a boundary in the abundances of planktonic foraminiferans with depth was related to the last deglaciation. Subsequent work has allowed construction of areal distribution charts for the 18 common planktonic species now living in the Atlantic (Phleger et al., 1953). From these charts, the foraminifera fall into three obvious groups: one confined to low latitudes near the equator, one abundant in middle latitudes, and one living primarily at high latitudes. Since the latitudinal distribution of species seems almost symmetrical

in the northern and southern hemispheres, water temperature appears to be the factor controlling their geographical distribution. Kane (1953) has shown from a study of species distribution in sediment surface layers and mean annual surface temperatures that the tests settle directly to the bottom. Thus this sensitivity towards temperature is of prime importance in unravelling past climatic changes. Further studies on species extinctions and changes in coiling direction, in long cores, have revealed other time and temperature dependent criteria in the Pleistocene.

Using the frequency in the abundance of the Globorotalia menardii complex, Ericson and coworkers (Ericson et al., 1956, 1961, 1964; Ericson and Wollin, 1968) have been able to construct what is claimed to be a complete record of the Pleistocene (Figure 1). The complete sequence has four major glaciations and three interglacials, obtained by overlapping zones in Atlantic cores from 30°N. to 30°S. Such an approach was necessary because globigerina ooze sediments accumulate at about 2 cm./10³yr., and cores taken from this type of sediment range from 5 to 15 metres in length. The Pliocene-Pleistocene boundary in this Atlantic suite was defined by the following micropaleontological criteria (Ericson et al., 1963):

- i) extinction of all discoasters at the boundary,

- ii) change in the coiling direction of the members of the Globorotalia menardii complex from 95% dextral coiling below the boundary to 95% sinistral coiling above,
- iii) appearance of Globorotalia truncatulinoides in abundance above the boundary,
- iv) extinction of Globigerinoides sacculifera fistulosa at the boundary,
- v) reduction of the Globorotalia menardii complex to a single fairly uniform race above the boundary,
- vi) increase in the average diameter of the tests of Globorotalia menardii and reduction in their number with respect to the total assemblage of foraminifera above the boundary.

There is no guarantee that these multiple criteria define the same event as the Calabrian fauna, and Selli (1967), McDougall and Stipp (1968), and Berggren et al. (1967, 1968) have suggested that a pre-glacial Pleistocene lasted 1 to 1.5 times as long as the glacial Pleistocene.

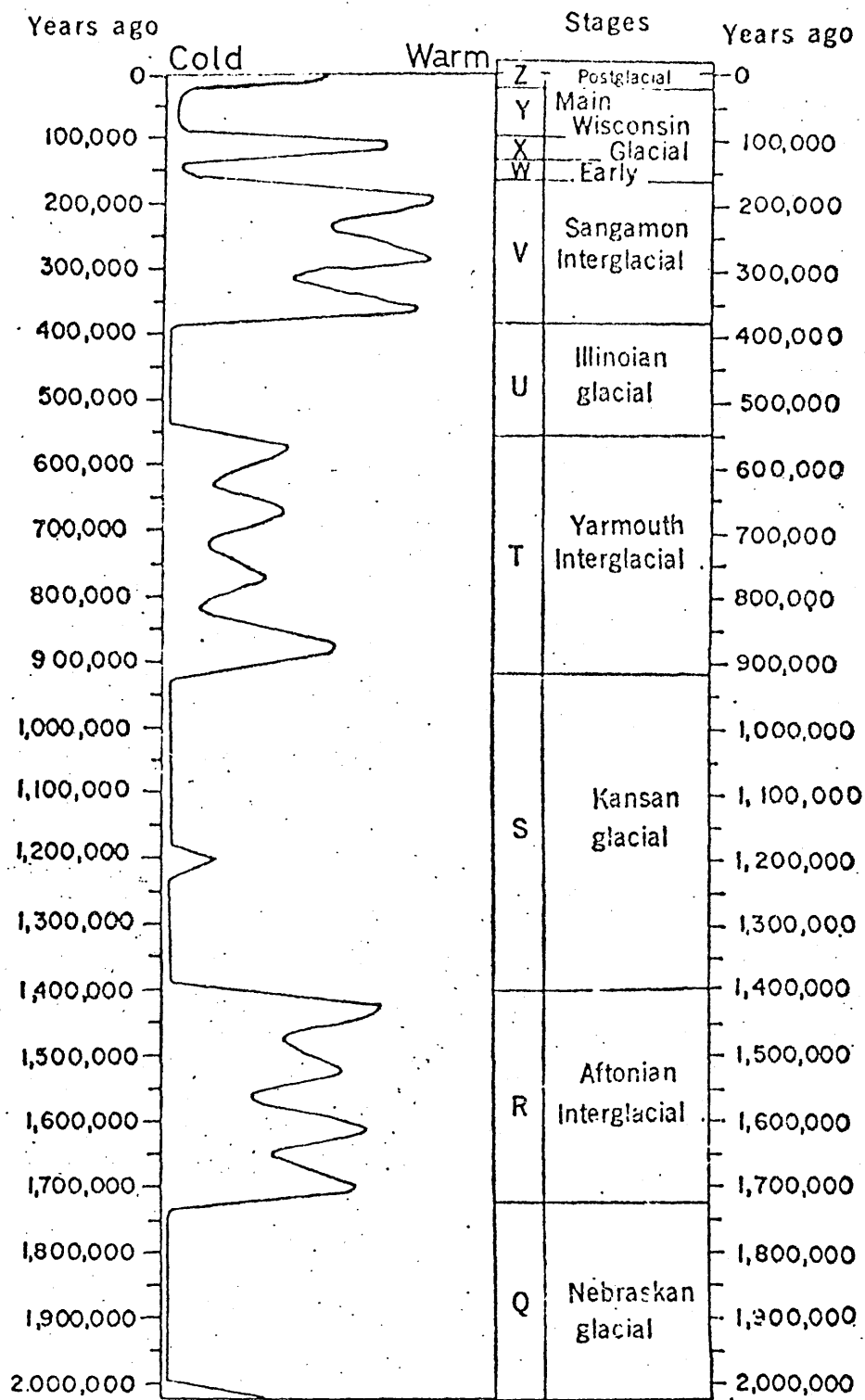


Figure 1: Ericson's Pleistocene Paleoclimatic Curve
(after Ericson and Wollin, 1968).

By far the most detailed information on past climate is found in the work of Emiliani (1955, 1958, 1964, 1966, 1969, 1971). This author performed O^{18}/O^{16} isotopic ratio measurements on different foraminiferal species in several cores from the Caribbean Sea and Equatorial Atlantic, and related the isotopic variations to ocean temperature changes. The method is based on the observation (Urey, 1947) that the oxygen isotopes in calcium carbonate precipitated from an aqueous solution are fractionated between water and carbonate ions, with a temperature-dependent fractionation factor. In consequence, the O^{18}/O^{16} ratio in calcium carbonate changes inversely by 0.00023 per Centigrade degree within the temperature range of normal biological formation (McCrea, 1950). At present, it is not certain whether the major factor giving rise to Emiliani's temperature curve is water temperature change (Emiliani, 1955, 1970), changes in the isotopic composition of sea water (Shackleton, 1967) or a roughly equal combination of both (Craig, 1965), but certainly no other approach has the sensitivity or reproducibility of this method. To obtain the generalised isotopic paleotemperature curve, Emiliani (1966) normalised data from several cores (Figure 2) in the same manner as Ericson et al. (1964) normalised the zone lengths designated warm and cold in their terminology.

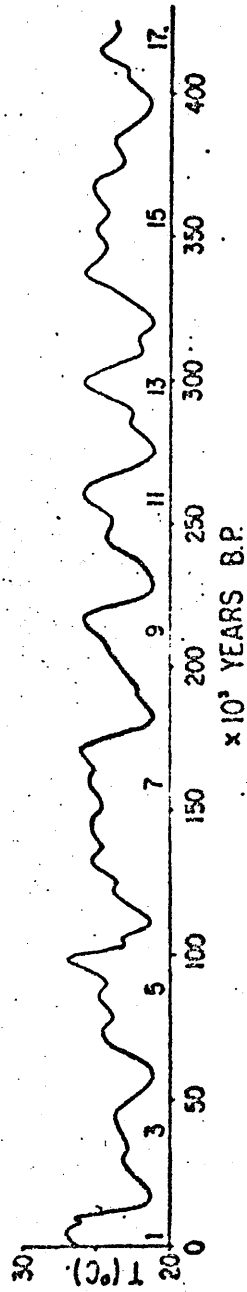
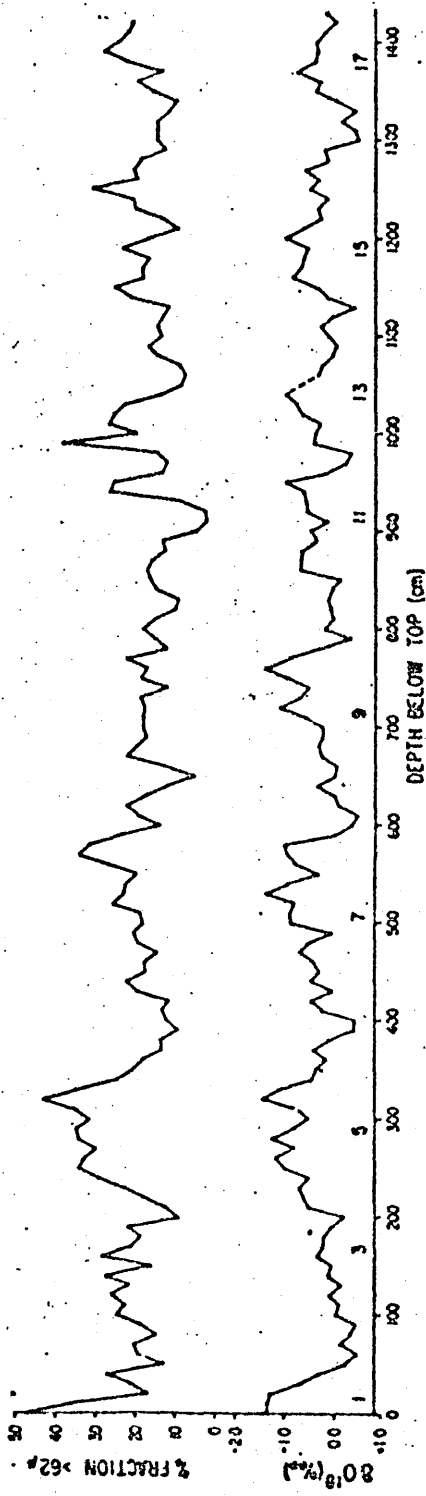


Figure 2. Emiliani's Paleotemperature Curve (lower).
 (Upper: > 62 micron fraction and $\delta^{18}O$ profiles for one core)
 (After Emiliani, 1966).

Early data obtained by Ericson and Emiliani around 1955 came from work done on the same core collection. Later the interests of the two workers diverged somewhat. Emiliani has exploited the fine detail of the paleotemperature curve to provide the most complete record of the "immediate" past. Since successive ice sheets and interglacial weathering have tended to destroy the evidence left by earlier glaciations, this is just the period from which most continental evidence remains. Emiliani's curve (Figure 2) shows successive cycles of alternating warm (interglacial) stages (odd integers with the present as stage 1), and shorter cold (glacial) stages (even integers), extended to stage 17 at about 425,000 yr. B.P. This apparent glacial/interglacial sequence has not been reconciled with the "classical" European sequence of four major Pleistocene glaciations (Emiliani and Flint, 1963). Good correlations have been shown to exist between the paleotemperature curve and anticipated biological abundances from continental and marine settings at low latitudes (Emiliani, 1970), and the relative abundances of several planktonic foraminifera (Lidz, 1966). Emiliani (1966, 1970) has estimated the glacial/interglacial temperature range to be 7 to 8 C. degrees in the Caribbean, 5 to 6 C. degrees in the equatorial Atlantic, and 3 to 4 C. degrees in the equatorial Pacific, with more marked ranges at higher latitudes.

Ericson's approach suffers from a lack of detail which is due, in part, to the choice of Globorotalia menardii as the best temperature indicator, and partly because the artificial boundary condition, which classes the species "very abundant" if more than "100 specimens per tray spread" are counted (Ericson and Wollin, 1956), abbreviates the available evidence (Emiliani, 1970). The climatic curve derived by Ericson attempts to go much further into the past, up to 2.1 million years (Glass et al., 1967; Ericson and Wollin, 1968). As Shackleton and Turner (1967) have pointed out, there is a progressive deterioration of confidence in Ericson's correlation between the marine record and the classical ice ages with increasing time before present. Nevertheless, criteria similar to those used by Ericson to define the Pliocene-Pleistocene boundary in Atlantic globigerina oozes have been found to demarcate a similar boundary in highly dissimilar Antarctic and Pacific sediments. These boundaries have been shown to be contemporaneous (Opdyke et al., 1966, Hays and Opdyke, 1967; Hays et al., 1969) by paleomagnetic dating (cf Section 1.4). In some cases there is also evidence of simultaneity in more recent boundaries, but in any event a Pleistocene duration, as defined by Ericson's criteria, of some 2 million years is indicated.

Together, the climatic curves of Ericson and Emiliani provide the best record of Pleistocene climate, and establishment of a

chronology for the curves provides a time scale against which rates of biological and geological development may be studied. The problem of chronology and the comparison of the curves is discussed in Section 1.5.

... of the ... in the ... of the ... This ... also ... in the ... and the ... of the ... is ... to the ... there exists ... (about ... years) ... less than 1 million years. The ... for this type of ...

... of radioactivity in deep sea sediments ... (1955) on top layer samples obtained during the ...

1.4 Natural Series Dating of Sediments.

The uranium ($4n + 2$), thorium ($4n$), and actino-uranium ($4n + 3$) series are three complex series of decay products which arise from the respective naturally occurring parents, U^{238} , Th^{232} and U^{235} . Since the various members of the series are isotopes of elements of widely dissimilar chemical properties, they behave differently towards the natural processes of weathering, solution and precipitation. Over geological time, this has resulted in the relative concentrations of the nuclides being quite different in the continents, oceans and sediments. This chemical fractionation also disrupts secular equilibrium in the series, and the subsequent growth of the members towards equilibrium is valuable in dating applications up to 500,000 years. Such a time span is ideally suited to the Pleistocene epoch, where there exists a gap between C^{14} dating (upper limit for deep sea dating about 35,000 years) and $K^{40} - Ar^{40}$ dating (lower limit less than 1 million years). The useful members of the series for this type of dating are shown in Figure 3.

The first analyses of radioactivity in deep sea sediments were made by Joly (1908) on top layer samples obtained during the 1872 Challenger expedition. The high values of Ra^{226} concentration relative to continental materials were confirmed by later workers (review by Piggot (1933)).

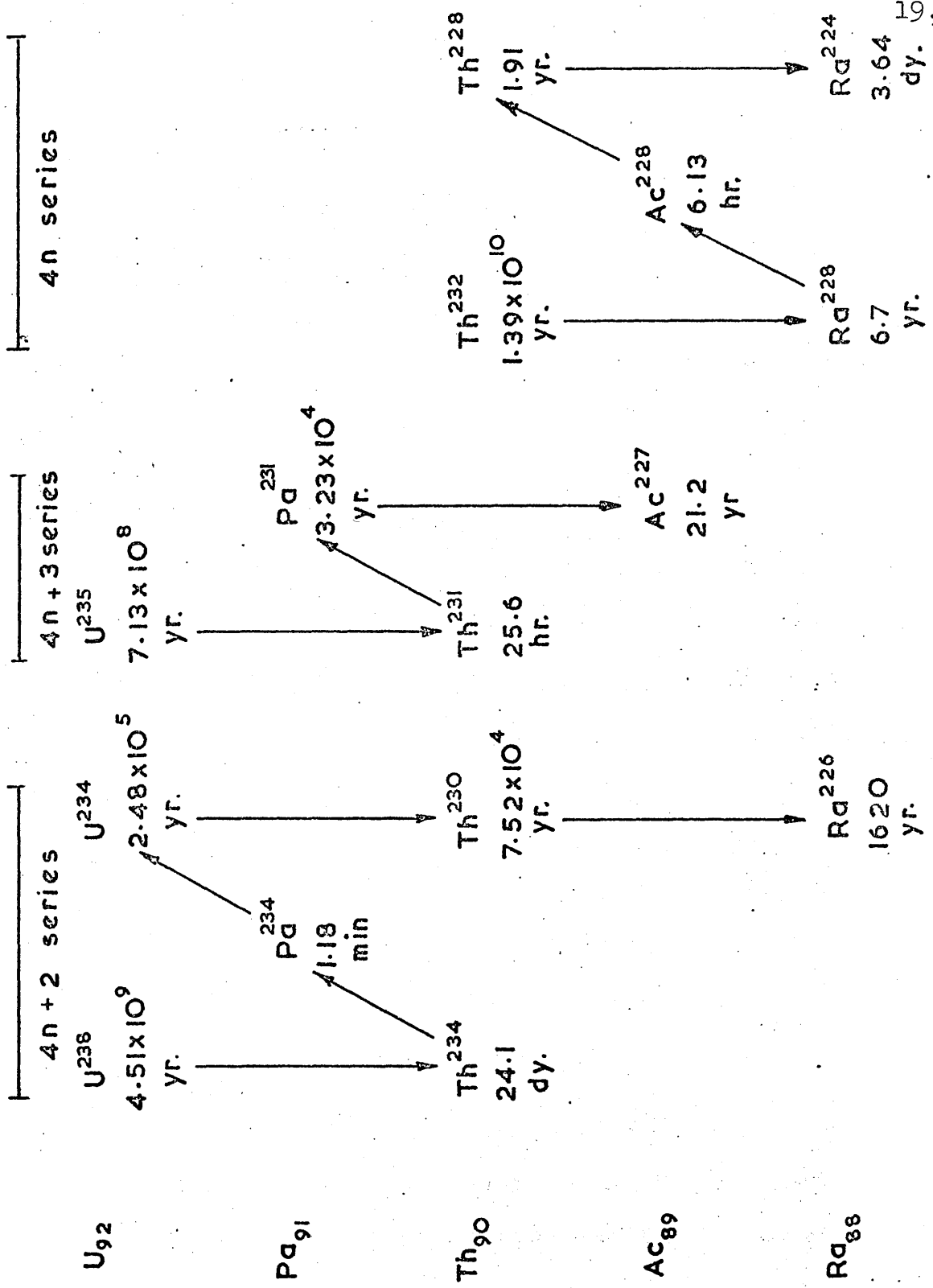


Figure 3: Natural series nuclides suitable for dating applications.

Red clay samples have been shown to have Ra^{226} concentrations ranging from 3 to 40×10^{-12} g. Ra^{226} /g., while globigerina ooze, with a higher sedimentation rate, gives concentrations ranging from 1 to 8×10^{-12} g. Ra^{226} /g. (Burton, 1965). The cause of these high values was reasoned by Pettersson (1937) to be due to precipitation of Th^{230} , the parent of Ra^{226} , from U^{234} dissolved in sea water. This explanation implied that the Ra^{226} concentration should increase with depth in a continuous core until it reached secular equilibrium with Th^{230} , then decrease from a peak in accordance with the half life of Th^{230} until secular equilibrium was attained with the U^{238} present in the sediment. Piggot and Urry (1939, 1941, 1942; Urry and Piggot, 1942) confirmed broadly that such a profile existed, with the peak maximum occurring at 7,000 to 9,000 years B.P. and the Ra^{226} concentration being independent of depth in excess of 400,000 years. Urry (1942, 1948, 1949) dated several cores by assuming that the Ra^{226} concentration was an indicator of the Th^{230} concentration when corrected for the U^{238} -supported fraction.

In an extensive study of cores taken by the Albatross during the 1947 Swedish expedition, Kroll (1953, 1954, 1955) revealed that Ra^{226} rarely followed the theoretical profile. In most of the cores studied, an erratic Ra^{226} distribution was found with secondary maxima and minima. Kroll questioned the assumptions of Urry, viz:

- i) that the unsupported Ra^{226} concentration is an index for unsupported Th^{230} , and
- ii) that either the Th^{230} concentration in the sediment on deposition has remained constant, or the rate of deposition of Th^{230} has remained constant irrespective of changes in deposition rate.

The first direct determinations of Th^{230} by Isaac and Picciotto (1954) on two Pacific cores confirmed that Th^{230} was the cause of the high Ra^{226} values and afforded support to Pettersson's (1951) suggestion that radium may migrate in the sediment column. This latter proposal was also sustained by Arrhenius and Goldberg (1955) who demonstrated a tendency for the Ra^{226} to accumulate in the authigenic mineral phillipsite, and by Goldberg and Koide (1963) who showed that Pb^{210} was deficient relative to Th^{230} in the upper zones of several types of sediment. It now seems fairly certain that both Ra^{226} and Ra^{228} diffuse rather freely from deep sea deposits, as shown by profiles of Ra^{226} concentration versus ocean depth (Koczy, 1958; Broecker et al., 1967), but the rates of diffusion are so low that some adsorption, possibly on clays, must take place (Koczy and Bourret, 1958; Koczy, 1963). As a result of this slow rate, Koczy and Bourret claimed that Ra^{226} diffusion becomes relatively unimportant in cores with sedimentation rates greater than $1 \text{ cm.}/10^3 \text{ yr.}$ In such cases it is possible that Ra^{226} measurements

may yield reasonable ages and thus explain the consistency of the results of Piggot and Urry. Volchok and Kulp (1957) repeated Ra^{226} analyses on two cores successfully determined by these workers and confirmed their results.

In an attempt to define a more satisfactory parameter, Picciotto and Wilgain (1954) suggested that the activity ratio $\text{Th}^{230}/\text{Th}^{232}$ be used as a geochronological index. This ratio would be independent of changes in the rate of total sedimentation or rate of thorium isotope deposition if:

- i) Th^{230} and Th^{232} are precipitated from sea water in a constant proportion,
- ii) the ratio $\text{Th}^{230}/\text{Th}^{232}$ in the water mass overlying the sediment has remained constant over the time interval concerned (about 500,000 years), and,
- iii) the amounts of Th^{230} or Th^{232} in lithogenic (terrigenous) phases of the sediment or of Th^{230} arising from uranium in authigenic phases are negligible, or corrections can be made for their contributions.

If these conditions hold, then the following equation should apply:

$$\left[\frac{\text{Th}^{230}}{\text{Th}^{232}} \right]_d = \left[\frac{\text{Th}^{230}}{\text{Th}^{232}} \right]_o \cdot e^{-(\lambda_1 - \lambda_2)t}$$

where: $(\text{Th}^{230}/\text{Th}^{232})_d$ is the activity ratio at depth d ,
 $(\text{Th}^{230}/\text{Th}^{232})_0$ is the activity ratio at the sediment
 water interface,
 t is the age corresponding to depth d ,
 λ_1 is the disintegration constant of Th^{230} ,
 λ_2 is the disintegration constant of Th^{232} .

The main criticisms of this method are that the geochemistry of U^{238} and U^{234} , the parents of Th^{230} , is quite different from that of Th^{232} , and the speciation of Th^{230} and Th^{232} should be quite different. It is questionable if Th^{232} ever enters solution, being carried to sediments in terrigenous materials in low concentration: values from 0.7 to $0.07 \times 10^{-6} \text{ g. Th}^{232}/10^3 \text{ l.}$ have been quoted for surface water (Moore and Sackett, 1964; Somayajulu and Goldberg, 1966, Kaufman, 1969). Th^{230} , on the other hand, is thought to be produced in solution as a $4+$ ion which is immediately hydrated. The mechanism conveying Th^{230} to sediments is uncertain: while Petterson (1937) assumed coprecipitation with hydrated iron or manganese, Holland and Kulp (1954) suggested adsorption on clays. Baranov and Kuzmina (1958) varied the $(\text{Th}^{230}/\text{Th}^{232})$ method by dating Indian Ocean cores by means of Th^{230} normalised against MnO and Fe_2O_3 .

In spite of the foregoing reservations, Goldberg and coworkers (Goldberg and Koide, 1958, 1962, 1963; Goldberg et al., 1963) used

the $\text{Th}^{230}/\text{Th}^{232}$ method to obtain sedimentation rates for most of the world's oceans. These workers leached all sediment samples with hot 6N HCl to avoid extraction of non-authigenic thorium isotopes. This procedure introduced a further uncertainty in that the fraction of total thorium leached could be variable. Mainly short cores were analysed, so no correction for U^{234} -supported Th^{230} was made. Almodovar (1960) attempted to refine the method by correction for U^{238} -supported Th^{230} , still using the same ratio. Only minor corrections were necessary to Goldberg's data for one core. Yokoyama et al. (1968) measured one Pacific clay core by nondestructive gamma spectrometry. Good agreement was found between rates determined by $(\text{Th}^{230}/\text{Th}^{232} - \text{U}^{238}/\text{Th}^{232})$ and $(\text{Th}^{230} - \text{U}^{238})$, but this core had very consistent U^{238} and Th^{232} concentrations, so that normalisation of Th^{230} against Th^{232} was of little importance.

In several cases, Goldberg and coworkers found an exponential decrease in the $\text{Th}^{230}/\text{Th}^{232}$ activity ratio with depth, but in others significant deviations were found. In a few instances, increases in the ratio with depth were found. These deviations were postulated by Goldberg and Koide (1962) to arise, at least in part, from top layer mixing by benthic organisms or water currents, or both. Particularly serious disagreement was found in Atlantic sediments between ages determined by $\text{Th}^{230}/\text{Th}^{232}$ and radiocarbon dating

(Goldberg et al., 1963). Ku et al. (1968) have also shown that sedimentation rates obtained by $\text{Th}^{230}/\text{Th}^{232}$ are too low by comparison with paleomagnetic measurements. This can be explained partly by Goldberg's interpretation of data, but it is possible that the main difference lies in Goldberg's choice of open barrel rather than piston cores (Ku et al., 1968; Goldberg, 1968). Although the validity of this method has been widely criticised (Rosholt et al., 1961; Sarma, 1964; Broecker, 1965), a good correlation has been established between the top layer $\text{Th}^{230}/\text{Th}^{232}$ ratio and the sedimentary basins of the world's oceans. The magnitude of the ratio is dependent on the continental area which drains into the basin relative to the ocean's size (Goldberg and Koide, 1962, 1963).

Data on unsupported Th^{230} in a core can be used in another way, as suggested by Volchok and Kulp (1957). If it is assumed that the uranium concentration in sea water has remained constant (3.3 $\mu\text{g.}/\text{l.}$; Rona and Gilpatrick, 1956; Wilson et al., 1960; Milner et al., 1961; Ku and Broecker, 1966) during the past 500,000 years, the mass of Th^{230} deposited in a depth of 4,000 metres can be calculated to be $2.21 \times 10^{-9} \text{ g. Th}^{230}/\text{cm}^2./10^3 \text{ yr.}$ (Prospero and Koczy, 1967). The sedimentation rate (S cm./ 10^3 yr.) should then be:

$$S = \frac{2.21 \times 10^{-9}}{C_{\text{Th}^{230}}}$$

where $C_{\text{Th}^{230}}$ is the concentration of Th^{230} in g.
at the dated level.

This method is obviously restricted to cores which have had a constant rate of accumulation over the period dated. To overcome this, some workers (Sarma, 1964; Ku, 1966; Ku and Broecker, 1966; Holmes et al., 1968) plot the logarithm of authigenic Th^{230} specific activity, ($\text{Th}_{\text{excess}}^{230}$), versus depth, and obtain a mean sedimentation rate (cm./ 10^3 yr.) from the gradient of the best fit line:

$$\ln. A = \ln. A_0 - (\lambda/S).x$$

where: A is the specific activity at depth x,

A_0 is the specific activity in freshly deposited sediment,

S is the mean sedimentation rate,

λ is the decay constant of Th^{230} .

If A_0 and S have been fairly constant over the sampled interval, the value of S allows sedimentary horizons to be estimated with fewer assumptions. Extrapolations beyond the depth sampled are still dubious. In spite of the suggestion that Th^{230} may migrate in sedimentary column (Sackett, 1964), this method, when applicable,

yields consistent results where other methods fail (Prospero and Koczy, 1967; Ku et al., 1968). Another variation of the ($\text{Th}^{230}_{\text{excess}}$) method is that adopted by Broecker and van Donk, (1970), where activities close to boundaries representing similar climatic changes are compared. If it is accepted that such periods exhibited similar conditions, the age difference thus obtained should be independent of intermediate changes in the sedimentation rate.

All the foregoing methods, including $\text{Th}^{230}/\text{Th}^{232}$, are generally used to yield an average rate of sedimentation. To surmount the effects of changes in sedimentation rate, Rosholt et al.

(1961, 1962) and Sackett (1960) introduced the idea of normalising unsupported Th^{230} against unsupported Pa^{231} , which should yield a series of dates for particular levels. These two nuclides appear uniquely suited for sediment dating. They are daughters of U^{234} and U^{235} respectively, and it is a necessary condition that the present uranium isotope abundances in sea water should have been maintained over the dating span of the method, viz:

- i) the activity ratio $\text{U}^{234}/\text{U}^{238}$ equals 1.15 ± 0.01
(Thurber, 1963; Somayajulu and Goldberg, 1966)
- ii) the isotope ratio $\text{U}^{238}/\text{U}^{235}$ equals 137.8
(Senftle et al., 1957; Strominger et al., 1958).

This latter assumption has some justification in that no deviations from the ratio have been found in natural environments (Hamer and Robbins, 1960). The second necessary assumption is that both Th^{230} and Pa^{231} , isotopes of elements highly insoluble in aqueous solution at the pH of sea water, should have comparable residence times in the ocean, short by comparison with their half lives. Measurements by Moore and Sackett (1964) on large volume sea water samples indicate residence times of less than 50 years for Th^{230} and less than 100 years for Pa^{231} . By the same token, the insolubility of the nuclides should make them resistant to post-depositional migration. The final and least firmly based assumption is that any uranium present in the terrigenous components of the sediment will have its decay products in radioactive equilibrium, so that unsupported or authigenic Th^{230} and Pa^{231} alone can be measured.

Early work employing this method (Rosholt et al., 1961, 1962; Sackett, 1960) showed good agreement with C^{14} dating, at least for cores taken from the Caribbean Sea, and its applicability to the determination of strata ages beyond the limit of radiocarbon dating seemed established. Unfortunately the determinations became less satisfactory in the light of redeterminations of half lives (Th^{230} : Attree et al, 1961; Pa^{231} : Kirby, 1961; Brown et al., 1968)

and the discovery that the U^{234}/U^{238} activity ratio in sea water was 1.15, not 1.00 as had been assumed. Although some workers have continued to use the $(Th_{\text{excess}}^{230}/Pa_{\text{excess}}^{231})$ ratio method, modified to take account of the new constants (Sackett, 1964; Rona and Emiliani, 1969; Emiliani and Rona, 1969) e.g.:

$$t = 8.26 \ln. 0.106 (Th_{\text{excess}}^{230}/Pa_{\text{excess}}^{231}) \times 10^4 \text{ yr.}$$

where t is the age of the level analysed

$(Th_{\text{excess}}^{230}/Pa_{\text{excess}}^{231})$ is the activity ratio of the uranium unsupported fractions of the two isotopes at the measured level,

Broecker and coworkers (Ku, 1966; Broecker and Ku, 1969) have suggested that the data are better used to plot $\ln(\text{specific activity})$ versus depth. This proposal stems from the work of Ku (1966), who found a 30% excess of unsupported Th^{230} relative to unsupported Pa^{231} on analysis of several cores. These results are believed to be superior to those of Rosholt et al. (1961, 1962) because Ku determined Pa^{231} directly whereas Rosholt determined it via its daughter Ac^{227} , which need not necessarily be in secular equilibrium with Pa^{231} (Broecker and van Donk, 1970). Sackett (1965), who also determined Pa^{231} directly, avoided extrapolation by comparison of the integrated Pa^{231} activity between the horizon to be dated and the core top with the total activity from the core top to the point where the activity became immeasurably small.

Until fairly recently there has been a dearth of dating methods against which natural series determinations may be cross-checked. Aside from C^{14} , other cosmic ray-produced nuclides such as Be^{10} , Al^{26} and Si^{32} have been employed, but difficulties in analysis and uncertainties regarding the necessary assumptions have resulted in relatively few data (review by Prospero and Koczy, 1967). A recent advance in the chronology of Pleistocene stratigraphy which has been of great value in confirming long term natural series disequilibrium dating is the establishment of a paleomagnetic sequence of polarity reversals. These result from the polarity of the earth's magnetic field having changed in a short interval at various times in the past. The timings of these reversals have been reasonably well established on land by $K^{40} - Ar^{40}$ dating of lava flows (Cox et al., 1961, 1964; Cox, 1969). The discovery of a similar paleomagnetic stratigraphy in deep ocean cores (Harrison and Funnell, 1964; Opdyke et al., 1966; Ninkovitch et al., 1966: Figure 4) allows a precise correlation between the marine and continental records since polarity changes are a global phenomena.

One drawback is that the last reversal occurred circa 0.7 million years B.P., which is a long time span to recover from some types of sediment. In areas of low sedimentation, cores which represent a much longer time can be taken and the natural remanent magnetism can be used to check the variability of sedimentation rates over 5 million years (Hays and Opdyke, 1967; Foster and Opdyke, 1970).

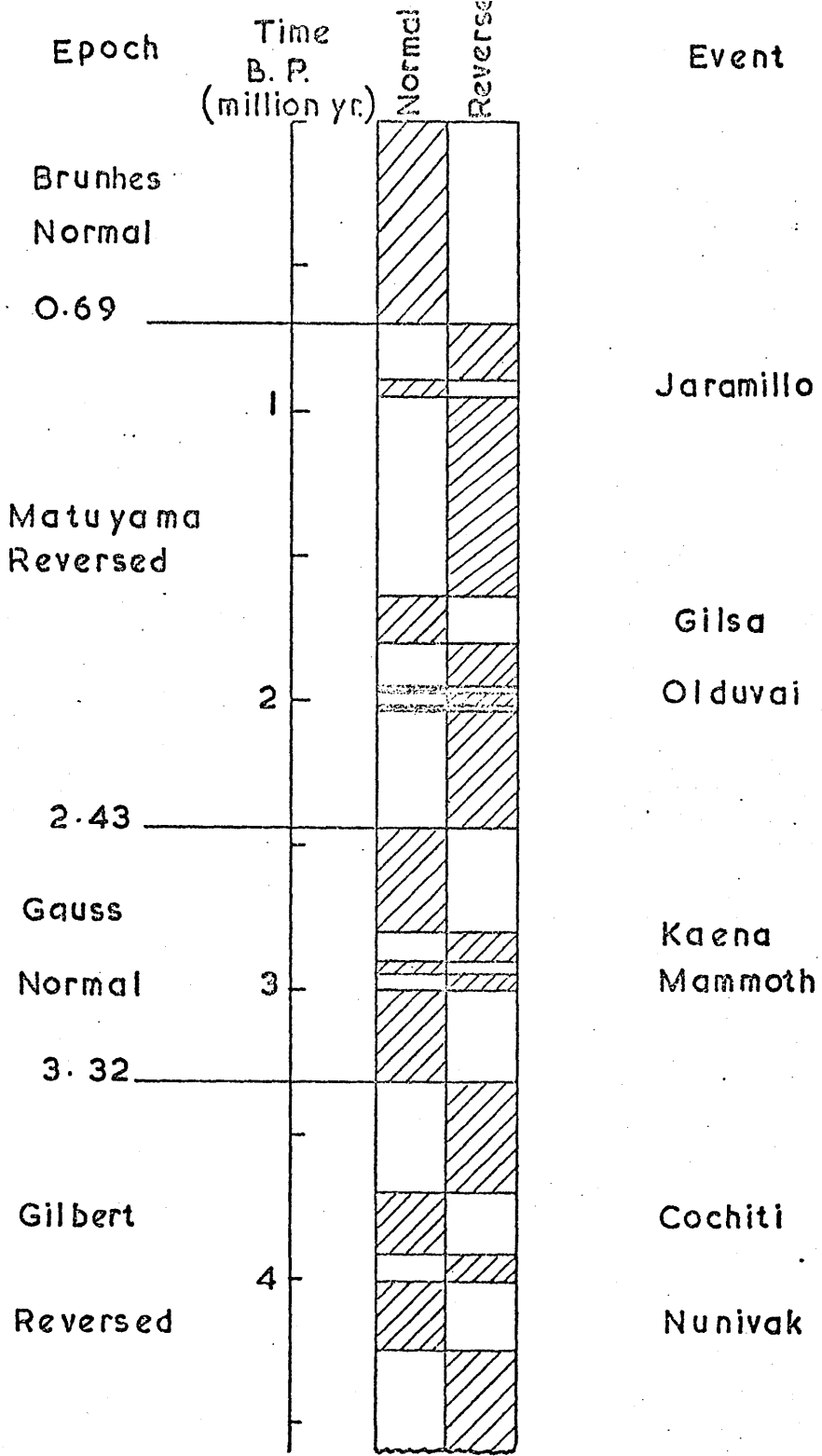


Figure 4 : Paleomagnetic Reversal Time scale (after Cox, 1969.)

By comparison with paleomagnetic data, Ku et al. (1968) confirmed the validity of accumulation rates determined by (Th^{230}_{excess}) where linearity exists in the radiometric data. A similar comparison of sedimentation rates in a few cores from Th^{230}/Th^{232} , remanent magnetism, and $K^{40} - Ar^{40}$ dating of volcanic glass shard layers suggested that it may take some time for the paleomagnetism to be "locked in" to the sediments (Dymond, 1969).

Absolute ages from coral terraces are also particularly pertinent to Pleistocene dating (Thurber et al., 1965). Corals grow only to a restricted water depth, so that elevated fossil terraces represent periods of high sea level, melting ice caps and high temperatures if the bedrock on which they stand is tectonically stable. Fossil coral dating, first demonstrated by Barnes et al. (1956), is based on the reverse phenomenon from (Th^{230}_{excess}) dating of pelagic sediments. Corals incorporate uranium isotopes according to their availability from sea water, with negligible thorium isotope inclusion. Typical uranium concentrations range from 2 to 4 parts per million (p.p.m.) (Broecker, 1963) in corals, in marked contrast to molluscs, which exhibit less than 1 p.p.m. when alive (Tatsumoto and Goldberg, 1958; Blanchard et al., 1967).

Thus the growth of Th^{230} towards equilibrium with U^{234} in the chemically closed system of a crystalline coral is dependent only on the

Th^{230} half life and the initial $\text{U}^{234}/\text{U}^{238}$ activity ratio. Broecker (1963) has derived the governing equation:

$$\left(\frac{\text{Th}^{230}}{\text{U}^{238}}\right)_p = (1 - e^{-\lambda_{\text{Th}}t}) + \left\{ \left[\left(\frac{\text{U}^{234}}{\text{U}^{238}}\right)_0 - 1 \right] \cdot \frac{\lambda_{\text{Th}}}{\lambda_{\text{U}} + \lambda_{\text{Th}}} \cdot (e^{-\lambda_{\text{U}}t} - e^{-\lambda_{\text{Th}}t}) \right\}$$

where $(\text{Th}^{230}/\text{U}^{238})_p$ is the present activity ratio of the nuclides,
 $(\text{U}^{234}/\text{U}^{238})_0$ is the initial activity ratio at the time
of formation,

λ_{Th} and λ_{U} are the disintegration constants of
 Th^{230} and U^{238} respectively,

t is the time since formation.

The potential limit for the method is about 300,000 years, but in practice dating beyond 200,000 years has proved difficult because of recrystallisation in very old corals. This results in open system behaviour (Thurber et al., 1965; Broecker and Thurber, 1965).

Ku (1968) has demonstrated that Pa^{231} dating of corals on a similar basis is in total accord with Th^{230} dating over its maximum span of about 120,000 years. Rosholt and coworkers (Rosholt, 1967; Szabo and Rosholt, 1969) have developed a method for dating molluscs by Th^{230} and Pa^{231} buildup which takes account of the open system behaviour characteristic of these species.

1.5. Dating of the Climatic Curve Sequences.

The obvious approach to correlate the continental and marine records is by comparison of determined ages from continental materials with ages of core levels anticipated to be contemporaneous. Radiocarbon dating of globigerina ooze cores has established that the most recent temperature minimum of the cores (Ericson's Y zone, Emiliani's stage 2) was synchronous with the last major (Wurm or Wisconsin) glaciation (Rubin and Suess, 1955, 1956; Ericson et al., 1956). The age of last glacial/interglacial boundary (Y/Z and 2/1 in Ericson's and Emiliani's terminology respectively) was established to be $11,000 \pm 1,000$ years B.P. (Broecker et al., 1960). Since the earlier stages in cores are beyond the range of the C^{14} method, their timing could only be estimated by extrapolation. The shortcomings of this approach have been outlined by Turekian (1964).

Absolute ages obtained by the $(Th_{\text{excess}}^{230}/Pa_{\text{excess}}^{231})$ method (Rosholt et al., 1961, 1962) have allowed the chronology to be extended to about 150,000 years. Emiliani (1966) used these results as the basis of the time scale for his generalised curve, pointing out that they were consistent with radiocarbon extrapolations. Support for this view was obtained by Rona and Emiliani (1969) who dated levels in two Caribbean cores using the new constants and an acid leach analytical process.

The most recent part of the time scale adopted by Ericson and coworkers was increased by Ku and Broecker (1966) who dated the W/X and U/V boundaries of one Caribbean core (V12-122) at 100,000 and 320,000 years B.P. respectively. These ages were obtained from $(\text{Th}^{230}_{\text{excess}})$ and $(\text{Pa}^{231}_{\text{excess}})$ rates of accumulation derived from totally dissolved samples, and were in agreement with Emiliani's interpretation. Broecker et al. (1968) subsequently revised the chronology in the light of paleomagnetic data (Glass et al., 1967), ages from coral terraces (Mesoletta et al., 1969), and a reinterpretation of the data from core V12-122. This revision, which suggests that Emiliani's time scale is 25% low beyond the span of radiocarbon dating, is supported by the fact that a high sea stand which occurs extensively in the world's oceans has been placed at $124,000 \pm 5,000$ years B.P. by fossil coral analysis (references in Emiliani and Rona, 1969; Veeh, 1966). This high sea level would be expected to be synchronous with the early part of Emiliani's stage 5 (Shackleton, 1969).

Broecker and coworkers (Broecker, 1966; Broecker et al., 1968; Broecker and van Donk, 1970) have demonstrated that the revised time scale agrees with the Milankovitch theory that perturbations in the earth's orbit, with concomitant variations of solar insolation, trigger climatic changes (Milankovitch, 1938; Varnekar, 1968). In addition, it is alleged that the generalised paleotemperature curve has been insufficiently normalised, and that there exists a

dominant asymmetric saw-tooth climatic cycle. This cycle has an average periodicity of approximately 90,000 years, a rather sharp change from cold to warm, and a gradual deterioration with secondary oscillations from warm to cold.

Emiliani (1966) has also claimed that his time scale shows a correspondence of paleotemperature minima with Milankovitch summer insolation minima. It is further claimed (Emiliani, 1971) that O^{18}/O^{16} analysis and Th^{230}/U^{234} dating of stalagmites and other speleothems from the continents are in agreement both with his temperature trends and time scale.

In summary, there exists a divergence in the calibration of the Pleistocene time scale of some 25% as recently as 100,000 years B.P. The facility with which both schools of thought fit data to their interpretation arises from the uncertainties (both theoretical and analytical) still associated with natural series dating.

1.6. Thesis Objectives.

The object of this work is to extend our knowledge of the Pleistocene time scale obtained from the marine record by use of established natural radioactive series methods. This is attempted by examination of two types of sample:

- i) sections of a globigerina ooze core, V16-200, and,
- ii) a suite of unrecrystallised fossil corals from the Upper Terrace of Aldabra Atoll.

Since the paleoclimatic zonations of V16-200 have been determined, the core provides an opportunity to estimate the time scale as recorded in equatorial Atlantic sediments. Most previous work of this nature has been performed on cores taken from the Caribbean Sea. Age determinations are made by consideration of authigenic Th^{230} and Pa^{231} data.

The excellent state of preservation of the Aldabra corals makes them ideal for high precision $\text{Th}^{230}/\text{U}^{234}$ dating of this ecologically important island.

CHAPTER 2.EXPERIMENTAL PROCEDURE.2. 1. Introduction.(a) Selection Criteria and Sample Description: V16-200.

The principal criterion which a sediment core must satisfy to be suitable for dating investigations is stratigraphic continuity. Experience has shown that uninterrupted particle-by-particle accumulation is not the norm, and cores taken without regard to bottom topography commonly contain evidence of slumping or phases of deposition by turbidity currents (Ericson, 1963.) A higher probability of undisturbed sections is achieved by taking cores from the tops or flanks of gentle rises. While turbidity currents normally give rise to abrupt textural changes, slumping does not affect texture, and can only be detected by cross-correlation of closely spaced cores. Although it is appreciated that the mechanics of coring may cause some depth distortion in the recovered sediment column, (cf. Chapter 1.2), micropaleontological comparisons indicate that a reproducible section is obtained from any one type of coring device. There also exists the possibility of losing some material from core tops : this can lead to uncertainties in determining absolute ages, but not sedimentation rates.

The core selected for this study, V16-200, is a piston core taken from the equatorial Atlantic Ocean ($01^{\circ} 58'N.$ $37^{\circ} 04'W.$; depth 4093 m.; length 1050cm.) on the sixteenth cruise of R.V. Vema of Lamont-Doherty Geological Observatory (1960).

On ship, the aim is to preserve retrieved cores as perfectly as possible for future study. The sediment column is pushed by a piston from the corer barrel into a plastic tray. Depth-in-core markings are made every 10cm. on both the wet sediment and storage tray, and the core then wrapped and sealed in a metal tube for protection. This minimises contamination and uncertainty in depth estimation when the core dries in the core laboratory.

The megascopic description of V16-200 is reproduced as Appendix 1. Selection of this core was guided by Professor D.B. Ericson, Lamont-Doherty Geological Observatory, Columbia University, New York. Investigation by Ericson et al. (1964), showed that the core contained undisturbed foraminiferans, and apart from minor variations in colour, the appearance is uniform throughout.

The core consists of foraminiferal lutite (globigerina ooze), and to a first approximation may be considered as an assemblage of biogenic calcium carbonate remains and terrigenous clay minerals in proportions varying with depth.

(b) Selection Criteria and Sample Description: Corals.

Corals secrete a skeleton of pure aragonitic calcium carbonate. Modern corals exhibit a restricted range of uranium concentrations (2 to 4 p.p.m. uranium with a U^{234}/U^{238} activity ratio of 1.15 ± 0.03), with very little incorporation of Th^{230} . Thus the growth of Th^{230} towards secular equilibrium with U^{234} in fossil corals provides an elegant dating method. Complications can arise, however, and Thurber et al. (1965) have established criteria which must be met if reliable data and ages are to be obtained. The most important of these criteria are:

- i) the fossil coral should contain as little calcite as possible. Calcite indicates that recrystallisation or cementation has taken place, which may lead to deviations from closed system behaviour.
- ii) the uranium concentration should be around 2 to 4 p.p.m. Evidence suggests that corals do not differentiate between Ca, Sr, Ra and U during growth, and the U/Ca ratio in corals is normally similar to that in sea water. This situation does not seem to have altered during the Pleistocene (Broecker, 1971), and recrystallised corals often have low uranium concentrations.

iii) the U^{234}/U^{238} activity ratio should be 1.15 ± 0.03 when corrected for age. This ratio appears to be constant in sea water with location and depth (Somayajulu and Goldberg, 1966). If this ratio has been constant since the coral formed, deviations from the above ratio are suspect.

iv) the Th^{230}/Th^{232} activity ratio should exceed 20. Since the concentration of Th^{232} in sea water is very low (Kaufman, 1969), measurable quantities of Th^{232} are neither expected nor found in modern corals. Contamination of an organism after death, by natural waters with typical Th^{230}/Th^{232} activity ratios of 1 to 4, would also add an uncertain amount of Th^{230} .

v) the Ra^{226}/Th^{230} ratio should be consistent with the age of the sample. If corals form with negligible Th^{230} and 10% of the equilibrium value of Ra^{226} , those of age greater than 70,000 years should have an Ra^{226}/Th^{230} ratio of unity. Chemical alteration occurring more than 7,000 years ago will not be detected from this ratio.

Corals analysed in this work were collected by Dr. W.J. Kennedy, University of Oxford, and samples were kindly supplied by Dr. J. Taylor, British Museum. (Natural History).

All samples were taken from their original positions of growth on Aldabra Atoll. Calcite/aragonite mineralogical analyses were supplied for each specimen. The lower limit of detection for calcite was 0.5%, and only samples with no detectable calcite were chosen for this study.

(c) Selection and Outline of Analytical Chemical Investigations.

For core samples, the nuclides of interest for natural series dating applications are authigenic Th^{230} and Pa^{231} , either alone, in combination with each other, or, in the case of Th^{230} , normalised against Th^{232} . Measurement of the unsupported abundances of those two isotopes necessitates determination of the respective parents U^{234} and U^{235} , the nuclides themselves, and Th^{232} . The straightforward approach to these analyses is alpha spectrometry, which allows determination of U^{238} and U^{234} from a uranium separation, and Th^{232} and Th^{230} from a thorium separation. The established isotopic abundance ratio of $\text{U}^{238}/\text{U}^{235}$ (137.8; Senftle et al., 1957; Stominger et al., 1958) allows the U^{235} abundance to be calculated. Pa^{231} , however, has a low activity and is normally determined at the higher detection efficiencies available in alpha proportional counters, since there is no other alpha-active protactinium isotope to interfere in these measurements.

In choosing an analytical separation route for uranium, thorium and protactinium, a decision must first be made whether:

- i) to dissolve the sediment sample completely, in which case the major proportion of the long-lived uranium and thorium isotopes (U^{238} and Th^{232}) will be derived from the detrital component of sedimentation, or
- ii) to leach the sediment sample in an attempt to dissolve only the authigenic isotopes.

The "acid leach" process favoured by Goldberg and coworkers was shown to release around 70% of the total Th^{232} in the sediment (Goldberg and Koide, 1962), and a similar technique employed by Rona (Rona and Emiliani, 1969) was estimated to release around 33% of the total uranium (Mo et al., 1971). In the present study, the total dissolution method was selected because the fraction of the radionuclides released to solution by the latter method above was considered to depend on such variables as degree of diagenesis, grain size and clay mineral composition. This made partial dissolution unsuitable for a long core such as V16-200.

The chemical separation scheme devised was based on those developed successively at Lamont-Doherty Geological Observatory, Columbia University, New York, by Thurber (1963), Kaufman (1964) and Ku (1966).

Analyses were performed to determine the isotopic abundances of U^{238} , U^{234} , Th^{232} , Th^{230} , Pa^{231} and Ra^{226} . The objectives of the separation scheme may be summarised as follows:

- i) dissolution of the entire sample by treatment with various acids, with U^{232} - Th^{228} or Pa^{233} tracers added at the outset. The final solution, containing all the nuclides of interest, has Cl^- as the major anion, since high boiling acids would complicate subsequent steps. An aliquot of this solution is taken for Ra^{226} analysis. No reducing agents are used to ensure that all U (IV) is oxidised to U (VI)
- ii) separation and purification of the uranium, thorium and protactinium isotopes by precipitation, solvent extraction and ion exchange.
- iii) thin source preparation of the purified uranium, thorium or protactinium for alpha analysis.

A flow chart of this scheme is given in Figure 5, and the alpha line spectra of the nuclides analysed in Figure 6. Subsidiary analyses were made to estimate the percentage of calcium carbonate and sodium chloride at each core interval sampled to determine the distribution of U^{238} and Th^{232} between the biogenic and terrigenous components.

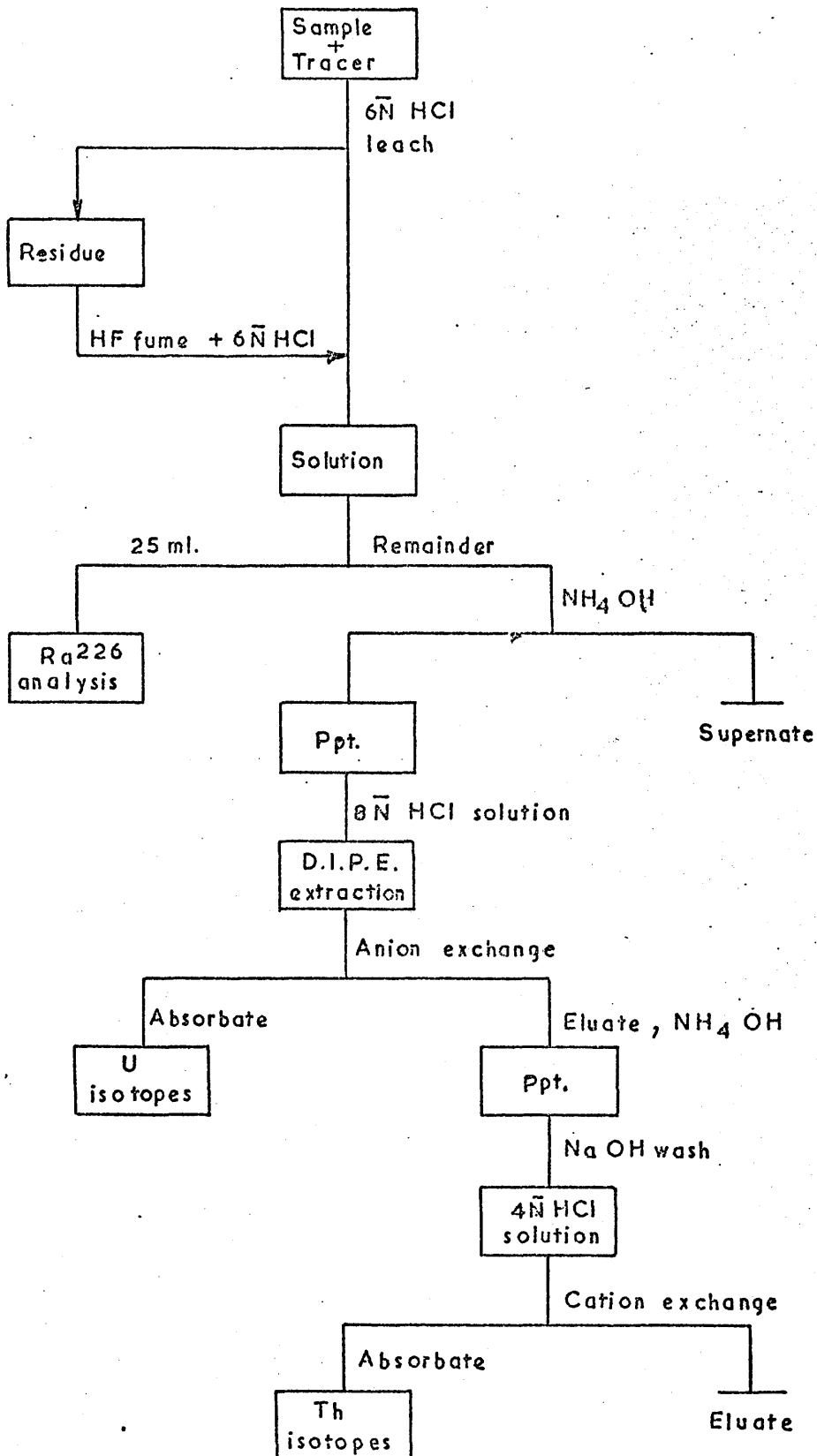


Figure 5: Separation flow chart.

Figure 6 : Alpha Line Spectra. (Data from Lederer et al., 1967)

a to c : Theoretical spectra derived from separates of a sample containing equal specific activities of U^{238} and Th^{232} with daughters at secular equilibrium.

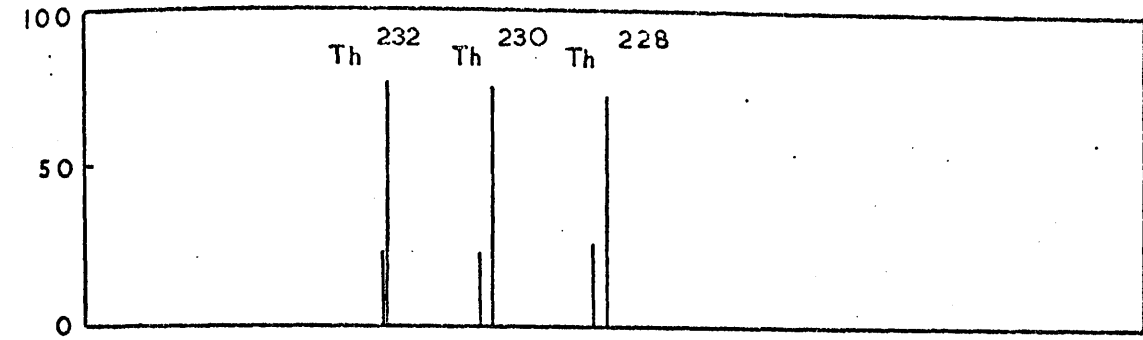
(This corresponds to a U/Th mass ratio of 0.33.)

a : Thorium separate

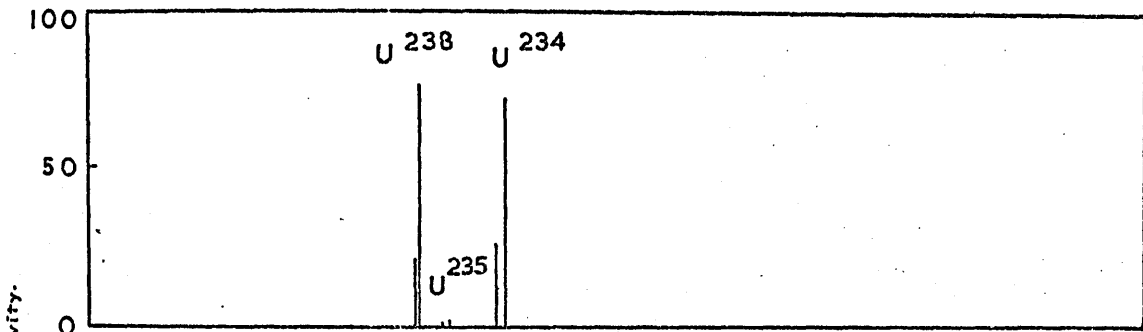
b : Uranium separate

c : Protactinium separate

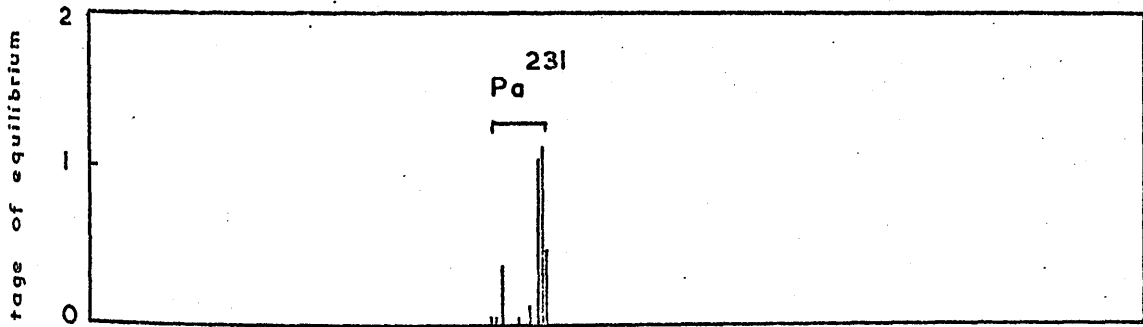
d : Theoretical alpha spectrum of U^{232} - Th^{228} spike and daughters at radioactive equilibrium.



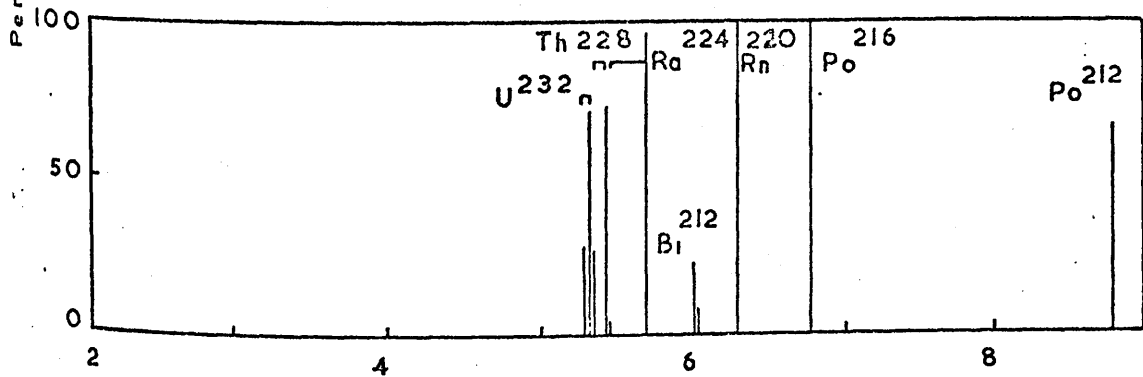
a



b



c



d

Alpha particle energy (Me V).

Corals are essentially pure calcium carbonate, and contain authigenic uranium with Th^{230} generation in situ. Thus there is no problem with detrital materials. All coral samples were merely dissolved, and U^{238} , U^{234} and Th^{230} determined as in sediment analysis.

... and facilitate subsequent dissolution. At firing was performed manually with an agate mortar and pestle, decrease preparation time a mixer mill (Coster Co. Model 280/10) with a tungsten carbide cylinder and ball in the later analysis. Dissolving was carried out using a... on a sieve with... ball.

Sample Preparation - Corals.

Some of the coral samples analyzed had a green-black outer... (possibly chlorite or other clay) which was...

2. 2. Sample Preparation and Subsidiary Chemical Analyses.

(a) Sample Preparation : V16-200.

Analyses were performed on 21 samples of V16-200 from depths between 5 and 927 cm. in the core. These samples were quarter-sections of 5 to 8 cm. depth intervals of the 6 cm. diameter core. Each section was dried overnight at 110°C. before the outer layer was scraped off to avoid possible surface contamination. The remaining sediment was ground to less than 200 mesh (75 μ m.) to homogenise it and facilitate subsequent dissolution. At first grinding was performed manually with an agate mortar and pestle, but to decrease preparation time a mixer mill (Glen Creston Ltd., Stanmore; M 280/11) with a tungsten carbide cylinder and ball was used in the later analyses. Sieving was carried out using a Perspex sieve with nylon boltcloth.

(b) Sample Preparation : Corals.

Some of the coral samples analysed had a green-black outer weathered crust (possibly glauconite or green algae) when received. This was removed, together with an underlying discoloured layer, by shaving with a diamond impregnated bronze wheel.

Any other obvious surface contamination was drilled out with a tungsten carbide tipped Vibratool (Burgess Products Ltd., Sapcote.) The remaining coral was covered with distilled water in an appropriately sized beaker, then ultrasonically vibrated for ten minutes. This process was repeated twice with fresh portions of water. The sample was dried overnight at 110°C . and crushed when cool in a pneumatic press with a steel cup and piston.

(c) Salt Analyses.

The salt content of the core material was taken to be the percentage of halides (Cl^- , Br^- and I^-) calculated as the percentage NaCl in the sample. This analysis was performed volumetrically by the Mohr method, titrating against standard silver nitrate solution with potassium chromate as indicator (Kolthoff and Sandell, 1956.)

About 25 mg. of the core section for analysis, dried and sieved, were weighed to 0.00001 g. on a tared piece of aluminium foil. The powdered sediment was poured into a 12 ml. centrifuge tube, 5 ml. distilled H_2O were added, and a Pasteur pipette used to mix the solution and leach salts from the sediment. After centrifugation, the aqueous solution was drawn off and transferred to a 50 ml. conical flask.

After addition of 2 drops $0.1\bar{M}$ K_2CrO_4 , the solution was titrated against an accurate $0.01\bar{M}$ $AgNO_3$ standard. At the end point, red-coloured Ag_2CrO_4 formed in the golden solution.

Each sample was run twice, with agreement between runs, after blank correction, of $\pm 3\%$. The blank was small and reproducible. A second leach with water on 3 samples released less than 0.5% of the total salt determined in the first analysis, indicating that one leach was sufficient.

(d) Carbonate Analyses.

Carbonate contents were determined according to Ku's (1966) modification of Turekian's (1956) method for acid soluble alkaline earths in deep sea sediments. The leached residue of the salt analysis was treated with 5 ml. dilute acetic acid (1:50 V./V.) When effervescence ceased, the contents of the tube were decanted into a 100 ml. conical flask, and heated to dryness on a hot plate. After addition of 5 ml. concentrated acetic acid and 30 ml. distilled H_2O , the residue was resuspended. About 2 mg. magnesium-dihydrogen ethylenediamine tetraacetate (Mg - E.D.T.A.) complex was added before titration to yield a sharper end point.

Next, 5 ml. NH_4Cl buffer solution (pH 10), 2 ml. KCN masking agent and 2 ml. Eriochrome Black - T indicator (Eastman Kodak: P6361) were added, and the mixture titrated against a 0.01M E.D.T.A. standard. At the end point, the wine-red colour of the solution turned light blue.

After blank correction, there was an agreement of $\pm 2\%$ between analyses, each sample again being duplicated. The reagent concentrations were those specified by Turekian (1956).

2. 3. Radiochemical Separations for Natural Series Isotopes.

(a) Dissolution of Samples : V16-200.

Depending on depth and composition, 5 to 10 g. of homogenised sediment were weighed to better than 0.01 g. and transferred to a 250 ml. Teflon beaker. The sediment was moistened with a few ml. of distilled H_2O , and concentrated HCl added slowly until effervescence ceased. A polyethylene lid was used to prevent loss at this stage. After addition of 25 ml. concentrated HCl and 5 ml. concentrated HNO_3 together with U^{232} - Th^{228} tracer or Pa^{233} tracer, the mixture was heated to dryness on a hot-plate. The dried residue was leached with 25 ml. $6\bar{N}$ HCl, and the leachate decanted after centrifugation into a second 250 ml. Teflon beaker. This process was repeated on the residue using a further 25 ml. $6\bar{N}$ HCl, followed by 25 ml. distilled H_2O .

At this stage, mainly the refractory clay minerals remained. Since these minerals contained most of the uranium and thorium, it was essential to effect their dissolution. In the earlier analyses this was achieved as follows. The residue was transferred to the original beaker and 100 ml. concentrated HF (40% W./ V.) with 10 ml. concentrated $HClO_4$ added. The mixture was heated on a hot-plate until fumes of $HClO_4$ were evolved.

When fuming ceased, the treatment with $6\bar{N}$ HCl and H_2O was repeated, and the leachates combined with those obtained previously. A variable volume of gelatinous residue normally remained. After addition of 10 ml. each of $6\bar{N}$ HCl and concentrated HNO_3 , the mixture was boiled. The solution was centrifuged when cool, and the supernate added to the leachates.

If any residue still remained, it was fused with sodium carbonate. The residue was dried and powdered, then mixed with five times its mass of Na_2CO_3 . This mix was transferred to a platinum crucible and heated strongly with swirling over a Meker burner for ten minutes. The cooled solid was dissolved in $6\bar{N}$ HCl: if any insolubles remained, they could be taken into solution by addition of an equal volume of concentrated HNO_3 followed by boiling.

In later experiments a faster procedure for dissolving the clays was used. The clay residue was dried and powdered, then placed in the 25 ml. cup of an acid digestion bomb (Parr Instrument Co. Illinois.; No. 4745, Figure 7.) A few drops of distilled H_2O were added, followed by 12 ml. concentrated HF. (40 or 48% W./V.)

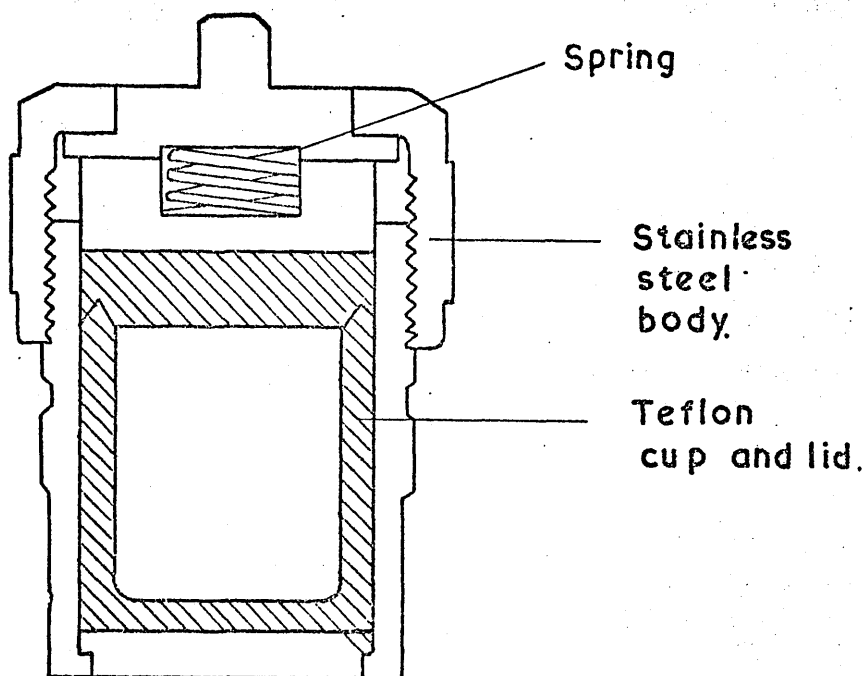


Figure 7: Parr 4745 Acid Digestion Bomb.

The cup, with its Teflon lid, was screwed into the body of the bomb, which was then heated at 150°C . in a thermostated oven for three hours. When cool, the contents of the cup were decanted into the original beaker, and the cup washed clean with $6\bar{\text{N}}$ HCl. After addition of 5 ml. concentrated HClO_4 , the mixture was heated until fuming ceased. The residue was leached with two 25 ml. portions of $6\bar{\text{N}}$ HCl. Any remaining residue was soluble in a boiling $6\bar{\text{N}}$ HCl/ HNO_3 mixture.

From the total measured volume of the combined leachates (150 to 250 ml.) a 25 ml. sample was taken by pipette for Ra^{226} analysis. No carriers were necessary for uranium, thorium or protactinium because the iron and aluminium present in solution carry these elements in hydroxide precipitates.

(b) Dissolution of Samples: Corals.

About 10 g. of the coarsely ground coral were weighed to better than 0.01 g. The sample was transferred to a 250 ml. Teflon beaker, and slowly treated with $8\bar{\text{N}}$ HNO_3 . Care was taken not to lose any of the solution, since dissolution was brisk. When effervescence ceased, 20 ml. concentrated HNO_3 , U^{252} - Th^{228} tracer, and 2 ml. HNO_3 /saturated $\text{Al}(\text{NO}_3)_3$ were added (see Chapter 2.3 h).

The mixture was heated until approximately two thirds of the original volume remained. If the cooled solution contained any insoluble material (contemporaneous detritus in the coral) it was filtered through acid hardened filter paper.

(c) Preliminary Enrichment.

The acid solution from the sample dissolution stage was heated strongly on a hot plate for one hour in the Teflon beaker to remove the last traces of CO_2 . (Uranium forms a stable and soluble carbonate complex, $\text{UO}_2(\text{CO}_3)_3^{4-}$.) The warm acid solution was neutralised with concentrated NH_4OH to a pH of 6 to 8. (The iron and aluminium hydroxide precipitate thus formed quantitatively scavenges uranium, thorium and protactinium under these conditions. If the pH exceeds 8 peptisation of $\text{Al}(\text{OH})_3$ occurs with subsequent difficulties in obtaining a true solution.) The solution and gelatinous precipitate were transferred to a 250 ml. Pyrex centrifuge bottle and separated by centrifugation. The supernate was decanted and discarded, and the precipitate completely redissolved in the minimum quantity of concentrated HCl. The precipitation and centrifugation were repeated, then the second precipitate was washed with twice its volume of distilled water. A few ml. of concentrated HCl were used to dissolve the washed precipitate, and the solution adjusted to $8\bar{N}$ with respect to HCl.

The volume of solution at this time was typically 50 to 100 ml. The solution was equilibrated with half its volume of diisopropyl ether (D.I.P.E.) in a 100 or 250 ml. separating funnel. (This removed most of the Fe(III) from solution, and permitted subsequent use of a smaller anion exchange column. Corals contain relatively little iron, and this step was omitted in coral analyses.) After separation, the aqueous phase was returned to the original beaker and warmed gently on a hot plate in a strong draught to remove the last traces of ether.

(d) Uranium Separation.

The first separation of uranium was performed by anion exchange. Bio-Rad AG 1 x 8 resin (100 to 200 mesh), previously expanded in distilled water, was settled into a 1 cm. diameter Pyrex chromatography column to a length of 12 cm. The column was pretreated with 30 ml. distilled H₂O followed by 30 ml. 8N HCl. The 8N HCl sample solution was then passed through the column, followed by a 40 ml. 8N HCl washing. (Fe (III) and U (VI) are adsorbed on the column at this stage, while Al(III) and Th(IV) are contained in the eluate (Kraus et al., 1956).) Uranium was eluted from the column by 25 ml. 0.1N HCl into a 100 ml. beaker.

The eluate was heated to dryness, the dried residue redissolved in 5 ml. $8\bar{N}$ HCl, and equilibrated with 5 ml. D.I.P.E. in a 25 ml. separating funnel to purify further from iron. The aqueous layer and a 5 ml. $8\bar{N}$ HCl washing from the D.I.P.E. were combined and heated to dryness. Next, 1 ml. concentrated HNO_3 was added, and the solution again evaporated to dryness. The nitrate residue was taken up in two 2 ml. portions of HNO_3 /saturated $\text{Al}(\text{NO}_3)_3$ mixture, and transferred to a 12 ml. centrifuge tube. After the addition of 5 ml. ethyl acetate (EtOAc), the layers were intimately mixed using a Pasteur pipette, centrifuged, and the EtOAc (now containing the uranium) drawn off into a second centrifuge tube using a fresh Pasteur pipette. The uranium was back-extracted from the EtOAc into 5 ml. distilled H_2O , and the organic layer discarded. The pH of the aqueous layer was adjusted precisely to 3 with a few drops of dilute NaOH (freshly prepared to minimise carbonate anion). Approximately 2 ml. of $0.4\bar{M}$ thenoyltrifluoroacetone (T.T.A.) in benzene were added, emulsified with the aqueous layer, and centrifuged. At this pH, U(VI) complexed with the T.T.A. chelate, and the organic layer was ready to be mounted for alpha counting.

Yields for uranium were initially low, since a thorium extraction stage at pH 1 on the final inorganic solution was included.

This step was found to be coextracting some uranium, and since no evidence of thorium isotopes was ever found, the step was omitted. After this, uranium yields of 35 to 75% were obtained routinely.

(e) Thorium Separation.

The eluate from the anion column was neutralised with concentrated NH_4OH to a pH of 7. This precipitate (mainly $\text{Al}(\text{OH})_3$ carrying $\text{Th}(\text{OH})_4$) was centrifuged and the supernate discarded. An equal volume of hot $3\bar{\text{N}}$ NaOH was added to the precipitate, mixed well, and centrifuged. (This removed the bulk of the $\text{Al}(\text{OH})_3$ and permitted the use of a smaller cation exchange column.) The remaining hydroxide precipitate was washed twice with 10 ml. distilled H_2O , the washings discarded, and the precipitate dissolved in about 25 ml. $4\bar{\text{N}}$ HCl . Gentle heating was often necessary to remove a slight opalescence in the solution due to peptisation.

A cation exchange column was used to purify the thorium from any remaining aluminium. A column of Bio-Rad AG 50W x 16 resin (400 minus mesh, 8 cm. x 8 m.m.) was prepared, and pretreated with 20 ml. $4\bar{\text{N}}$ HCl . The sample solution, containing thorium in $4\bar{\text{N}}$ HCl , was then added to the column, followed by 16 ml. $4\bar{\text{N}}$ HCl .

(The Th(IV) isotopes were now adsorbed on the column, while Al(III) passed through in the eluate (Kraus and Moore, 1950).)

Thorium was eluted with 40 ml. 0.75 \bar{M} oxalic acid into a 100 ml. beaker. After the addition of 5 ml. concentrated HNO_3 and 5 ml. concentrated HClO_4 , the mixture was heated to dryness on a hot-plate. The beaker was washed down with 2 ml. concentrated HClO_4 and the solution again fumed to dryness. (Since the presence of oxalic acid interferes with subsequent steps, its complete decomposition was necessary.) A further 2 ml. concentrated HNO_3 were added, and the process repeated.

The purified thorium fraction was dissolved in two 3 ml. portions of dilute HNO_3 (0.035 \bar{M} , pH 1.5) and transferred to a 12 ml. centrifuge tube. The thorium was then extracted into 2 ml. 0.4 \bar{M} T.T.A. in benzene by emulsification using a Pasteur pipette. The chelate was then ready to be mounted for alpha counting after centrifugation.

Yields for thorium ranged from 40 to 70%.

(f) Protactinium Separation.

Protactinium analyses were performed separately from those for uranium and thorium.

Protactinium is an element which appears to be characterised by irreproducible chemical behaviour: colloid formation is common. Accordingly, all apparatus used for the protactinium analyses was constructed from Teflon, polyethylene or polypropylene. The partitioning of protactinium between phases in the solvent extraction steps was followed by monitoring the 0.31 MeV. Pa²³³ peak, using a NaI (Tl) crystal gamma detector coupled to a multichannel analyser.

After the sample (with added Pa²³³ tracer) had been dissolved, the D.I.P.E. extraction for Fe(III) was performed. The aqueous layer from this extraction was neutralised with NH₄OH, and centrifuged. The precipitate was treated with hot 3N NaOH as in the separation procedure for thorium. This hydroxide residue was dissolved in concentrated HNO₃ after washing with H₂O, reprecipitated with NH₄OH, and further washed with H₂O. The precipitate was dissolved in 2 ml. concentrated H₂SO₄ and 10 ml. concentrated HNO₃, transferred to a 100 ml. Teflon dish and heated on a hot plate until H₂SO₄ fuming commenced. (Fuming the residue with H₂SO₄ removed any traces of F⁻. Pa(V) forms a stable (PaF₆)⁻ anion, which renders extraction into organic phases impossible.) The fuming was not taken to dryness, and when cool the pasty residue was dissolved in 10 ml. concentrated HCl.

This solution was equilibrated with 10 ml. diisobutyl carbinol (D.I.B.C.) in a polyethylene separating funnel. Protactinium was extracted into the D.I.B.C. and the phases were separated by centrifugation. The D.I.B.C. was transferred back to the separating funnel, and scrubbed with two successive portions of $6\bar{N}$ HCl. Next the protactinium was back-extracted into 5 ml. $0.1\bar{N}$ HF/ $12\bar{N}$ HCl. After separation, 1 ml. concentrated H_2SO_4 was added to the inorganic phase, and the mixture heated to fuming in the original dish. When cool, 4 ml. concentrated HCl were added, and the protactinium was again extracted into 5 ml. D.I.B.C. After centrifugation, the organic phase was washed with two 5 ml. portions of $6\bar{N}$ HCl by mixing with a polyethylene pipette while in the centrifuge tube. Protactinium was back-extracted from the D.I.B.C. into 5 ml. $0.1\bar{N}$ HF/ $12\bar{N}$ HCl in the same fashion. The acid was scrubbed with two 5 ml. portions of benzene, transferred to a 10 ml. Teflon beaker, and heated to dryness. After addition of 1 ml. concentrated HNO_3 , the solution was again heated to dryness. Next 1 ml. $0.5\bar{M}$ H_2SO_4 was added to the beaker, and heated until fuming commenced. After dilution with 1 ml. distilled H_2O , the solution was transferred to a 12 ml. polyethylene tube. (Sometimes slight heating was necessary to obtain a clear solution). The pH of the resultant acid was 0.2 to 0.5, and in this range the protactinium was stripped into 1 ml. $0.4\bar{M}$ T.T.A. in benzene.

The complex was now ready to be mounted for alpha determination.

Protactinium tracer yields ranged from 40 to 70%.

(g) Radon Separation.

The system used in this laboratory for Ra²²⁶ analysis has been described by Conlan et al. (1969), and is based on a separation scheme suggested by Lucas (1963). The method involves the "emanation technique" and the physical separation of Rn²²² ($t_{1/2} = 3.823$ days) from a solution containing the parent Ra²²⁶, followed by gas phase alpha scintillation counting. Radium analyses were performed by Mr. M.C. Jarvis under the author's supervision.

The 25 ml. aliquot of the dissolved sample taken for Ra²²⁶ analysis was made up to 200 ml. with a solution of 2 g. BaCl₂/l. 6N HCl, and stored in a 250 ml. flask with inlet and outlet necks. The sealing time of the equilibration flask was noted so that the percentage buildup of Rn²²² towards secular equilibrium with Ra²²⁶ could be calculated. Samples were stored for at least ten days before counting.

Figure 8 shows the separation apparatus.

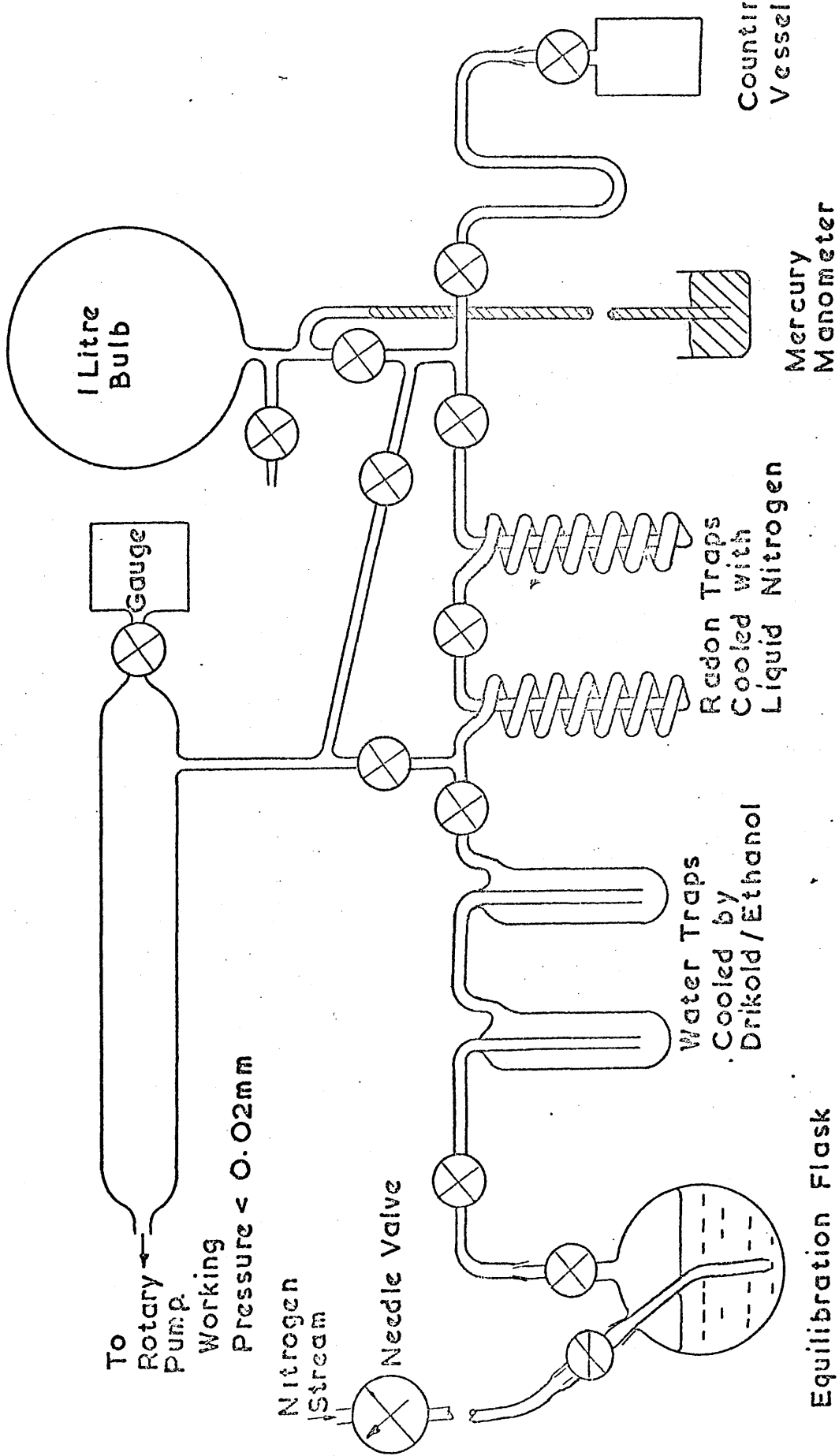


Figure 8: Radon Separation Apparatus.

The entire vacuum line, apart from the equilibration vessel, was evacuated to a pressure of about 0.01 torr. The rotary pump was then isolated, and Dewar vessels containing Drikold/ethanol and liquid nitrogen emplaced as indicated. Radon was swept from the equilibration flask in a stream of commercial nitrogen (British Oxygen Company Ltd., London), to be condensed in the spiral traps. When the nitrogen pressure in the line had reached atmospheric, as shown by the manometer bubbler, the flow was shut off. The litre bulb and the moisture traps were isolated from the radon traps and the counting vessel, and this latter section of the line pumped to remove nitrogen. Pumping was stopped when the working vacuum had been attained, and the radon distilled from the warmed spiral traps into the U section, now cooled by liquid nitrogen. When the spiral traps were at room temperature, they were isolated from the U tube, the liquid nitrogen vessel was removed, and the U tube warmed. The radon contained therein was carried into the counting vessel by opening the tap to the nitrogen stored in the litre bulb. The counting vessel was sealed immediately and removed from the line.

To ensure a consistent radon separation yield from the system, the entire sequence of manipulations was performed to a strict schedule.

(h) Chemical Apparatus, Reagents and Carriers.

All glass apparatus used in the analyses was Pyrex (borosilicate glass). Between analyses, all apparatus, glass, Teflon and polyethylene, was scrubbed with Pyroneg (Diversey Ltd., Barnet.), rinsed, and heated in a 5% solution of Decon-75 (Medical Pharmaceutical Developments Ltd., Brighton.) for at least three hours at around 60°C. After rinsing, all glass and Teflon apparatus was heated in 8N HNO_3 for at least three hours at the same temperature. Polyethylene apparatus was treated similarly, but in 6N HCl . All were thoroughly washed with tap water, and further rinsed with distilled water immediately before use.

"Analar" grade reagents and distilled water were used throughout.

As mentioned previously, the sediment samples did not require any carriers. For the coral samples and blank runs, an aluminium carrier was prepared by dissolving 315 g. $\text{Al}(\text{NO}_3)_3 \cdot 6\text{H}_2\text{O}$ in a mixture of 142 ml. distilled H_2O and 28 ml. 16N HNO_3 (May and Grimaldi, 1954). This solution was extracted for possible uranium contamination by scrubbing with an equal volume of ethyl acetate. (This mixture was also used for salting out in the uranium analyses.)

The iron carrier used in the blank analyses was prepared by extracting 10 ml. $1\bar{M}$ FeCl_3 in $8\bar{N}$ HCl with 10 ml. D.I.P.E. Ferric ion was back extracted from the D.I.P.E. with 10 ml. distilled H_2O , and 2 ml. of this solution was taken as Fe (III) carrier.

work employed cobalt decomposer that is suggested by Thurt

A 2" x 2" collar (1" i.d., 0.001" thick) was placed on a levelled 200W. hotplate and heated at full power. A 1" stainless steel counting planchette (1" diameter with a 3/8" diameter dimple) was placed centrally on the collar. The collar was supplied by a power line drawn from the wall outlet with a 2" power cord and a lead shielded to the plane. A temperature gradient existed radially across the plan

2. 4 Nuclear Counting Techniques.

(a) Alpha Source Preparation.

Alpha spectrometry requires thin sources (a few tens of $\mu\text{g./cm}^2$.) to give good energy resolution and reduce low energy tail contributions. The preparation of thin sources has been reviewed by Yaffe (1962), and alpha counting in general by Schneider and Harmon (1958). The standard methods for source preparation are electrodeposition and vacuum sublimation, but this work employed chelate decomposition as suggested by Thurber (1963).

A brass collar, (1" o.d., 0.5" deep, 0.125" thick) was placed on a levelled 600W. hotplate and heated at full power. A stainless steel counting planchette (1" diameter with a shallow 0.5" diameter dimple) was placed centrally on the collar. The metal - T.T.A. complex in benzene was drawn from the centrifuge tube with a Pasteur pipette and dropped slowly on to the planchette. A temperature gradient existed radially across the planchette and together with the depression this kept the benzene solution localised while evaporation occurred. When all the benzene had evaporated, the planchette was flamed over a Meker burner until bright red.

This left an oxidised deposit of the element mounted on the disc: while there were obvious inhomogeneities because the benzene dried in concentric rings, the resolution appeared equal to that of a vacuum deposited source.

Notes. This method of mounting was simple and rapid, the only problems encountered being:

- i) any aqueous material inadvertently added with the T.T.A.- benzene caused sputtering and a "thick spot" on the mount.
- ii) in uranium extractions, the pH had to be adjusted precisely to 3, otherwise other elements were extracted into the T.T.A., causing a thickening of the source.
- iii) the purity of the T.T.A. was important. It was recrystallised from benzene, placed in a light-tight flask, and pumped to a vacuum of approximately 10^{-3} torr. At this pressure, volatile impurities were allowed to distil overnight into a liquid nitrogen trap. The purified T.T.A. and all T.T.A. - benzene solutions were maintained in well stoppered, light-tight flasks.

(b) Alpha Spectrometry: Theory

The terrigenous component of deep sea sediments exhibits uranium

and thorium concentrations around 2.6 and 13.4 p.p.m. respectively (Ku, 1966), which correspond to activities of 2 to 3 d.p.m./g. Since biogenic components have much lower concentrations than these (e.g. foraminifera contain 0.0x p.p.m. uranium (Ku, 1965)), it follows that either long counting times are necessary to reduce counting uncertainties to a few percent, or that large samples must be processed. In general the quantity of sediment available for destructive analysis is limited, but in any case the volumes derived from large samples complicate chemical separations.

Prior to about 1960, alpha spectrometric analysis had to be performed by a Frisch gridded ionisation chamber. Although this type of instrument has the desirable features of high inherent alpha resolution (0.6% width at half maximum for 5 MeV. alpha particles), low background (0.1 to 1 alphas per minute) and good counting geometry (50%), its use is hampered by instability during long counts. In the past decade, the availability of silicon surface barrier (S.B.) detectors has greatly facilitated routine alpha spectrometric work.

The S.B. detector (Dearnley and Northrup, 1966) is essentially a large area diode, having a thin atmospherically oxidised p-type layer as sensitive face on a high purity n-type silicon wafer.

Electrical contacts are made to the faces of the disc by a uniform vacuum deposition of gold (40 ug./cm^2 .) on the sensitive surface, and through a thicker aluminium contact to the rear n-type surface. When a reverse bias is applied to the detector, charge carriers are swept from a voltage dependent depth behind the sensitive face, known as the depletion depth.

When a charged particle impinges on the front surface of the detector, it loses its energy (EeV.) by ionisation, expending $3.6 \text{ eV. / electron-hole pair}$ in the silicon. (This is to be compared with an expenditure of about 30 eV./ion-pair in a gas.) If the depletion depth is greater than the particle range in silicon, all the energy will be lost, forming $E/3.6$ electron-hole pairs, each comprising 1.6×10^{-19} coulombs of charge. Since both electrons and holes have high mobilities in silicon, the reverse bias voltage sweeps them apart with a collection time of a few nanoseconds. It has been observed experimentally that the rate of charge carrier formation is independent of particle energy and ionisation density. Thus a charge (q) dependent only on incident energy is produced, provided that the depletion depth is sufficient and the field in the depletion zone is large enough to separate the charge carriers before recombination can occur.

The high resolution inherent in S.B. detectors is limited

by preamplifier noise. Since the capacitance of an S.B. detector is a function of bias voltage and environmental conditions, a low noise charge sensitive preamplifier is used. The input differentiating time constant of such a preamplifier is much greater than the detector collection time, so a voltage $V_{in} = q/C_T$ is developed at the input of the preamplifier from a particle of energy E, where:

$$C_T = C_d + C_s + C_p$$

C_T is the total capacitance

C_d is the total detector capacitance

C_s is the total stray capacitance

C_p is the dynamic input capacitance

of the amplifier.

For a feedback operational amplifier,

$$C_p = A.C_f$$

C_f is the feedback capacitance

A is the open loop voltage gain

and normally C_p is so large that:

$$C_T = C_p$$

Therefore, $V_{in} = q/C_p = q/A.C_f$

and $V_{out} = (q/A.C_f).A = q/C_f$.

i.e. the output is independent of diode and stray capacitances.

Finally, for such a charge sensitive preamplifier, V_{out} for a totally stopped particle of energy EeV. is:

$$V_{\text{out}} = \frac{E \times 1.6 \times 10^{-19}}{3.61 \times C_f}$$

For alphas, this pulse is typically tens or hundreds of mV. per MeV. input. A pulse of this size can be amplified conveniently by normal nucleonic amplifiers, with appropriate pulse shaping to enhance signal-to-noise ratio.

The signal from the amplifier system, still linearly proportional to particle energy, is fed to a multichannel analyser after suitable discrimination. The analyser sorts the incoming pulses according to their amplitude, and assigns each pulse to a channel in the memory corresponding to a particular voltage increment. During counting, the analyser accumulates a spectrum of the number of particles of a specific energy received (channel contents) versus the particle energy (channel number). A quantitative estimation of the relative abundances of particles with different energies recorded can be found by integration.

(c) Alpha Spectrometry: Spectrometer System.

In alpha spectroscopy studies, S.B. detectors are normally operated under vacuum for the following reasons:

- i) alpha attenuation is minimised. (Alpha ranges in air are approximately 1 cm./ MeV.)

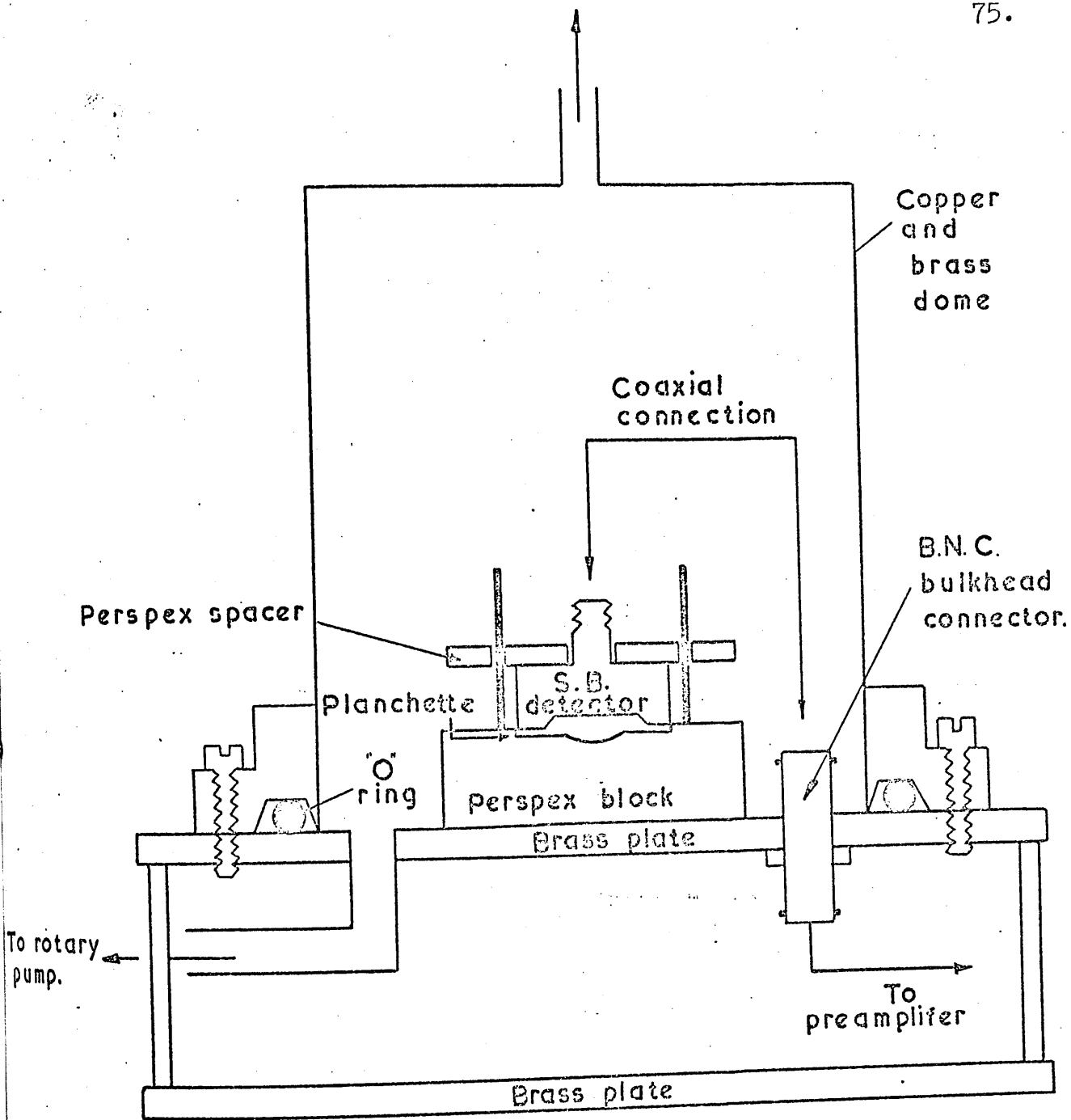
ii) the detector, when under bias, is sensitive to gases and organic vapours. These can cause trapping centres in silicon which degrade the detector resolution.

iii) since the diode is light sensitive, a darkened enclosure reduces noise.

The design of the vacuum chambers used in this work is shown in Figure 9. Two detectors were used in the study, allowing two samples to be counted simultaneously.

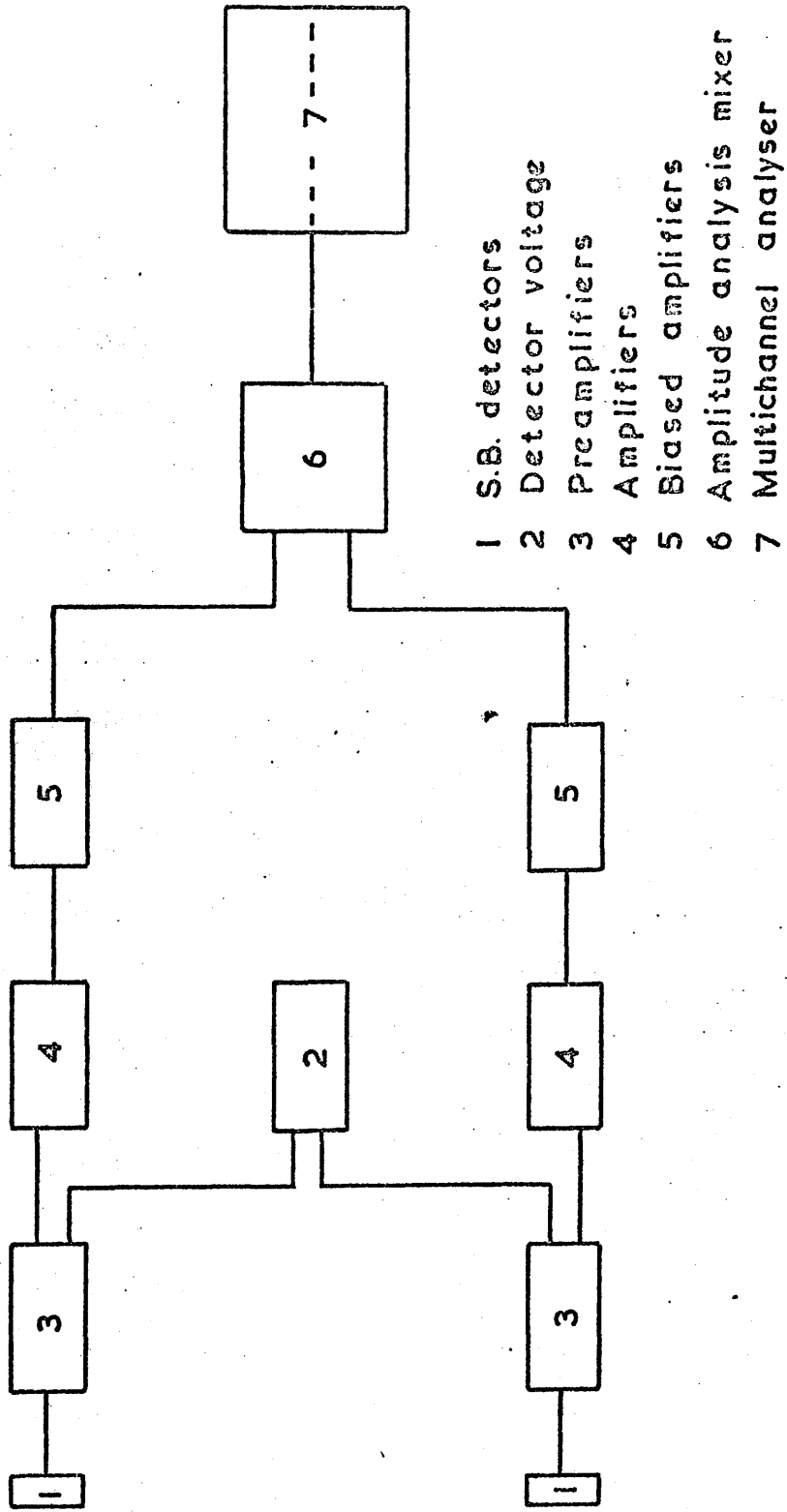
Bias voltage was applied to detectors from a dual supply detector voltage unit (NE 5321), and the amplifier systems consisted of preamplifier (NE 5287), amplifier (NE 5259) and biased amplifier (NE 5261), all manufactured by Nuclear Enterprises Ltd., Edinburgh. The biased amplifier outputs were fed into a 400 channel analyser (Laben, Milan; Spectroscope MOD 400) through an amplitude analysis mixer (Laben M400). This unit enabled the outputs to be recorded simultaneously in two 200 channel banks of the analyser memory. A block diagram of the electronic system is shown in Figure 10.

A double stage rotary pump with liquid nitrogen trap was used to attain a vacuum of 0.1 torr in 10 minutes in the chambers, at which point bias was applied to the detectors. Subsequently a vacuum of 0.05 to 0.03 torr was reached and maintained throughout counting.



- Figure 9:

Vacuum chamber for surface barrier detector. Scale: 1 cm. represents 2.54 cm (approx.)



- 1 S.B. detectors
- 2 Detector voltage
- 3 Preamplifiers
- 4 Amplifiers
- 5 Biased amplifiers
- 6 Amplitude analysis mixer
- 7 Multichannel analyser

Figure 10: Block diagram of alpha spectrometer.

Both detectors used in this study had an active area of 300 mm^2 and a depletion depth of 100 μm . (20th Century Electronics Ltd., Croydon; SSN020M -100; and ORTEC, Oak Ridge; A-045-300-100).

The detector operating voltages quoted by the manufacturers (37V. and 50V. respectively for the 20th Century and ORTEC detectors) were confirmed by maximising the resolution through the system of a 3 nuclide source (Radiochemical Centre, Amersham; source AMR 33, containing Pu^{239} , Am^{241} and Cm^{244} , guaranteed resolution 20 KeV. at full width half maximum (f.w.h.m.)).

Detector leakage current values determined by the manufacturers allowed suitable preamplifier load resistors to be selected (such that the leakage current produced a 1V. drop across the resistors) and dictated that time constants of 0.5 microsecond single differentiation and single integration be used in shaping. The total system resolution found was 75 KeV. f.w.h.m. for the 20th Century detector, compared with the quoted 40 KeV. f.w.h.m., and 65 KeV. f.w.h.m. for the ORTEC detector, compared with 23 KeV. f.w.h.m. This discrepancy was probably due to the large capacitance in the cables and connectors between detectors and preamplifiers. Resolutions up to 120 KeV. f.w.h.m. are tolerable because of the alpha energy differences of the nuclides being analysed (Figure 6). The amplifier gains and discriminators were adjusted to correspond to an energy range of 3 to 6.5 MeV. in 200 channels,

giving an energy increment of 17.5 KeV/channel, and a peak maximum separation of around 40 channels for the nuclides of interest (cf. Section 2.6a).

Spectrometer systems are subject to channel drift due to environmental changes in temperature and humidity, and component ageing. Some drifting was observed in this study, but small drifts were tolerable since the peaks were well separated. When larger drifts occurred the data were rejected.

The counting efficiency of both detectors measured against a calibrated source (Radiochemical Centre, Amersham; source AMR 22, containing vacuum sublimed Am²⁴¹ with a certified emergence rate of 1.781×10^4 alpha particles per minute (\pm less than 5%) and 2 pi to 4 pi conversion factor of 1.96) was 33%, but for typical sample mounts with the activity spread on an 0.5" diameter dimpled planchette the efficiency was 24%.

Since high purity materials are used in the construction of S.B. detectors, a new detector has a negligible alpha background. The background increases with usage due to recoil nuclides attracted to the negatively charged detector face. The magnitude of this background depends on the half lives of the daughter nuclides and the activities of the parent nuclides counted. In these

studies the only buildup of importance was that of Th^{228} from U^{232} . Other activities, such as U^{234} from U^{238} or Th^{230} from U^{234} were negligible, and the short lived daughters of Th^{228} had alpha energies higher than those of the natural nuclides measured. Even for Th^{228} , the background was 12 counts per day in the peak region at the end of the study on the older 20th Century detector (Figure 11).

Mounts prepared from sediment samples were counted for 1 to 3 days, which accumulated several hundred to a few thousand counts for each isotope and gave final counting uncertainties of a few percent (Figures 12 and 13). Coral separates were normally counted for over 4 days to reduce uncertainties since a higher precision of measurement was required (Figures 14 and 15).

Figure 16 demonstrates the energy to channel number linearity of the system.

(d) Low Alpha Background Proportional Counter.

Total Pa^{231} activities in the core material were very small (0.1 to 0.3 d.p.m./g.) and since this is the only natural, long-lived, alpha-active isotope of this element, it was desirable to maximise the counting efficiency. A low alpha background proportional counter was used (Nuclear Measurements Corporation,

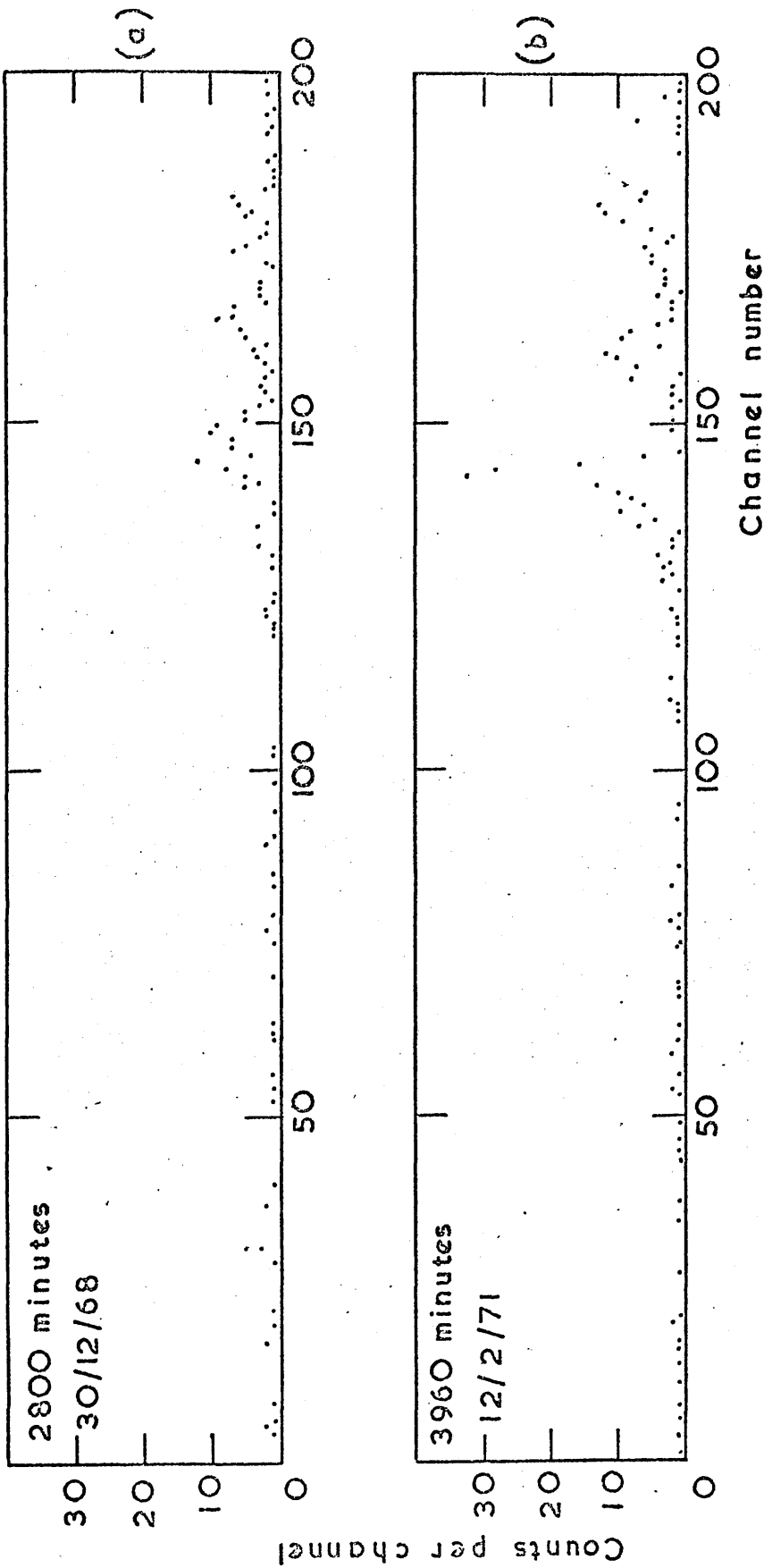


Figure II: Alpha backgrounds of 20th Century detector.

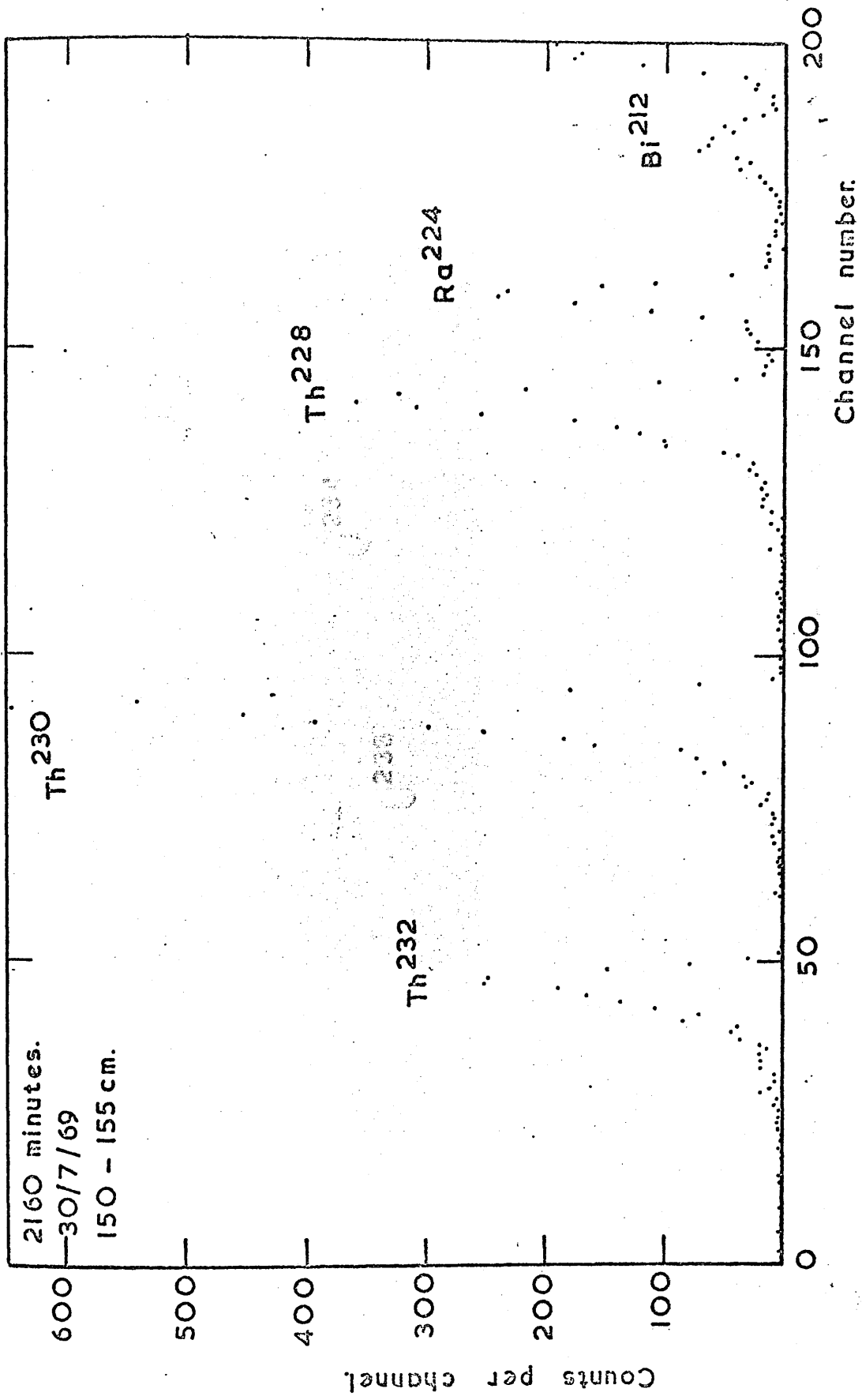


Figure 12: Thorium alpha spectrum from a sediment sample.

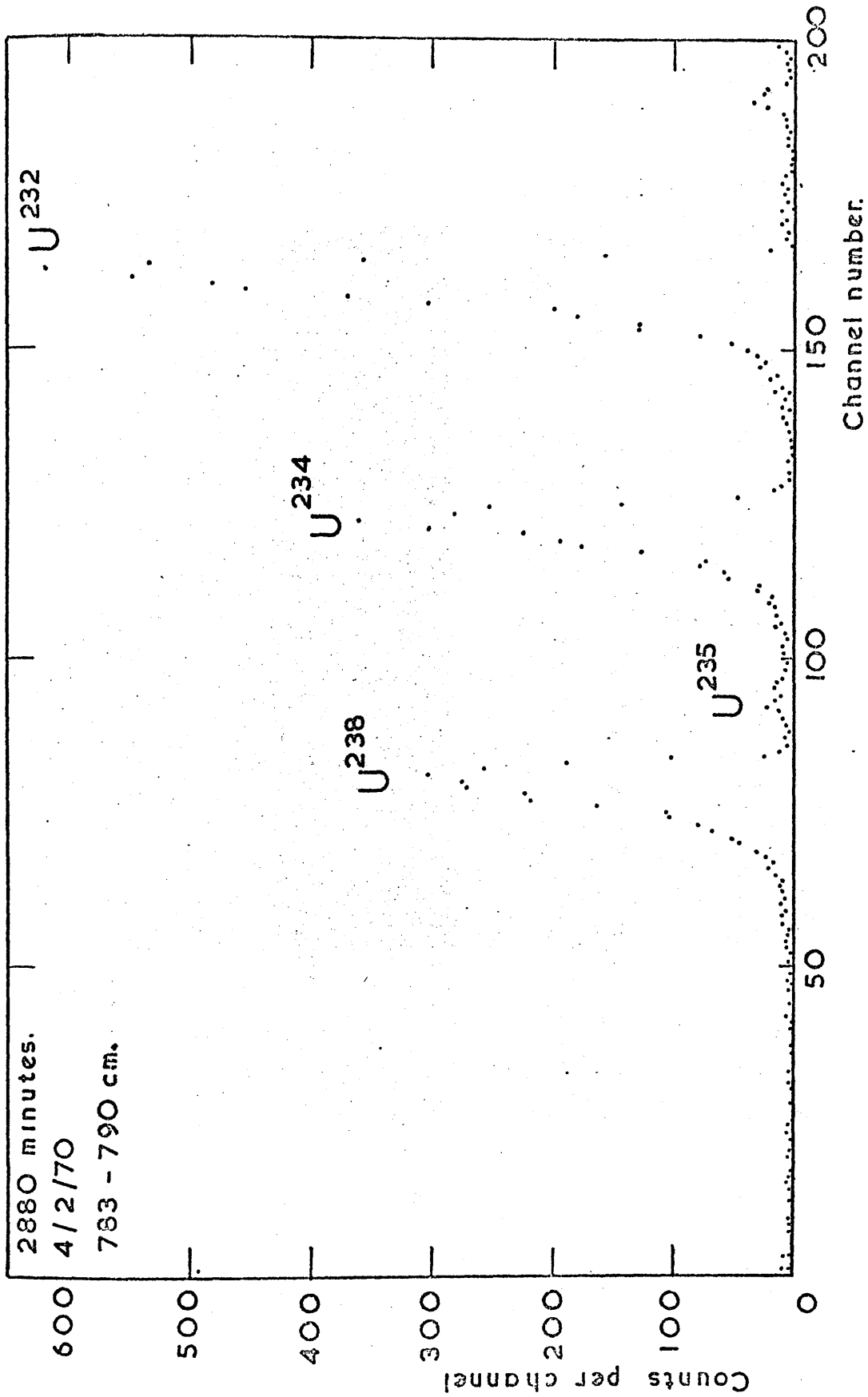


Figure 13: Uranium alpha spectrum from sediment sample.

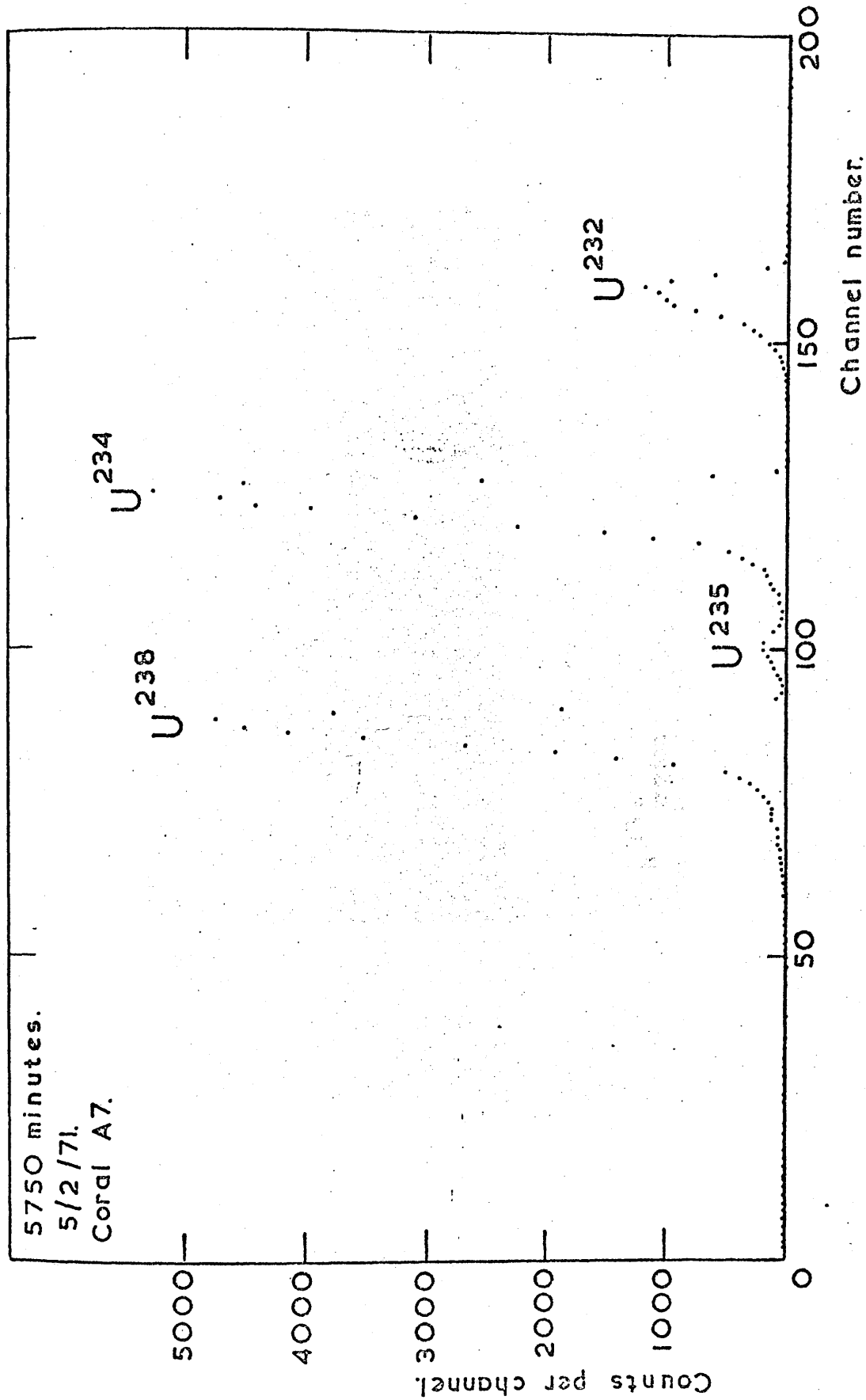


Figure 14 : Uranium alpha spectrum from a coral sample.

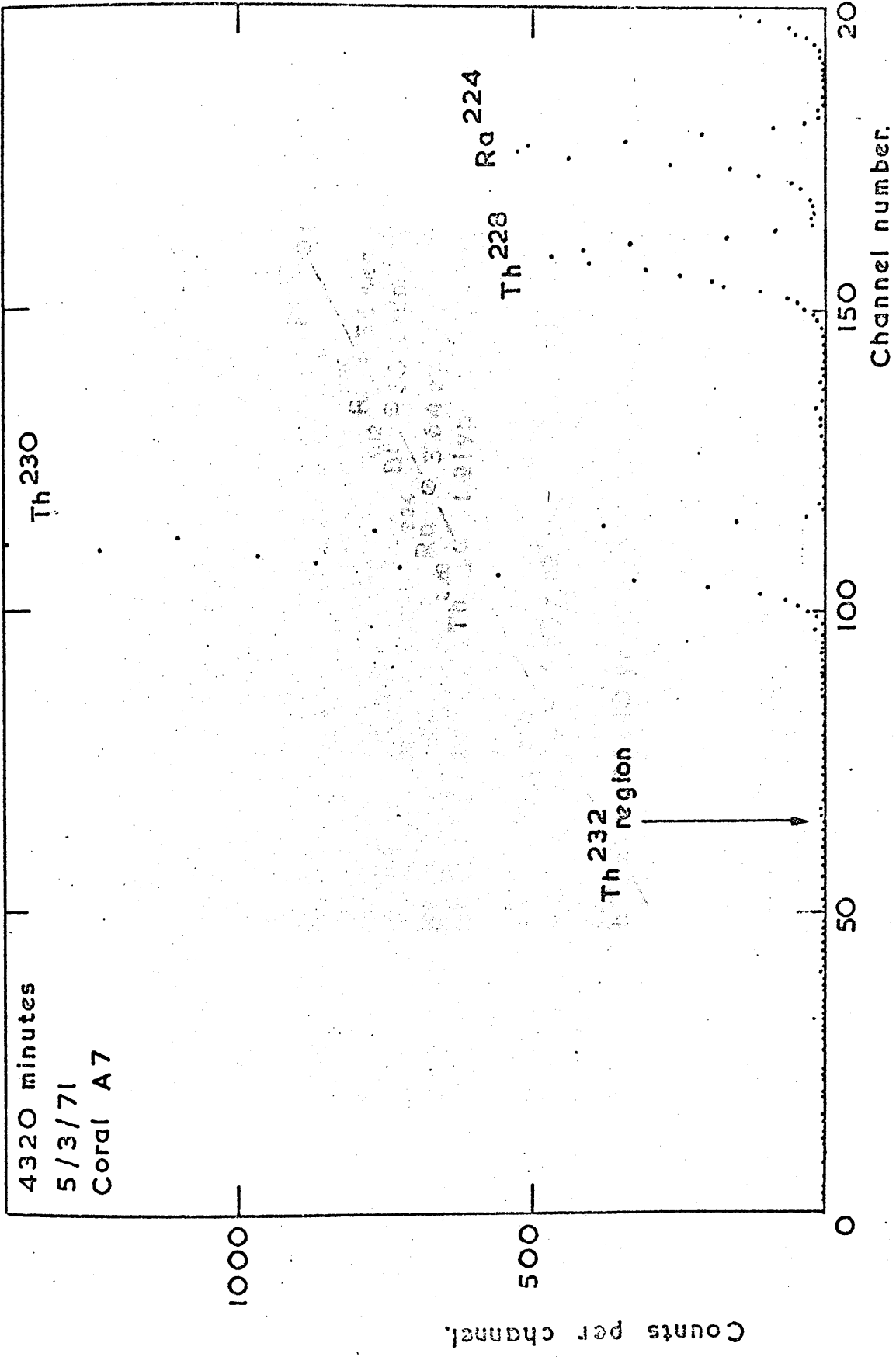


Figure 15: Thorium alpha spectrum from a coral sample.

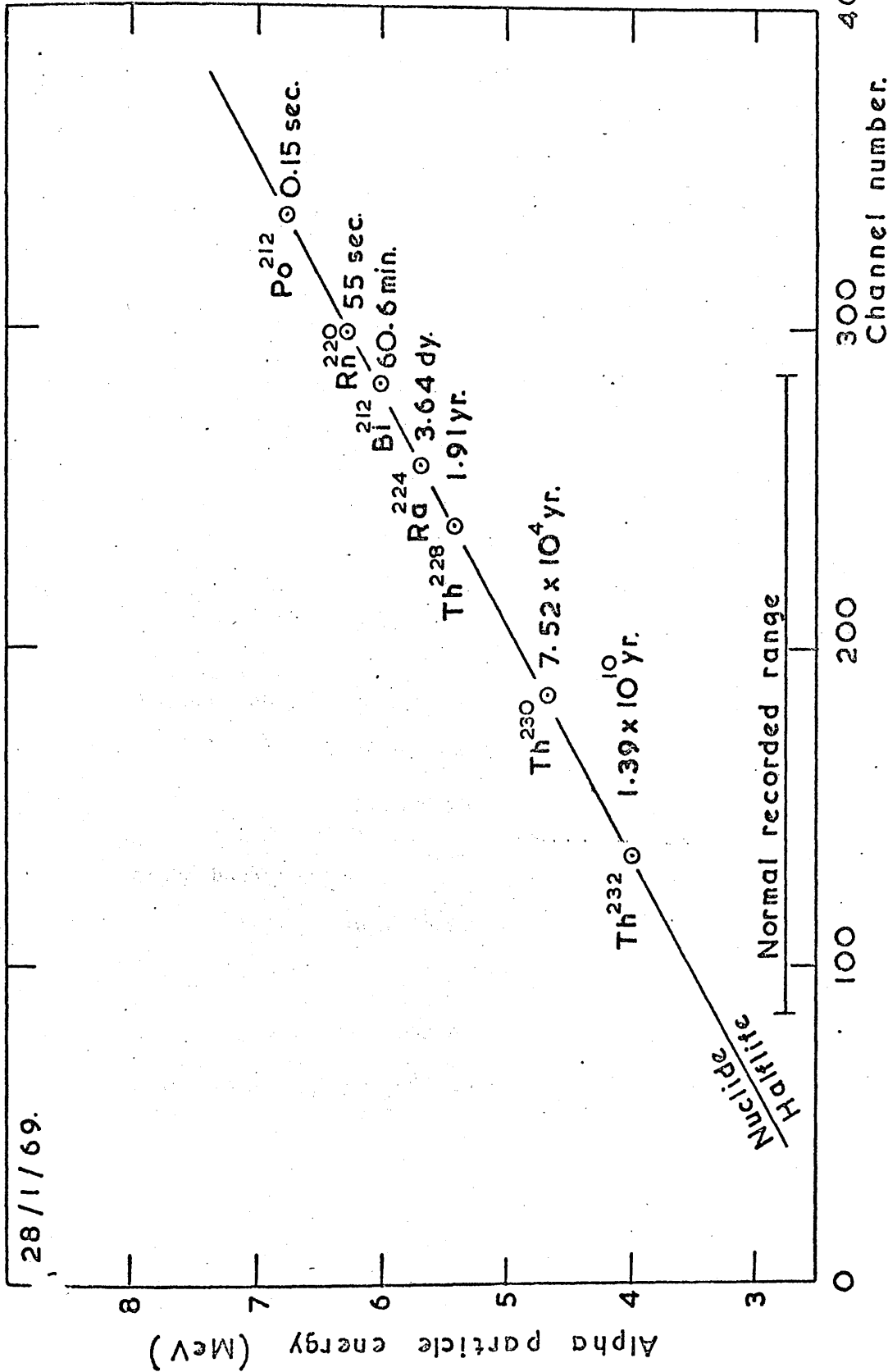


Figure 16: Energy to channel linearity of the alpha spectrometer.

Indianapolis, PC-3T). This is a windowless gas flow counter, with a 2.25" diameter hemispherical chamber and a small loop anode. Both the hemisphere and bottom tray of the counter are fabricated from low alpha stainless steel. Such a chamber gives optimum geometry for planchette counting, and the same counter was used also for Pa²³³ estimation to determine chemical yield. The manufacturer's specifications for the instrument are:

Counter yields:

From thin samples: alpha and beta, 2 pi plus backscattering less self absorption.

Alpha, 51%; beta, 55 to 75%

Plateaux character:

Alpha, 900 to 1200V. Beta, 1700 to 1900V.

(Both with slope less than 1% per 100V.)

Alpha background:

less than 2 counts per hour.

The alpha plateau was determined to be between 950 and 1250V. using the Am²⁴¹ calibrated source (AMR 22), and the beta plateau from 1600 to 1950V. using a C¹⁴ source (Nuclear Measurements Corporation, Gold Standard). Figure 17 illustrates the plateaux.

In practice, both the alpha background and plateaux were dependent on the cylinder of P-10 flow gas (British Oxygen Company,

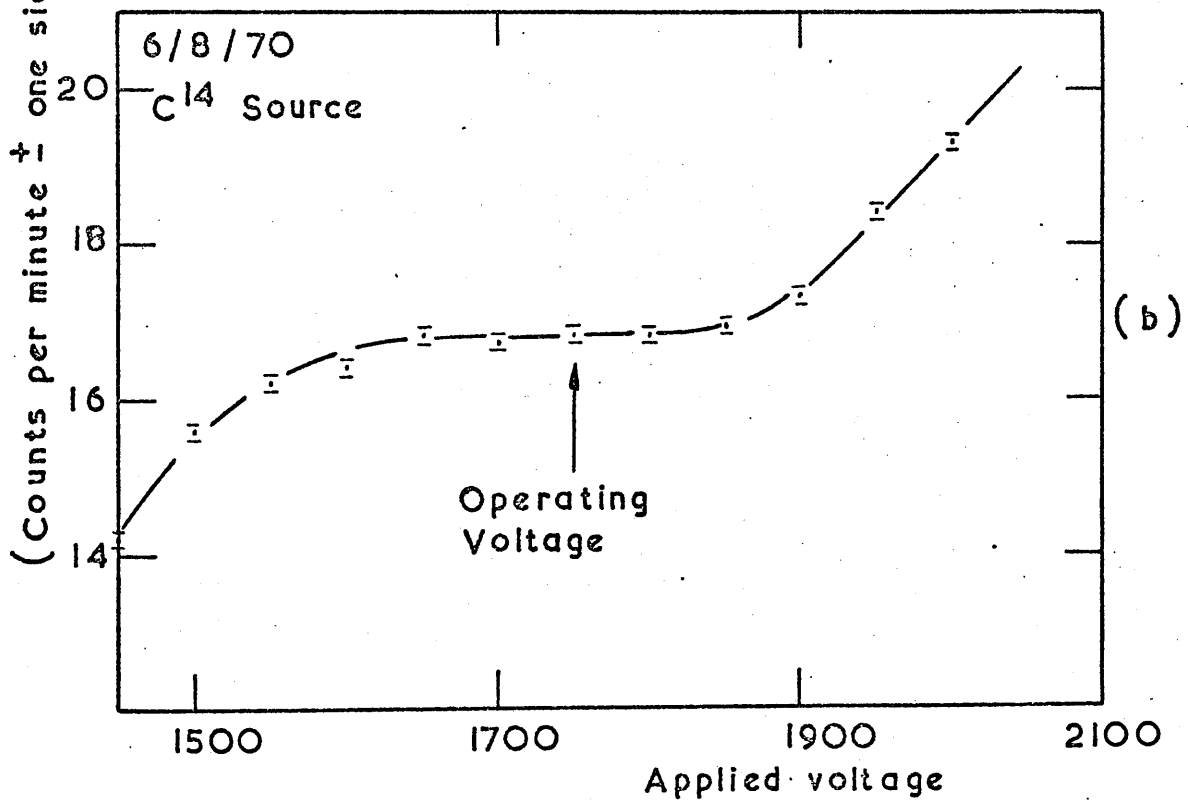
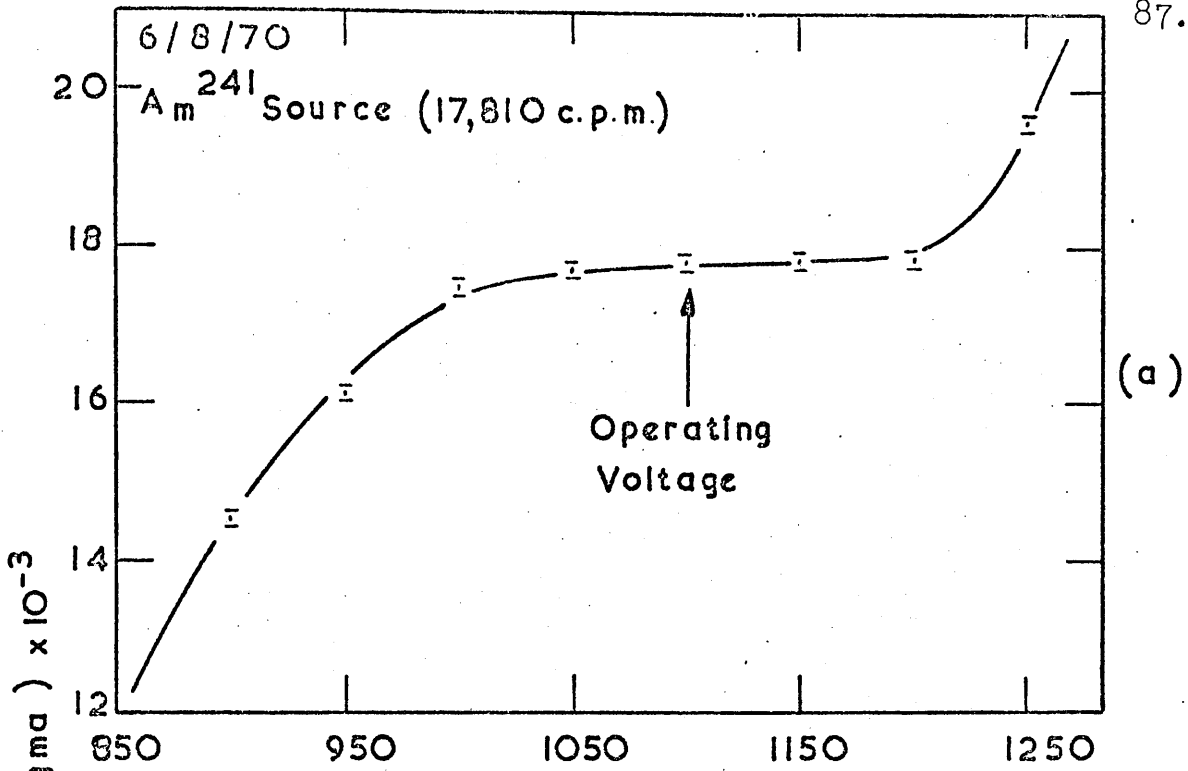


Figure 17: N.M.C counter a) Alpha plateau. b) Beta plateau.

90% argon, 10% methane mixture) used, but were very stable for each cylinder. In each case, the alpha voltage setting was determined by equalising the Am^{241} source count rate at a flow of 2 bubbles per second. This gave an alpha detection efficiency of $50.7 \pm 0.7\%$. (The large error arose mainly from the 3 sigma error of the source calibration count and associated analytical error.) Values selected for the alpha and beta counting voltages were 1050 to 1100V. and 1750 to 1800V. respectively. Under these conditions, backgrounds on a clean stainless steel planchette ranged from 0.015 to 0.035 c.p.m. for alphas, and 62 ± 3 c.p.m. for betas.

Before inserting the protactinium samples, the beta background was monitored for 20 minutes. The sample beta count was then taken for a time appropriate to yield more than 20,000 counts. This count was repeated to give another estimate agreeing within counting statistics. Next, 4 tracer discs, prepared by careful evaporation of 1 ml. Pa^{233} spike solution directly on clean 1" dimpled platinum planchettes, were counted for the same time as the sample. The count rates of the tracer discs agreed to $\pm 3\%$ of their mean, and all separation yields were calculated relative to the same 4 discs. (Note. Platinum planchettes were used since the acid solution in which Pa^{233} was stored attacked stainless steel. Also the sample protactinium separates were not counted on platinum planchettes because those available had alpha backgrounds 2 to 5 times higher than the stainless steel planchettes used.)

The Pa²³¹ activity of the sample was monitored for 3 to 5 days to yield 3,000 to 10,000 total alpha counts. Readings were taken periodically to check that the count rate remained constant. The Am²⁴¹ source rate was checked at the selected voltage before and after each count. Between sample counts, the alpha background was monitored for 1 to 4 days with a clean planchette in the counting chamber.

The alpha spectrum of a protactinium mount is shown in Figure 18.

(e) Radon Counters.

The design of the radon counters used in Ra²²⁶ analysis was similar to that suggested by di Ferrante (1963). The internal diameter of the chamber used to contain the radon (Figure 19) is less than the range in air of the alphas to be counted, so that any alpha particle released in the chamber should produce a scintillation at the detector wall. Since two of the short lived daughter nuclides of Rn²²² are also alpha emitters, the apparent activity is increased threefold (Figure 20).

The vessel to be counted was coupled to the face of a 2" photomultiplier tube (20th Century Ltd., Croydon; VMP 11/44F) with silicone oil (Midland Silicones Ltd.; 550). A copper shield was

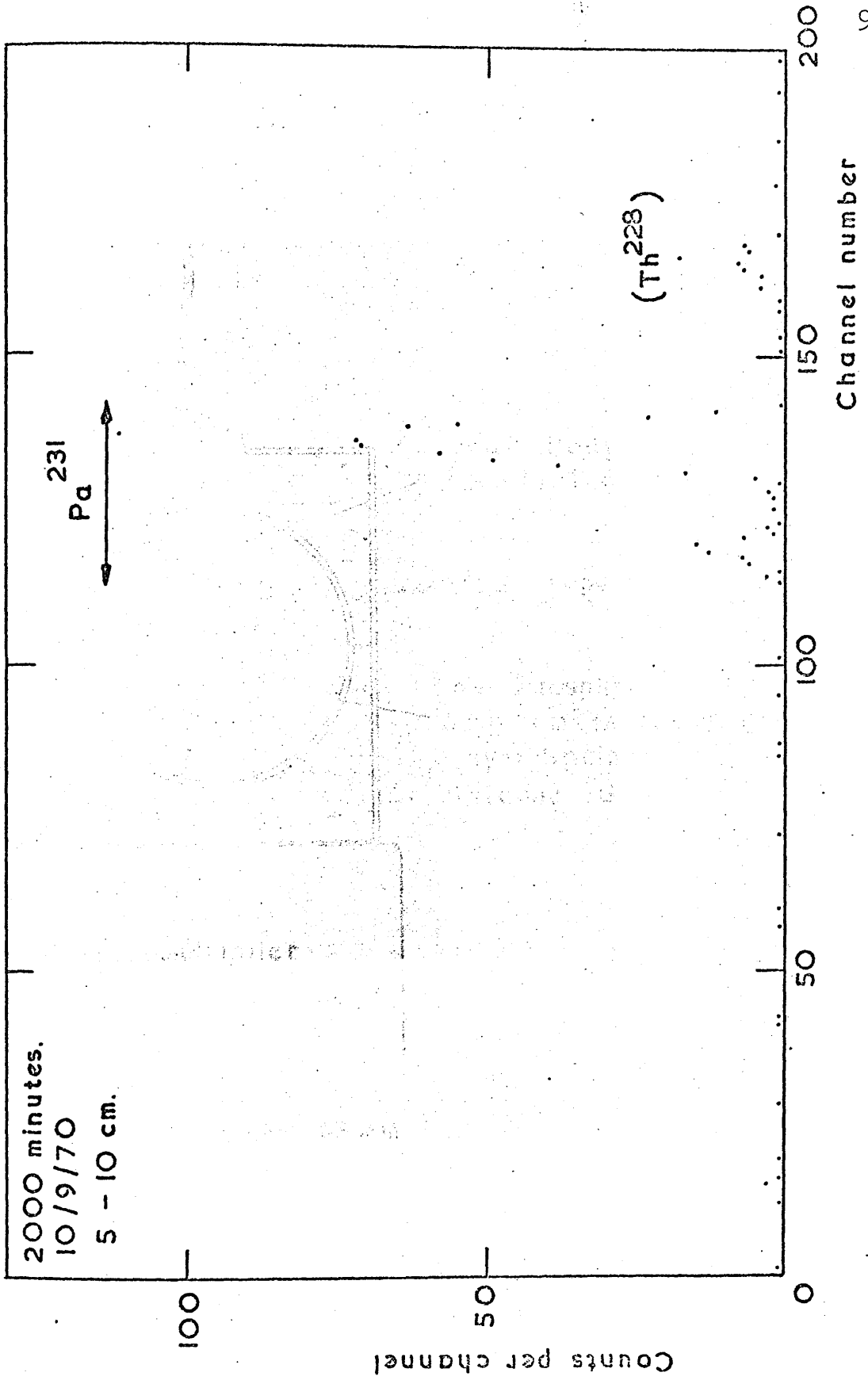
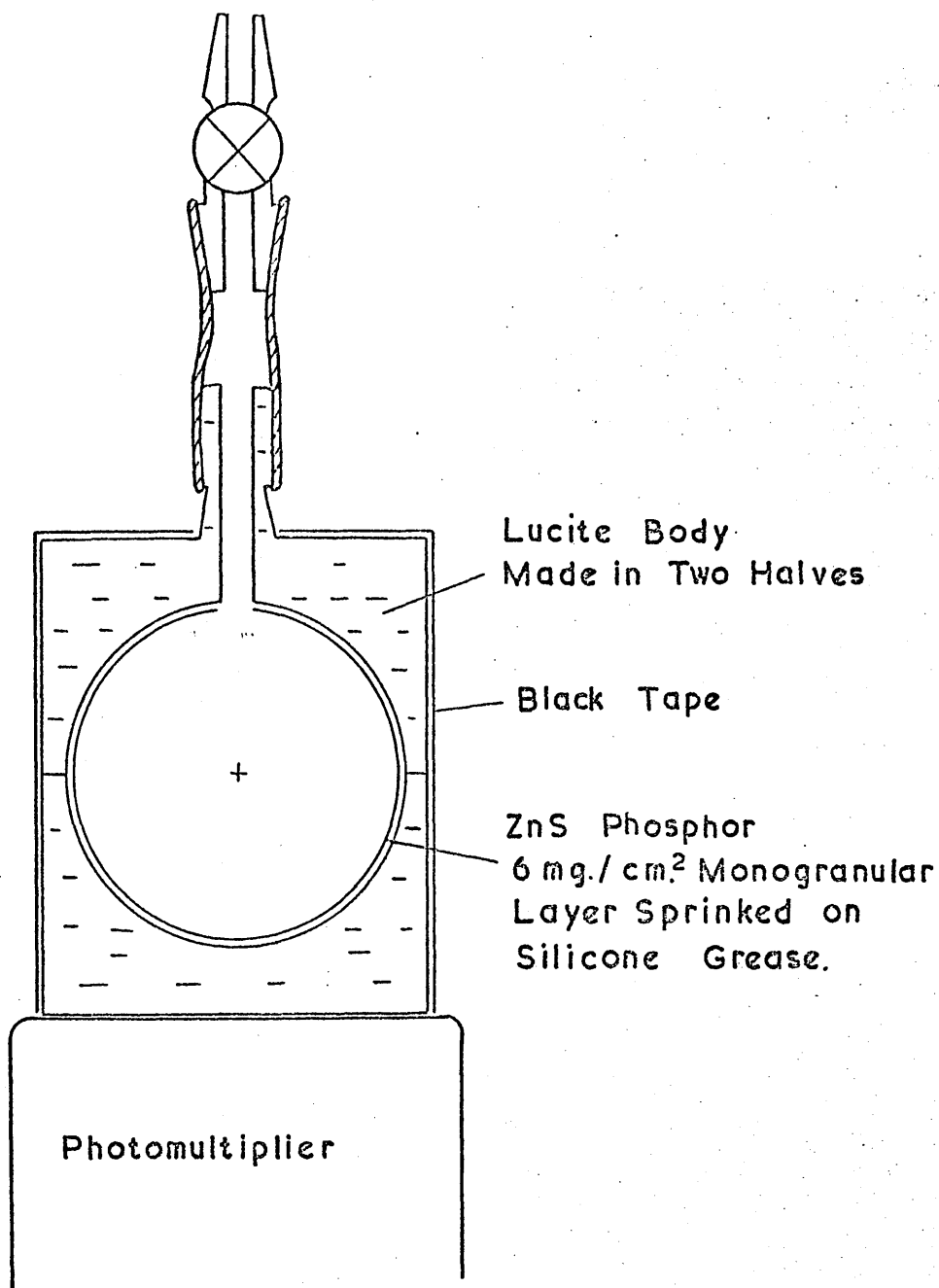


Figure 18: Protactinium alpha spectrum from a sediment sample.



Internal Diameter 45 mm.
Capacity 48 cm³

Figure 19: Radon Counting Vessel.

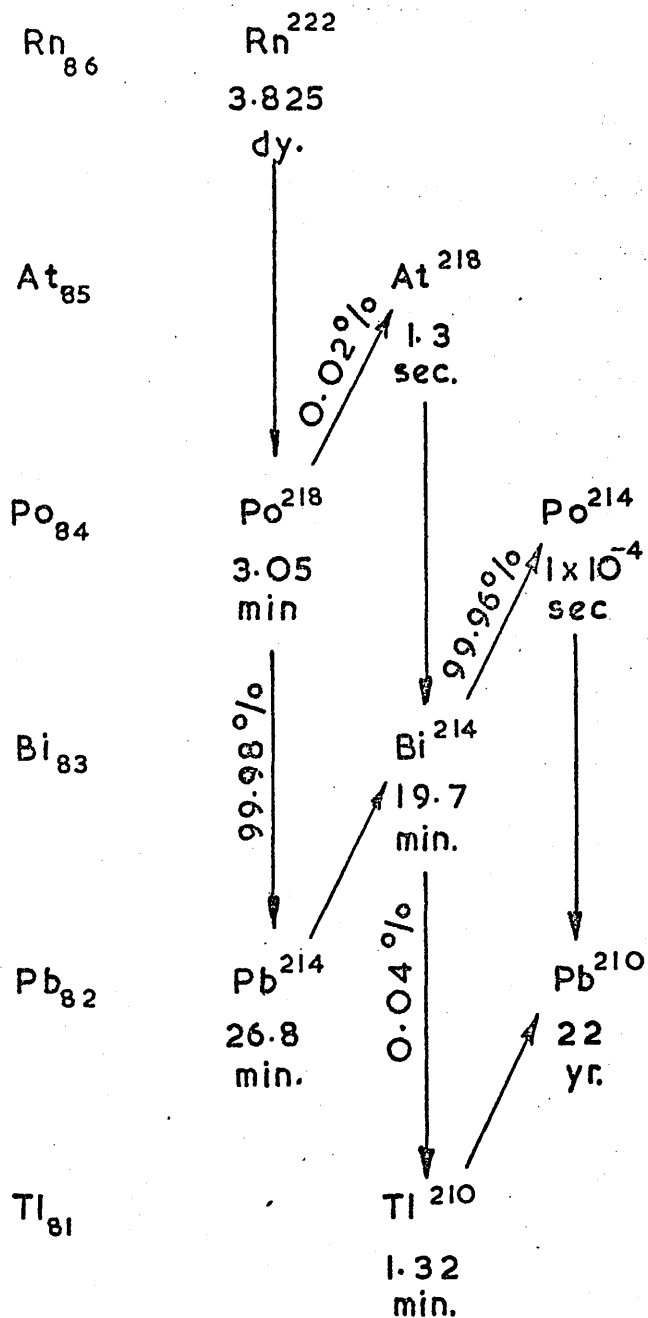


Figure 20:

 Rn^{222} and daughter nuclides.

screwed over the detector on to the photomultiplier housing to exclude light. The associated electronics consisted of a White cathode follower (Ekco Electronics Ltd., Southend; 691A), amplifier (Ekco; 640A) and scaler with H.V. supply and discriminator (Ekco; 529D). The system had a plateau 200V. long, with a slope of 0.5% per 100V. (Figure 21), and all detectors were counted at 725V., the midpoint of the plateau. The system was operated at minimum gain (X25), with a discriminator level of 1.5V.

Under these conditions, the background of all 3 detectors used was 0.4 c.p.m., due mainly to impurities in the ZnS (Ag) phosphor. Each detector was calibrated for combined system separation and detection efficiency by separating and counting solutions containing 52 d.p.m. Ra²²⁶ (calculated as Rn²²² plus 2 daughters). The overall efficiency for each detector was different, with mean values and standard deviations as shown in Table 1.

The radioactive daughters of Rn²²² were not removed by the preliminary evacuation. Therefore vessels were not counted until 3 hours after filling to allow secular equilibrium between radon and supported daughters to be established. The vessel was placed on the photomultiplier tube some time before this, however, because of a slight memory effect when the photomultiplier tube had been exposed to light.

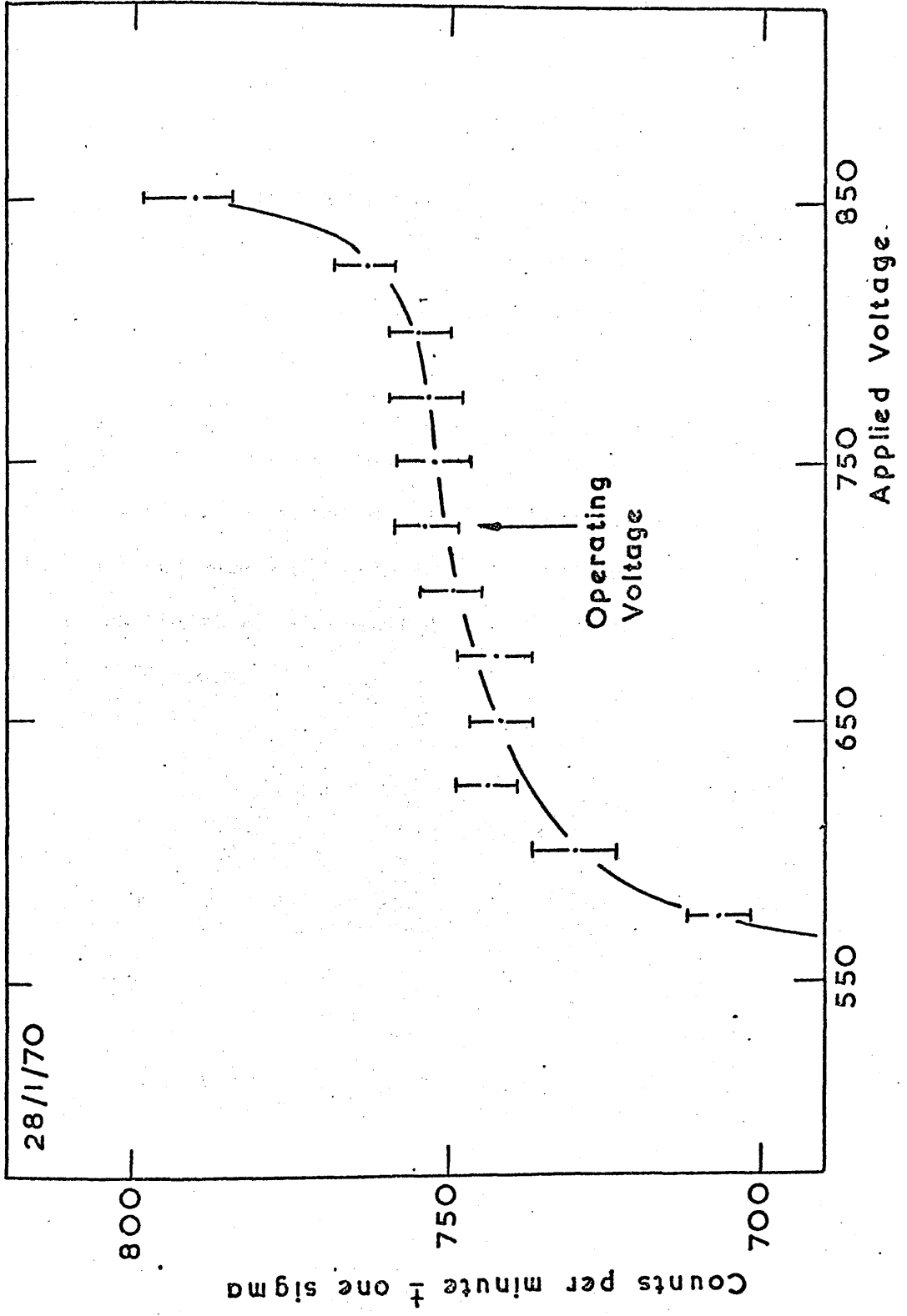


Figure 21: Radon counter plateau.

For each sample, more than 2,000 counts were recorded, reducing the uncertainty on the count to less than 2.5%. Repeated analyses on the same sample and results from duplicated samples indicated that individual analyses were good to better than $\pm 10\%$, but most samples were separated more than once, further reducing the uncertainty.

Background determinations were made by separating a solution of 25 ml. distilled water plus 175 ml. $\text{BaCl}_2/6\bar{\text{N}} \text{HCl}$. Count rates thus obtained were similar to the inherent background of the detectors (Table 2) and resulted in a background correction of 0.38 ± 0.09 c.p.m.

efficiency

64.4

60.7

64.6

TABLE 1.

Radon Detector Separation and Counting Efficiencies.

| Counting Vessel | V1 | V2 | V3 |
|-----------------------|------|------|------|
| | 63.1 | 39.2 | 54.7 |
| | 63.6 | 40.2 | 56.8 |
| | 65.5 | 38.2 | 55.1 |
| Combined separation | 65.2 | 40.2 | 52.9 |
| and counting | | 37.7 | 55.5 |
| efficiencies. | | 43.5 | 53.6 |
| | | 47.4 | 53.4 |
| | | 39.4 | |
| | | 38.0 | |
| | | 42.5 | |
| Mean efficiency | 64.4 | 40.7 | 54.6 |
| Standard deviation on | 1.2 | 2.8 | 1.4 |
| each separation | | | |

TABLE 2.

Radon Detector Background and Blank Count Rates.

| | | |
|-----------------------|-----------|-------------|
| Blank count rate | (6/2/70) | 0.43 c.p.m. |
| | (13/2/70) | 0.26 c.p.m. |
| | (20/2/70) | 0.42 c.p.m. |
| | (27/2/70) | 0.30 c.p.m. |
| | (6/3/70) | 0.35 c.p.m. |
| | (12/3/70) | 0.40 c.p.m. |
| Background count rate | (4/3/70) | 0.50 c.p.m. |

| | | |
|----------------------------|--|-------------|
| Mean count rate | | 0.38 c.p.m. |
| Root mean square deviation | | 0.09 c.p.m. |

2.5 Standards and Spikes for Radiochemical Analysis.

(a) U^{232} - Th^{228} spike.

This alpha spike was selected because it yielded uranium and thorium isotope activities directly without calibration of the S.B. detectors or knowledge of chemical yield, and thus avoided beta counting of tracers and samples. These considerations are important because the overall efficiency of the S.B. detectors, with their small active area, depends on the localisation of material on the source. Also, difficulties occur in the analysis of beta active uranium and thorium isotopes because of their complex decay schemes and the necessity to reproduce similar mounts for accurate beta counting. These factors outweighed the disadvantages of the method, which were:

- i) the absolute activity of the spike (d.p.m./ml.) and the Th^{228}/U^{232} activity ratio had to be known accurately.
- ii) corrections, sometimes quite large, had to be made to the Th^{228} peak sum, increasing the statistical uncertainty on thorium analyses (see Section 2.6a).

The calibrated spike solution was obtained from Dr. A. Kaufman, Lamont-Doherty Geological Observatory, Columbia University, New York.

A neutron bombardment procedure was used to produce U^{232} , and uranium purification was performed in January, 1950. Kaufman (1964) has determined the activity of the spike solution by alpha spectrometry. U^{238} and Th^{230} standards were used to calibrate U^{232} and Th^{228} respectively, with agreement within experimental error between the experimental and calculated activity ratio. The theoretical activity ratio was also confirmed by comparison of the U^{232} and Th^{228} activities against the U^{238} and Th^{230} activities of a concordant uraninite.

The spike had an activity of 5.4 d.p.m./ml. in August, 1968, when the activity ratio Th^{228}/U^{232} equalled 1.03, the transient equilibrium value. It was stored carrier free in $8N HNO_3$ in a Pyrex flask. Two aliquots of the solution were taken, Fe (III) and Al (III) carriers were added, and uranium and thorium separated by ion exchange according to the procedures described in Sections 2.3d and 2.3e. The uranium mounts exhibited an alpha contribution from U^{233} falling in the U^{234} peak region, with a U^{233}/U^{232} activity ratio of 0.022, confirming the value found by Ku (1966). The thorium mounts showed no contamination in the Th^{232} or Th^{230} peak regions.

(b) Pa^{233} Spike.

Pa^{233} ($t_{1/2}$ 27.4 days) was selected as the tracer for Pa^{231}

analyses because it is the protactinium isotope with the next longest half life to Pa²³¹. The spike was obtained by milking Pa²³³ from its parent, Np²³⁷. Approximately 10mg. neptunium oxide were obtained from the Radiochemical Centre, Amersham (Code NGS 1) and dissolved in concentrated HNO₃ with a few mg. KBrO₃ added. The solution was heated to dryness and the residue dissolved in a mixture of 2 ml. concentrated H₂SO₄ and 10 ml. concentrated HCl, and purified by 3 cycles of extraction into D.I.B.C. as described for sample analysis (Section 2.3f). The purified Pa²³³ was stored in 12N HCl/0.1N HF in a thick-walled polyethylene bottle. Radiochemical purity of the Pa²³³ was checked by following the decay of the 4 tracer discs over 3 months ($t_{\frac{1}{2}} = 27.3$ days cf. 27.4 days, Lederer et al., 1967), and by alpha spectrometry of the discs, which showed no alpha active impurity.

(c) Ra²²⁶ Standards.

Three standards, each containing 52 d.p.m. Rn²²² plus daughters at equilibrium, were prepared. An Ra²²⁶ standard (National Bureau of Standards, Washington; No. 4950A, containing 10⁻⁹ g. Ra²²⁶ ± 0.15%) was diluted to 250ml. with distilled H₂O. Aliquots of 2 ml. from this solution were made up to 200 ml. with 23 ml. distilled water and 175 ml. BaCl₂/6N HCl solution in equilibration flasks. Standards were separated and counted in exactly the same way as samples.

2.6 Treatment of Data.

(a) Uranium and Thorium Spectra.

Alpha spectrometric peaks obtained from uranium and thorium mounts (Figures 12 to 15) were normally asymmetric, with a sharp high energy cutoff and a low energy tail. This was due partly to the fine structure of the alpha emissions of the nuclides analysed (Figure 6) and partly to source broadening. Nevertheless, the peaks were well resolved, with about 36 channels between U^{238} , U^{234} and U^{232} peak maxima, 45 channels between Th^{232} and Th^{230} , and 55 channels between Th^{230} and Th^{228} . Each peak was integrated by summing a 25 channel envelope which included 7 or 8 channels on the high energy side and 16 or 17 channels on the low energy side.

Integrations in uranium analyses were straightforward, the only correction being subtraction of 2.2% of the U^{232} peak sum from the U^{234} sum to allow for the U^{233} contribution (Section 2.5a). In thorium analyses, the only corrections made were to the Th^{228} peak sum, where the following assumptions were made:

- i) Th^{228} from the core material was in secular equilibrium with Th^{232} . This assumption should be affected only by Ra^{228} ($t_{\frac{1}{2}} = 6.7$ years) migration in the core. Thus the sum of the Th^{232} peak was subtracted from the total Th^{228} peak sum.

(Coral spectra did not require this correction, since they contained negligible Th^{232} .)

ii) 4.9% of the Ra^{224} alphas fell in the Th^{228} envelope (Lederer et al., 1967). The Ra^{224} peak total was therefore multiplied by 0.052 and this figure also subtracted from the total Th^{228} peak.

The disintegration rates of the natural uranium and thorium isotopes were calculated by multiplying their ratios relative to U^{232} or Th^{228} respectively by the known activities of the added tracers. From this absolute activity, the disintegration rates were expressed in d.p.m./g. sample, and uranium and thorium concentrations converted to p.p.m. (i.e. ug./g.) using the values of 4.51×10^9 years and 1.39×10^{10} years for the half lives of U^{238} and Th^{232} respectively (Lederer et al., 1967).

The unsupported Th^{230} activity, ($\text{Th}_{\text{excess}}^{230}$), was calculated as (d.p.m./g. Th^{230} - d.p.m./g. U^{234}). A typical sample calculation is included in Appendix 2.

(b) Protactinium Data.

Protactinium alpha count rates were converted to Pa^{231} disintegration rates using the formula:

$$\text{d.p.m. Pa}^{231} = \frac{\text{c.p.m. Pa}^{231} - \text{background}}{\text{chemical yield} \times \text{counting efficiency}}$$

From this value, the Pa^{231} absolute activity was expressed as d.p.m./g. sample. The unsupported Pa^{231} activity, ($\text{Pa}_{\text{excess}}^{231}$), was calculated using the relationship:

$$(\text{Pa}_{\text{excess}}^{231}) = (\text{d.p.m./g. Pa}^{231} - 0.046 \times \text{d.p.m./g. U}^{238}),$$

assuming the activity ratio $\text{U}^{235}/\text{U}^{238} = 0.046$ (Strominger et al., 1958). A typical sample calculation is reproduced in Appendix 2.

(c) Radium Data.

Count rates determined from Rn^{222} separates were corrected for background and for the time elapsed between separation and counting. Normally this was the time between separation and the midpoint of the counting time, but if the counting period exceeded 12 hours, a shorter time, calculated by the method of Hoffman and Van Camerik (1967), was used to allow for decay during counting. A graph was prepared to show the percentage Rn^{222} remaining after this period.

Corrected count rates were then converted to disintegration rates using the appropriate overall efficiency of the counting vessel. From a graph of Rn^{222} buildup towards secular equilibrium with Ra^{226} during storage, this rate was normalised to the Rn^{222} equilibrium disintegration rate. Division by 3 gave the Ra^{226} activity in solution, from which the activity (d.p.m./g.) in the

sediment was calculated. The half life of Ra²²⁶ used in the calculation was 1622 years (Ramthun, 1966). A typical sample calculation is included in Appendix 2.

2. 7. Errors and Reproducibility.

(a) Analytical Errors.

Any analytical procedure has an inherent error associated with measurement processes, e.g. pipetting or weighing. In the present case, such errors exist only in measurement of:

- i) the volume of tracer added. Aliquots of 1 ml. were delivered from pipettes of better than 1% tolerance.
- ii) the mass of sample. All weighings were made to 4 decimal places, so that even for small (5 g.) samples the error was considerably less than 1%.

These errors were considered insignificant relative to the statistical errors associated with activity determinations (cf. Table 6). Nevertheless precautions were taken as follows to ensure accurate analysis:

- i) during sample pretreatment, care was taken to avoid contamination by extraneous material: grinding was carried out using a tungsten carbide mill, sieving with a Perspex sieve and nylon boltcloth.
- ii) during preliminary acid treatment of tared samples, effervescence was controlled to avoid sample loss before spike addition.

iii) mechanical loss of insoluble residues before total dissolution was avoided.

All spike methods hinge on equilibration of tracer and sample isotopes. In the case of sediment samples this was ensured by heating the partial solution with added spike to dryness (Section 2.3a), and for coral samples by total dissolution before spike addition with subsequent prolonged heating in $8N$ HNO_3 (Section 2.3b).

Another possible source of error was addition of contamination from reagents or glassware. To this end, blanks were run for uranium, thorium and protactinium as follows: Fe (111) and Al(111) carriers were added to 1 ml. aliquots of the respective tracers and the blanks treated alongside authentic samples with the same quantities of reagents at every stage. The apparatus employed for these blank analyses had been used in many cycles of sample analysis, so this also served as a check on the decontamination procedure. The protactinium mount thus obtained showed no alpha activity above background, while the uranium and thorium mounts, with typical tracer yields, had alpha activities of around 8 counts per day in the U^{238} and U^{234} regions and 15 to 20 counts per day in the Th^{232} and Th^{230} peak regions (Tables 3 and 4). These values in uranium and thorium spectra were small by comparison with the peak sums normally recorded on sample mounts (Section 2.6a), and in a small (5 g.) sample would

TABLE 3.

Protactinium Blank Analysis

| Sample | Date | Count Period (minutes) | Count | Rate (c.p.m. \pm 1 Sigma) |
|-------------------------|---------|---------------------------|-------|--------------------------------|
| Planchette | 26/8/70 | 4325 | 72 | 0.017 \pm 0.002 |
| Pa ²³¹ blank | 30/8/70 | 1290 | 20 | 0.016 \pm 0.003 |
| Planchette | 8/9/70 | 5894 | 87 | 0.015 \pm 0.001 |

TABLE 4.

Uranium and Thorium Blank Analysis,

(1440 minute counts, 25 channel integrations.)

| Isotope | Blank (24/2/70) | Background (26/2/70) | Yield % | D.p.m. | D.p.m./5g. |
|-------------------|--------------------|-------------------------|------------|--------|------------|
| U ²³⁸ | 8 | 1 | - | 0.036 | 0.007 |
| U ²³⁴ | 8.5 | 1 | - | 0.038 | 0.008 |
| U ²³² | 1181 | 6 | 63 | 5.4 | - |
| Th ²³² | 19 | 6 | - | 0.082 | 0.015 |
| Th ²³⁰ | 14 | 5 | - | 0.061 | 0.012 |
| Th ²²⁸ | 1284 | 10 | 67 | 5.56 | - |

have been interpreted as 0.007 d.p.m./g. U^{238} and 0.015 d.p.m./g. Th^{232} .

The possibility of a systematic error in the analyses arising from an error in the calibration of the $U^{232} - Th^{228}$ spike was recognised. Two well characterised samples were run, the Mississippi Spergen Limestone and a sample solution of the concordant uraninite K-120a (Table 5). The results show good agreement with previous studies of these samples, and, as a corollary, confirm the transient equilibrium condition of the spike solution.

(b) Counting uncertainties and errors.

Measurements of radioactive decay in a properly functioning counter exhibit fluctuations about the "average" behaviour predicted by the decay law. Since radioactive decay rates follow binomial distribution statistics, a single observation gives estimates of both the mean and the variance of the mean. If a reasonably large number of counts (N) are recorded in a time short by comparison with $t_{\frac{1}{2}}$ for the nuclide measured, then:

$$\sigma = N^{\frac{1}{2}}$$

$t_{\frac{1}{2}}$ is the half life

t is the count period

σ is the standard deviation of the mean.

TABLE 5.

Analytical Results on "Standard" Materials.

1. Uraninite K120-a.

| | U^{234}/U^{238} * | Th^{230}/U^{234} * |
|-----------|---------------------|----------------------|
| This work | 0.99 ± 0.01 | 1.01 ± 0.02 |
| Ku (1966) | 0.99 ± 0.01 | 1.01 ± 0.01 |

2. Mississippi Spergen Limestone

| | U^{234}/U^{238} * | Th^{230}/U^{234} * | U p.p.m. |
|------------------|---------------------|----------------------|-----------------|
| This work | 1.01 ± 0.01 | 1.03 ± 0.02 | 1.07 ± 0.02 |
| | 1.01 ± 0.01 | 1.02 ± 0.02 | 1.10 ± 0.02 |
| Ku (1966) | 1.02 ± 0.02 | 1.03 ± 0.03 | -- |
| Mo et al. (1971) | -- | -- | 1.02 to 1.10 |

* - Activity ratio.

In this work, all uncertainties quoted are 1 sigma errors calculated from counting data, except for CaCo_3 and NaCl determinations which were estimated from agreement between duplicate analyses (Sections 2.2c and 2.2d), and Ra^{226} data where the error includes standard deviations of the vessel efficiencies calculated from several standard separations (Section 2.6c). Errors were calculated by means of the formulae:

Error on a sum or difference

i.e. $f = (a + b)$ or $f = (a - b)$

$$\sigma_f = \left(\sigma_a^2 + \sigma_b^2 \right)^{\frac{1}{2}}$$

Error on a product or quotient

i.e. $f = (a \cdot b \cdot c)$ or $f = (a \cdot b / c)$.

$$\sigma_f = \left[f^2 \left(\frac{\sigma_a^2}{a^2} + \frac{\sigma_b^2}{b^2} + \frac{\sigma_c^2}{c^2} \right) \right]^{\frac{1}{2}}$$

A true counting error may exist in Pa^{231} analyses. Here the alpha detection efficiency of the N.M.C. proportional counter was obtained using the known activity of the flat, stainless steel calibrated Am^{241} source (AMR 22). The activity of the Pa^{233} tracer was determined from dimpled platinum tracer discs in the same counter. Both alpha and beta sample activities from Pa^{231} and Pa^{233} respectively were measured on dimpled stainless steel discs.

The possibility exists therefore, that a small difference in alpha detection efficiency may arise from different source geometries, and in beta detection efficiency as a result of different back-scattering from platinum and stainless steel. Unfortunately, small differences here could affect the small Pa²³¹ activities measured.

An attempt was made to assess this uncertainty as follows. The N.M.C. counter was calibrated relative to the U²³² - Th²²⁸ spike by evaporating 1 ml. aliquots of the spike on dimpled stainless steel planchettes. The observed activity, corrected for the counter efficiency, was from 91 to 94% of the theoretical value calculated as U²³² plus 5 supported alpha-active daughters with an activity ratio of 1.03. These slightly low values may be due to:

- i) some sputtering in the preparation of the spike mounts, and
- ii) alpha attenuation in the "thick" aqueous mounts.

(c) Reproducibility.

A stringent test of the reliability of an analytical method is the agreement between repeated analyses of the same material. Several samples were run in duplicate in this research, the results of which are shown in Table 6. Although separation yields were low during early stages of the work, resulting in lower count rates and poorer statistics, the replicate analyses agreed well within 1 sigma counting statistics. The results of a later duplicated coral

TABLE 6.

Results of Duplicate Analyses.

| Sample | U^{238} * | U^{234} * | $\frac{U^{234}}{U^{238}}$ + | Th^{232} * | Th^{230} * | $\frac{Th^{230}}{Th^{232}}$ + | Ra^{226} * |
|------------|-----------------|-----------------|-----------------------------|-----------------|-----------------|-------------------------------|-----------------|
| 642-650cm. | 1.09 ± 0.08 | 1.13 ± 0.09 | 1.03 ± 0.07 | 1.88 ± 0.10 | 1.53 ± 0.08 | 0.81 ± 0.02 | 1.21 ± 0.09 |
| | 1.01 ± 0.08 | 1.14 ± 0.09 | 1.13 ± 0.08 | 1.75 ± 0.12 | 1.37 ± 0.09 | 0.78 ± 0.03 | 1.46 ± 0.15 |
| | 0.78 ± 0.09 | 0.62 ± 0.08 | 0.81 ± 0.08 | 1.32 ± 0.14 | 1.31 ± 0.14 | 1.00 ± 0.07 | --- |
| | 0.67 ± 0.07 | 0.55 ± 0.05 | 0.83 ± 0.08 | 1.17 ± 0.08 | 1.59 ± 0.11 | 1.08 ± 0.04 | --- |
| 450-456cm. | 1.08 ± 0.09 | 1.03 ± 0.08 | 0.95 ± 0.08 | 2.00 ± 0.13 | 1.84 ± 0.12 | 0.92 ± 0.03 | 2.19 ± 0.05 |
| | 1.01 ± 0.05 | 0.93 ± 0.05 | 0.92 ± 0.05 | 1.95 ± 0.16 | 1.67 ± 0.14 | 0.86 ± 0.03 | 1.84 ± 0.13 |
| | 0.81 ± 0.03 | 0.74 ± 0.03 | 0.90 ± 0.04 | 1.93 ± 0.13 | 2.08 ± 0.14 | 1.08 ± 0.04 | --- |
| 385-390cm. | 0.93 ± 0.05 | 0.75 ± 0.03 | 0.80 ± 0.04 | 1.75 ± 0.10 | 1.95 ± 0.11 | 1.11 ± 0.03 | --- |
| | 2.66 ± 0.03 | 2.89 ± 0.03 | 1.09 ± 0.01 | --- | 2.01 ± 0.03 | --- | --- |
| Corals 1,2 | 2.63 ± 0.03 | 2.91 ± 0.03 | 1.11 ± 0.01 | --- | 2.01 ± 0.03 | --- | --- |

* - Specific activity, d.p.m./g.

+ - activity ratio.

analysis are also given, where better statistics and excellent agreement were obtained. It is concluded that the uncertainty defined by the counting statistics represents the major uncertainty in the analytical procedure.

CHAPTER 3.RESULTS AND EVALUATION : V16-200.3. 1 Data Presentation

The results of the analyses on the 21 sections of core V16-200 are presented in Tables 7a and 7b. All errors associated with specific activities and isotopic activity ratios are derived from one sigma counting uncertainties only, except in the case of Ra²²⁶ analyses (Section 2.6c). In general, the errors on uranium and thorium concentrations are better than 5% and 7% respectively. The errors on calcium carbonate and salt determinations are better than 2% and 3% respectively, as derived from replicate analyses. The specific activities ($\text{Th}_{\text{excess}}^{230}$) and ($\text{Pa}_{\text{excess}}^{231}$) in the core are those of the isotopes unsupported by the corresponding quantities of their respective parents, U²³⁴ and U²³⁵, at the various depths.

TABLE 7a

Analytical Data on Core V16-200

| Depth Interval | U^{238} dpm/g | U^{234} dpm/g | Th^{232} dpm/g | Th^{230} dpm/g | Ra dpm/g | Pa ²³¹ dpm/g | CaCO ₃ wt. % | NaCl Wt. % | U^{*} ppm | Th^{*} ppm | $\frac{U}{Th}$ |
|----------------|--------------------|--------------------|---------------------|---------------------|----------------|----------------------------|----------------------------|---------------|----------------|-----------------|----------------|
| 5- 10 | 0.52 +0.02 | 0.51 +0.02 | 1.03 +0.04 | 8.63 +0.21 | 4.92 +0.36 | 0.34 +0.01 | 69.8 | 2.9 | 2.56 | 15.29 | 0.17 |
| 15- 20 | 0.60 +0.02 | 0.58 +0.02 | 1.30 +0.07 | 8.20 +0.38 | 5.19 +0.23 | 0.31 +0.01 | 65.9 | 2.6 | 2.55 | 16.64 | 0.15 |
| 25- 30 | 1.11 +0.03 | 1.04 +0.03 | 2.25 +0.09 | 7.43 +0.26 | 4.96 +0.24 | 0.32 +0.01 | 40.4 | 2.7 | 2.63 | 16.05 | 0.16 |
| 45- 50 | 0.99 +0.04 | 0.94 +0.04 | 2.33 +0.16 | 7.00 +0.46 | 6.96 +0.15 | 0.22 +0.01 | 38.3 | 1.3 | 2.22 | 15.67 | 0.14 |
| 75- 80 | 1.00 +0.02 | 0.97 +0.02 | 2.23 +0.12 | 6.14 +0.11 | 6.88 +0.17 | 0.23 +0.01 | 42.4 | 1.2 | 2.39 | 16.07 | 0.15 |
| 105-110 | 1.04 +0.03 | 0.99 +0.03 | 1.54 +0.11 | 3.85 +0.28 | 10.01 +0.33 | 0.18 +0.01 | 43.0 | 1.5 | 2.54 | 11.27 | 0.23 |
| 150-155 | 1.19 +0.05 | 1.09 +0.05 | 2.40 +0.23 | 5.47 +0.51 | 5.67 +0.41 | 0.20 +0.01 | 26.6 | 1.4 | 2.24 | 13.54 | 0.17 |
| 180-185 | 1.06 +0.04 | 0.97 +0.04 | 2.04 +0.09 | 4.27 +0.17 | 3.64 +0.13 | 0.12 +0.01 | 34.6 | 2.1 | 2.26 | 13.11 | 0.17 |
| 220-225 | 0.71 +0.02 | 0.73 +0.02 | 1.40 +0.07 | 2.95 +0.14 | 3.27 +0.28 | 0.12 +0.01 | 53.6 | 1.7 | 2.15 | 12.72 | 0.17 |
| 260-265 | 0.67 +0.05 | 0.63 +0.05 | 1.69 +0.08 | 2.95 +0.13 | 2.49 +0.11 | 0.12 +0.01 | 50.5 | 1.5 | 1.90 | 14.29 | 0.13 |

TABLE 7a (continued)

| | | | | | | | | | | | |
|---------|---------------|---------------|---------------|---------------|---------------|---|-------|------|------|-------|------|
| 280-285 | 0.74 +0.03 | 0.70 +0.02 | 1.61 +0.08 | 2.91 +0.15 | 3.96 +0.10 | — | 50.0 | 1.0 | 2.04 | 13.34 | 0.15 |
| 310-315 | 0.85 +0.03 | 0.80 +0.03 | 1.63 +0.10 | 2.21 +0.13 | 3.47 +0.19 | | 42.8 | 3.4 | 2.14 | 12.31 | 0.17 |
| 385-390 | 0.84 +0.03 | 0.74 +0.02 | 1.82 +0.08 | 2.00 +0.09 | 1.86 +0.20 | | 41.4 | 1.2 | 1.99 | 12.88 | 0.15 |
| 450-458 | 1.03 +0.04 | 0.96 +0.04 | 1.98 +0.10 | 1.77 +0.09 | 2.04 +0.07 | | 28.2 | 2.7 | 2.01 | 11.63 | 0.17 |
| 480-486 | 0.43 +0.08 | 0.39 +0.05 | 0.90 +0.05 | 1.23 +0.06 | 1.38 +0.10 | | 67.8 | 2.3 | 1.94 | 12.19 | 0.16 |
| 552-560 | 0.71 +0.06 | 0.57 +0.04 | 1.21 +0.07 | 1.48 +0.09 | 1.51 +0.09 | | 50.3 | 0.8 | 1.97 | 10.06 | 0.20 |
| 642-650 | 1.05 +0.06 | 1.13 +0.06 | 1.83 +0.08 | 1.45 +0.06 | 1.35 +0.09 | | 39.7 | 2.3 | 2.45 | 12.80 | 0.19 |
| 712-720 | 0.87 +0.03 | 0.70 +0.03 | 2.17 +0.09 | 1.26 +0.05 | 1.39 +0.08 | | 44.5 | 2.2 | 2.21 | 16.53 | 0.13 |
| 783-790 | 0.95 +0.03 | 0.82 +0.02 | 1.86 +0.13 | 0.98 +0.07 | 1.86 +0.18 | | 41.9 | 1.2 | 2.25 | 13.27 | 0.17 |
| 850-857 | 1.09 +0.03 | 0.95 +0.03 | 1.69 +0.14 | 0.84 +0.07 | - | | 32.6 | 2.3 | 2.26 | 10.53 | 0.21 |
| 922-927 | 1.48 +0.05 | 1.64 +0.05 | 2.12 +0.15 | 1.91 +0.13 | 1.73 +0.12 | | 39.7 | 2.0 | 3.43 | 14.77 | 0.23 |
| Mean | | | | | | | 44.95 | 1.92 | 2.29 | 13.57 | 0.17 |

* On a CaCO₃ and NaCl free basis.

Table 7b

Analytical Data on Core V16-200 (continued)

| Depth Interval | $\frac{U^{234}}{U^{238}}$ | $\frac{Th^{230}}{U^{234}}$ | Ra 226 $\frac{Th^{230}}$ | Th 230 excess dpm/g | Pa 231 excess dpm/g | Pa 231 excess dpm/g | Th 230 excess $\frac{Th^{230}}{Pa^{231}}$ | Th 230 excess | |
|----------------|---------------------------|----------------------------|-----------------------------|---------------------------|---------------------------|---------------------------|---|--------------------|-------------------|
| 5- 10 | 0.98 ± 0.04 | 16.92 ± 0.78 | 0.57 ± 0.04 | 8.12 ± 0.21 | 26.9 ± 0.8 | 0.32 ± 0.01 | 1.06 ± 0.03 | 7.88 ± 0.37 | 25.5 ± 0.7 |
| 15- 20 | 0.97 ± 0.04 | 14.14 ± 0.81 | 0.63 ± 0.04 | 7.62 ± 0.38 | 22.3 ± 1.2 | 0.28 ± 0.01 | 0.82 ± 0.04 | 5.86 ± 0.43 | 27.1 ± 1.8 |
| 25- 30 | 0.94 ± 0.03 | 7.14 ± 0.32 | 0.67 ± 0.04 | 6.39 ± 0.26 | 10.7 ± 0.5 | 0.27 ± 0.01 | 0.45 ± 0.01 | 2.84 ± 0.16 | 23.9 ± 1.2 |
| 45- 50 | 0.95 ± 0.04 | 7.45 ± 0.58 | 1.00 ± 0.07 | 6.06 ± 0.46 | 10.4 ± 0.8 | 0.18 ± 0.01 | 0.29 ± 0.01 | 2.60 ± 0.27 | 34.0 ± 2.6 |
| 75- 80 | 0.97 ± 0.02 | 6.32 ± 0.17 | 1.12 ± 0.04 | 5.17 ± 0.11 | 8.98 ± 0.30 | 0.18 ± 0.01 | 0.32 ± 0.01 | 2.32 ± 0.13 | 28.3 ± 1.0 |
| 105-110 | 0.95 ± 0.03 | 3.88 ± 0.31 | 2.60 ± 0.21 | 2.86 ± 0.28 | 5.02 ± 0.50 | 0.13 ± 0.01 | 0.23 ± 0.01 | 1.88 ± 0.23 | 22.2 ± 2.2 |
| 150-155 | 0.92 ± 0.04 | 5.03 ± 0.52 | 1.03 ± 0.12 | 4.38 ± 0.51 | 5.97 ± 0.70 | 0.15 ± 0.01 | 0.20 ± 0.01 | 1.83 ± 0.28 | 29.6 ± 3.6 |
| 180-185 | 0.92 ± 0.04 | 4.40 ± 0.25 | 0.85 ± 0.05 | 3.30 ± 0.17 | 5.05 ± 0.28 | 0.07 ± 0.01 | 0.11 ± 0.01 | 1.62 ± 0.11 | 44.6 ± 3.3 |
| 220-225 | 1.03 ± 0.04 | 4.04 ± 0.22 | 1.11 ± 0.11 | 2.22 ± 0.14 | 4.78 ± 0.32 | — | — | 1.59 ± 0.13 | — |
| 260-265 | 0.94 ± 0.09 | 4.68 ± 0.43 | 0.84 ± 0.05 | 2.32 ± 0.14 | 4.69 ± 0.30 | — | — | 1.37 ± 0.11 | — |

Table 7b (continued)

| | | | | | | | |
|---------|---------------|---------------|---------------|----------------|----------------|---|----------------|
| 280-285 | 0.95 +0.04 | 4.16 +0.24 | 1.36 +0.08 | 2.21 +0.15 | 4.42 +0.31 | — | 1.37 +0.12 |
| 310-315 | 0.94 +0.03 | 2.76 +0.19 | 1.57 +0.13 | 1.41 +0.13 | 2.47 +0.23 | — | 0.87 +0.10 |
| 385-390 | 0.85 +0.03 | 2.70 +0.15 | 0.93 +0.12 | 1.26 +0.09 | 2.15 +0.16 | — | 0.69 +0.06 |
| 450-458 | 0.93 +0.04 | 1.79 +0.13 | 1.15 +0.07 | 0.87 +0.10 | 1.21 +0.14 | — | 0.44 +0.06 |
| 480-486 | 0.91 +0.09 | 3.15 +0.43 | 1.12 +0.10 | 0.84 +0.08 | 2.60 +0.25 | — | 0.93 +0.10 |
| 552-560 | 0.82 +0.06 | 2.52 +0.24 | 1.02 +0.09 | 0.91 +0.10 | 1.83 +0.20 | — | 0.75 +0.09 |
| 642-650 | 1.07 +0.05 | 1.27 +0.09 | 0.93 +0.07 | 0.32 +0.08 | 0.53 +0.13 | — | 0.17 +0.04 |
| 712-720 | 0.80 +0.03 | 1.80 +0.10 | 1.10 +0.08 | 0.56 +0.06 | 1.01 +0.11 | — | 0.26 +0.03 |
| 783-790 | 0.86 +0.03 | 1.20 +0.09 | 1.90 +0.24 | 0.16 +0.07 | 0.27 +0.12 | — | 0.09 +0.04 |
| 850-857 | 0.87 +0.02 | 0.88 +0.02 | — | -0.11 +0.07 | -0.16 +0.10 | — | -0.07 +0.04 |
| 922-927 | 1.11 +0.03 | 1.16 +0.09 | 0.91 +0.09 | 0.27 +0.14 | 0.45 +0.23 | — | 0.13 +0.07 |

3. 2 Natural Series Element Concentrations and Activity Ratios.

a) Uranium and Thorium Concentrations.

The uranium and thorium concentrations of the analysed sections of core V16-200, expressed as p.p.m. of total sediment, are plotted in Figure 22. A comparison of these distribution curves with the "calcium carbonate plus salt" profile of the core (Figure 23) shows a marked inverse relationship. If the elemental concentrations are expressed on a "carbonate and salt free" basis (Table 7b), the scatter in values is reduced, implying that both elements were transported primarily in the clay fraction. Mean values in the clay fraction of 2.29 ± 0.07 p.p.m. uranium, 13.57 ± 0.42 p.p.m. thorium, with a mean U/Th ratio of 0.17 are obtained, and there is no systematic trend in either concentration with depth.

These values agree closely with previously determined concentrations of the two elements in the clay fractions of pelagic sediments. Ku (1966) found 2.6 p.p.m. uranium, 13.4 p.p.m. thorium, with a mean U/Th ratio of 0.19 as the average values for pelagic clay from about 90 analyses on 11 cores. He concluded that there was no correlation of the two concentrations either with depth in the cores or with the clay sedimentation rates.

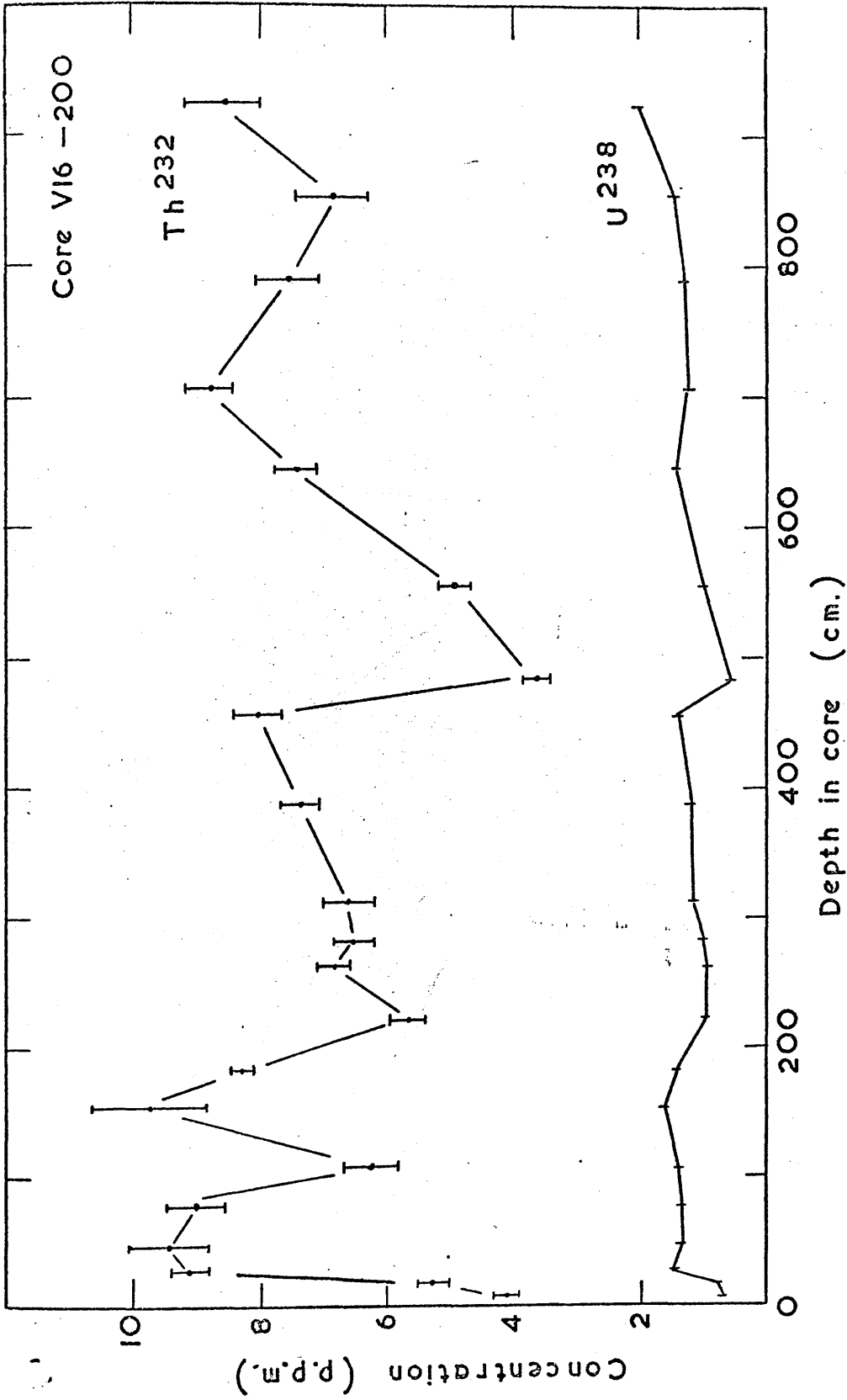


Figure 22: Uranium and thorium concentrations versus depth.

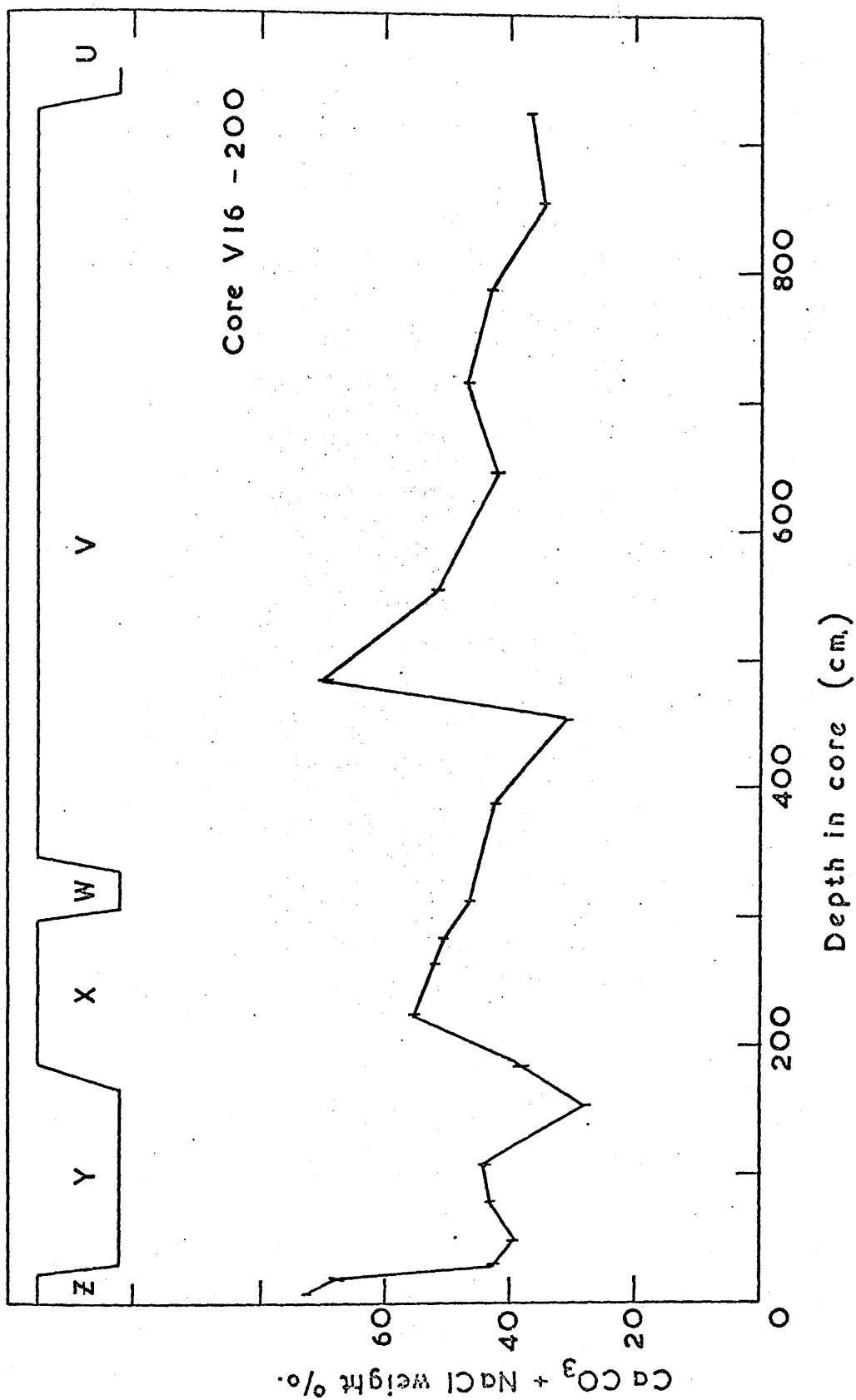


Figure 23: ¹⁴CaCO₃ + NaCl weight percentage versus depth.
 (Inset: Ericson's climatic curve.)

Heye (1969) calculated the mean U/Th ratio in pelagic clay to be 0.179 ± 0.005 from 134 analyses on 25 cores quoted in the literature.

The average values found in igneous rocks (Adams et al., 1959; Rogers and Adams, 1969) are 3.5 ± 0.5 p.p.m. uranium, 13.5 ± 1.5 p.p.m. thorium, with a U/Th ratio of around 0.29. Since clays are the ultimate weathered residues of igneous rocks after water-borne transportation, it appears therefore that more than one third of the total uranium is leached by weathering process during transport, while thorium is scarcely soluble at all. This is in accord with the known geochemistries of the elements. Whereas uranium is readily oxidised to the soluble U (VI), the Th (IV) ion is hydrated and precipitated in the conditions prevalent in ocean and river waters.

The results from core VI6-200 indicate that the clay fraction has consistent uranium and thorium concentrations at all depths. Indirect support for this homogeneity of the clay comes from the studies of Murray (1970) and Bowles (1970), who examined tropical North Atlantic and equatorial Atlantic cores respectively. Both workers found a uniform clay composition, in respect of both mineralogy and size, over an inferred period of up to 1 million years B.P.

b) U^{234}/U^{238} Activity Ratios.

The determined values of the U^{234}/U^{238} activity ratios in core V16-200 (Table 7b) range from 0.80 to 1.11, with a mean value of 0.94 ± 0.02 , and again no progressive trend with depth is evident. Heye's (1969) compilation resulted in a mean U^{234}/U^{238} activity ratio of 0.925 ± 0.006 for pelagic sediments, derived from analyses of core samples at various depths. A deficiency of U^{234} compared with the secular equilibrium value of the ratio, 1.00, therefore exists in core V16-200 and other sediments. This phenomenon of uranium isotope fractionation in the marine environment has been extensively studied in recent years.

Most of the uranium in V16-200 is detrital and contained in the clay fraction, but other sediment types may also contain authigenic uranium precipitated from sea water. The initial U^{234}/U^{238} activity ratio of authigenic uranium should be 1.15 ± 0.02 , the value found in recently formed oolites, corals and open ocean water (Thurber, 1962; Koide and Goldberg, 1965). Thus, in general, the U^{234}/U^{238} activity ratio in freshly deposited sediment is dependent on the relative quantities of detrital and authigenic uranium, and on the initial activity ratio in the detrital component. If these contributions remain constant in time, and the resultant sediment forms a chemically closed system, then the secular equilibrium value

of the U^{234}/U^{238} ratio will be attained at depth after times long compared with the half life of U^{234} (2.48×10^5 yr.). Ku (1965) evaluated this possible geochronological use of the U^{234}/U^{238} ratio by analysis of three highly homogenous red clay cores with low sedimentation rates. The results of this study are best illustrated by the North Atlantic core V10-95, in which the ratio decreased from a surface value of 0.95 through a minimum of 0.80, then gradually increased towards 1.00 with depth. Ku explained this profile in terms of upward migration of a fraction of the U^{234} atoms through the sediment, with a constant loss of U^{234} at the sediment-water interface. An equation was formulated to generate the profile in terms of 3 parameters : S, the sedimentation rate; D, the diffusion coefficient; and F_m , the (constant) fraction of the U^{234} produced which was free to diffuse. The three cores studied had different sedimentation rates and diffusion rates, but in each F_m equalled 30%.

The significance of this value was explained by Kolodny and Kaplan (1970) who attempted to date an extensive collection of phosphorite nodules from widely spaced localities of the sea floor. Phosphorite contains reasonably high concentrations of authigenic uranium (50 to 200 p.p.m.), with variable proportions of both oxidation states present, i.e. U (IV) and U (VI).

Analyses were performed on each nodule to determine the U^{234}/U^{238} activity ratios and uranium concentrations in the whole sample and in the U (IV) fraction. The values for the U (VI) fraction could then be calculated. The results showed distinctly different U^{234}/U^{238} activity ratios in the U (VI), total uranium, and U (IV) fractions. Mean values of the ratios found were as follows:

| | | |
|-----------------|---|-----------------|
| U (VI) fraction | : | 1.57 ± 0.40 |
| total uranium | : | 0.97 ± 0.04 |
| U (IV) fraction | : | 0.71 ± 0.06 |

Thus the U (IV) in phosphorite was visualised, not as a chemically closed system, but as a semi-closed, "valve-type" system, to which no uranium could be added, but from which U^{234} could escape.

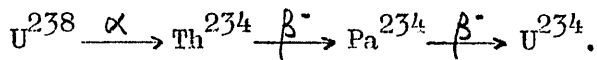
With the assumptions that:

- i) a fraction R of radiogenic U^{234} in the U (IV) fraction of phosphorite is oxidised to U (VI),
- ii) this fraction remains constant with time,
- iii) any oxidation process not related to radioactive decay does not distinguish between U^{234} and U^{238} ,

Kolodny and Kaplan showed that their results could be explained with a value of R equal to 0.3. A phosphorite which formed with a U^{234}/U^{238} activity ratio of 1.15, solely in the form U (IV), may be calculated to attain a U^{234}/U^{238} ratio of 1.00 after only 200,000

years, if 30% of the U^{234} were oxidised to U (VI), rather than the corresponding closed system time of over 1 million years.

The mechanism for the uranium isotopic fractionation is postulated to be relocation of daughter U^{234} atoms in a lattice by recoil and radiation damage during the decay sequence:



As a result of this displacement, the U^{234} atoms are more readily oxidised than the U^{238} parent (Cherdyntsev et al., 1955; Starik et al., 1958; Kolodny and Kaplan, 1970).

In the case of core V16-200 and the clay cores studied by Ku (1965), the mechanism for migration of U^{234} is possibly oxidation to U (VI) followed by complexing to the soluble uranyl carbonate. Any U (VI) which is not locked in mineral grains is probably leached before deposition occurs. It is suggested that given "normal" deep sea conditions and sufficient time, about one third of the radiogenic U^{234} will be in the mobile U (VI) oxidation state.

The profile of U^{234}/U^{238} activity ratios down core V16-200 is quite different from those found by Ku (1965). This may be due to the erratic detrital mineral fraction of this core (i.e. the inverse of the "calcium carbonate plus salt" profile (Figure 23)), because this fraction contains most of the total uranium.

Ku's model assumed a constant upward diffusion of U^{234} in the sediment column. It was recognised, however, that the low value calculated for the diffusion coefficient implied that the mobile U^{234} was exchanged between pore water and mineral grains many times during migration. Thus the ideal profile is not found if local differences in absorption occur, and Ku (1966) did not find a regular trend in two long globigerina ooze cores, V12-122 from the Caribbean Sea and V9-29 from the equatorial Atlantic Ocean. The mean value of 0.94 ± 0.02 found for the U^{234}/U^{238} activity ratio in core V16-200 indicates that fractionation has taken place, but it is impossible to calculate the relative contributions of fractionation during transport and in the sediment column itself.

c) (Th_{excess}^{230}) Specific Activities and Th^{230}/U^{234} Activity Ratios.

The Th^{230} specific activity in V16-200 again has two sources, one fraction being authigenically removed from ocean water, the other being contained in the detrital fraction. In this case the authigenic (Th_{excess}^{230}) contribution is greater than the unsupported detrital contribution.

Scott (1968) studied size fractions of sediments from five rivers of the east and south coasts of the U.S.A., and determined the specific activities of U^{238} , U^{234} , Th^{232} and Th^{230} . The small size fractions analysed (less than 0.2 to 2 μm .) may be considered

analogous with the terrigenous component of pelagic sedimentation, although the uranium concentrations found (2.4 to 4.8 p.p.m.) are somewhat higher than those found in pelagic clays (cf. Section 3.2a). Sediments from two of the rivers exhibited high organic contents, which were considered to have been derived from the surface layers of soil cover. Rosholt et al. (1966) have shown that organic rich surface layers may "fix" mobile uranium leached from lower levels of the soil profile, with consequent enrichment of U^{234} . The remaining three rivers had U^{234}/U^{238} activity ratios ranging from 0.83 to 0.96, Th^{230}/U^{234} activity ratios from 1.17 to 1.92, and unsupported Th^{230} activities from 0.41 to 2.21 d.p.m./g. Although it is clear that such isolated results must be treated with caution, Scott (1968) assumed a maximum (Th^{230}_{excess}) in clays of 0.5 d.p.m./g., and a deep sea accumulation rate for this component of $lg./cm./10^3 yr.$ The resultant value of 0.5 d.p.m. (Th^{230}_{excess})/ $10^3 yr.$ is to be compared with 8.8 d.p.m. (Th^{230}_{excess})/ $10^3 yr.$ deposited authigenically (based on a mean ocean depth of 3,800 m. and 3 $\mu g./l.$ uranium in sea water with a U^{234}/U^{238} activity ratio of 1.15 (Ku 1966)).

This combined unsupported Th^{230} activity is of prime importance in sedimentation rate estimation. The very properties which cause authigenic Th^{230} precipitation might be expected to ensure that Th^{230} does not suffer post-depositional migration. In fact, this conclusion has been confirmed by Bonatti et al. (1971) who analysed an East Pacific hemipelagic core in which oxidation-reduction phenomena had caused migration of uranium and several transition metals, and by Bernat

and Goldberg (1968) who analysed samples representing the total sediment, the detrital clay fraction, and the authigenic mineral phillipsite in a North Pacific clay core. Therefore, if the conditions of sedimentation have remained relatively constant, an exponential decrease in the $\text{Th}^{230}/\text{U}^{234}$ activity ratio with depth will occur towards the secular equilibrium value (1.00) with a "half life" of 107,000 years.

Figure 24 shows that the $\text{Th}^{230}/\text{U}^{234}$ ratio in core V16-200 exhibits a fairly regular exponential decrease. The "scatter" in the experimental values of the ratio is most likely a result of two factors:

- i) the variable fractions of carbonate and clay in the depth intervals analysed (Table 7a), and,
- ii) migration of U^{234} in the sediment column.

The variability of carbonate and clay contents presumably reflect climatically controlled changes in sedimentation with time. Ku and Broecker (1966) noted that the ($\text{Th}_{\text{excess}}^{230}$) data of Caribbean core V12-122 showed a more regular logarithmic decrease when plotted on a "carbonate-free" basis than on a "total sediment" basis. This implies either that authigenic Th^{230} is absorbed on to clays from sea water, or that the individual authigenic Th^{230} and terrigenous deposition rates are more constant than the biogenic carbonate deposition rate.

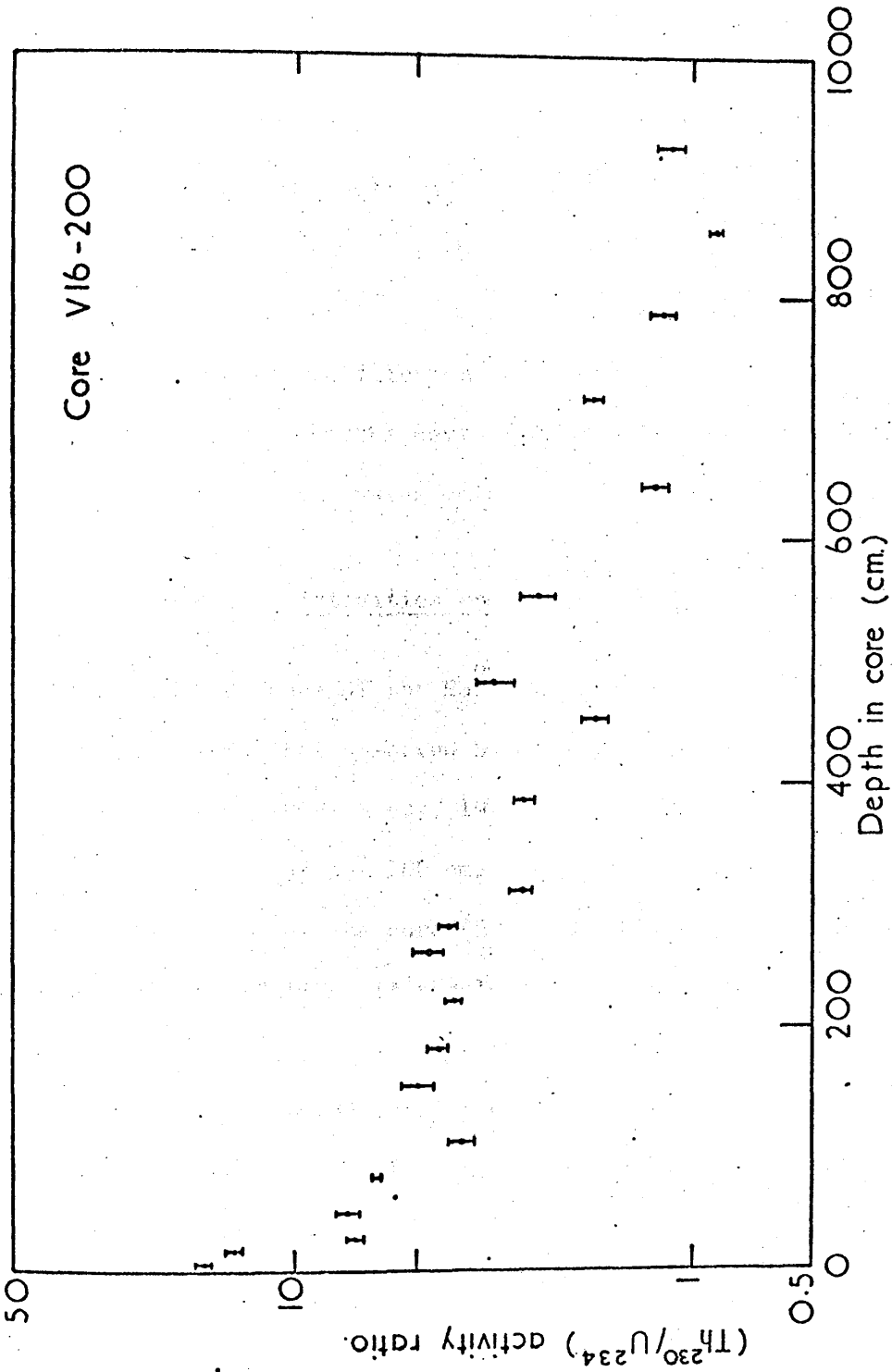


Figure 24. (Th²³⁰/U²³⁴) activity ratio versus depth.

As discussed in Section 3.2b, the U^{234}/U^{238} data indicate that U^{234} cannot follow a pattern of constant migration in core V16-200. The effect of this migration on the Th^{230}/U^{234} activity ratio is small in the upper reaches of the core where a large excess of Th^{230} exists, but as the specific activity of the unsupported Th^{230} decreases as secular equilibrium is approached with depth, U^{234} migration may cause further deviations of the ratio, in either sense, from the closed system value.

d) Ra^{226} Specific Activities and Ra^{226}/Th^{230} Activity Ratios.

The general shape of the Ra^{226} profile in core V16-200 (Figure 25) is similar to that observed by other workers (Urry and Piggot, 1942; Pettersson, 1949; Koczy, 1963). The maximum Ra^{226} specific activity exists at around 100 cm. in the core, whereas from the sedimentation rate of the core (2.20 cm./ 10^3 yr. : cf. Section 4.2b) and the Ra^{226} half life, it should be reached at about 22 cm. (6 half lives). This discrepancy can be explained by assuming that the Ra^{226} atoms diffuse, under the influence of a concentration gradient, in both directions away from the maximum level, and pass out through the surface sediment layer into the ocean at a constant rate (Koczy and Bourret, 1958).

It is evident that the Ra^{226} specific activities show some fluctuations from a smooth curve. A similar observation may be made

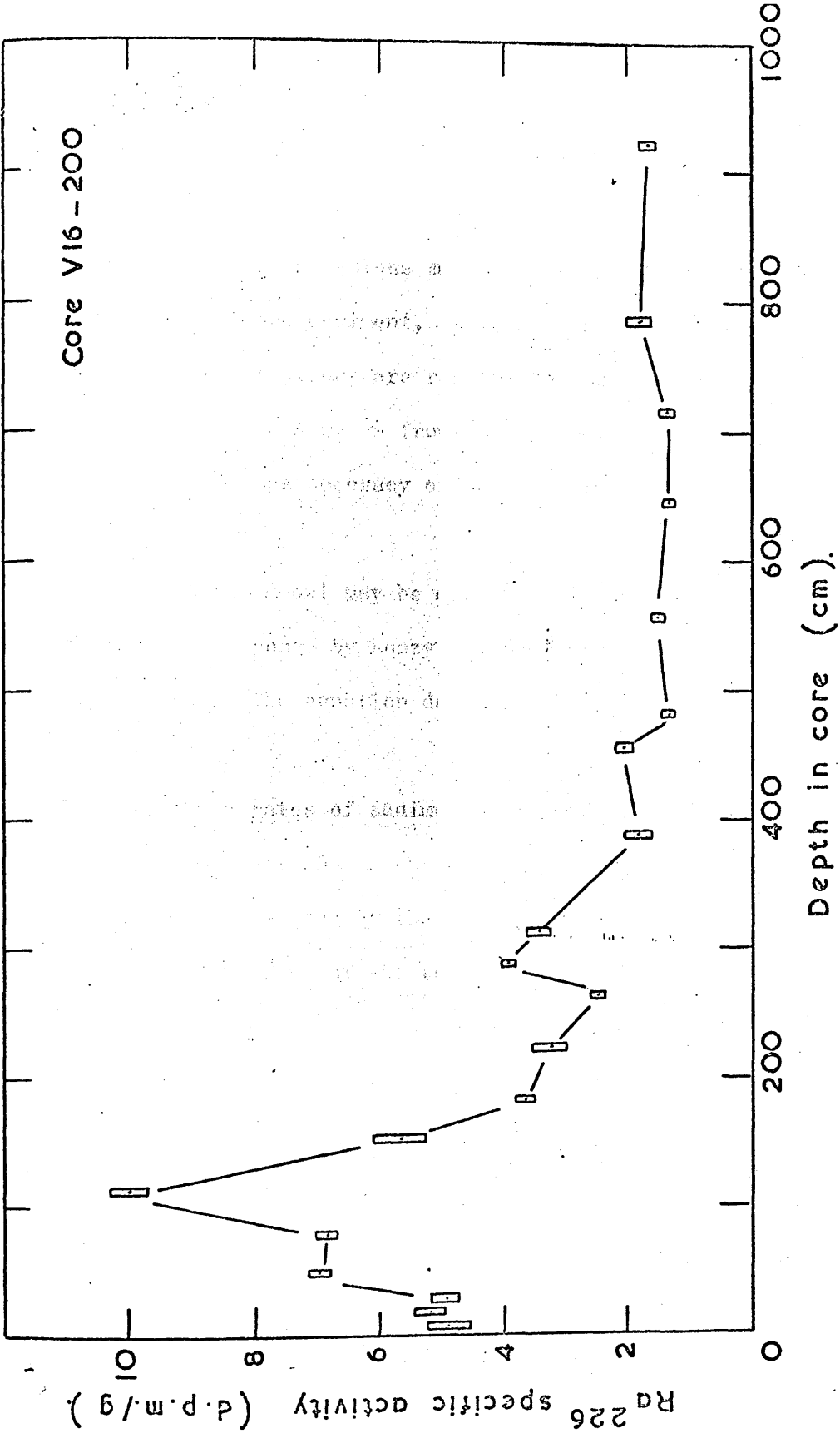


Figure 25 : Ra²²⁶ specific activity versus depth.

about the $\text{Ra}^{226}/\text{Th}^{230}$ activity ratio plot versus depth (Figure 26). While in part these fluctuations may be caused by experimental uncertainties, local variations may also occur in the absorption characteristics of the sediment, as in U^{234} diffusion (Section 3.2b). Provided these fluctuations are random, they do not affect any qualitative conclusions drawn from the general shape of the profile, but they do reduce the accuracy of quantitative data derived from it.

A mathematical model may be developed to evaluate Ra^{226} diffusion in the core, as proposed by Koczy and Bourret (1958) and Goldberg and Koide (1963). The equation depends on the following assumptions:

- i) the rates of sedimentation and Th^{230} deposition did not change appreciably during the period represented by the core,
- ii) reworking of the top layer of sediment, e.g. by burrowing organisms, may be ignored,
- iii) the Ra^{226} activity in the core is derived solely from Th^{230} in the sediment,
- iv) diffusion of Ra^{226} is controlled only by the concentration gradient, i.e. absorption is the same at all levels in the core, and,
- v) Ra^{226} diffuses into the ocean from the sediment surface at a constant rate.

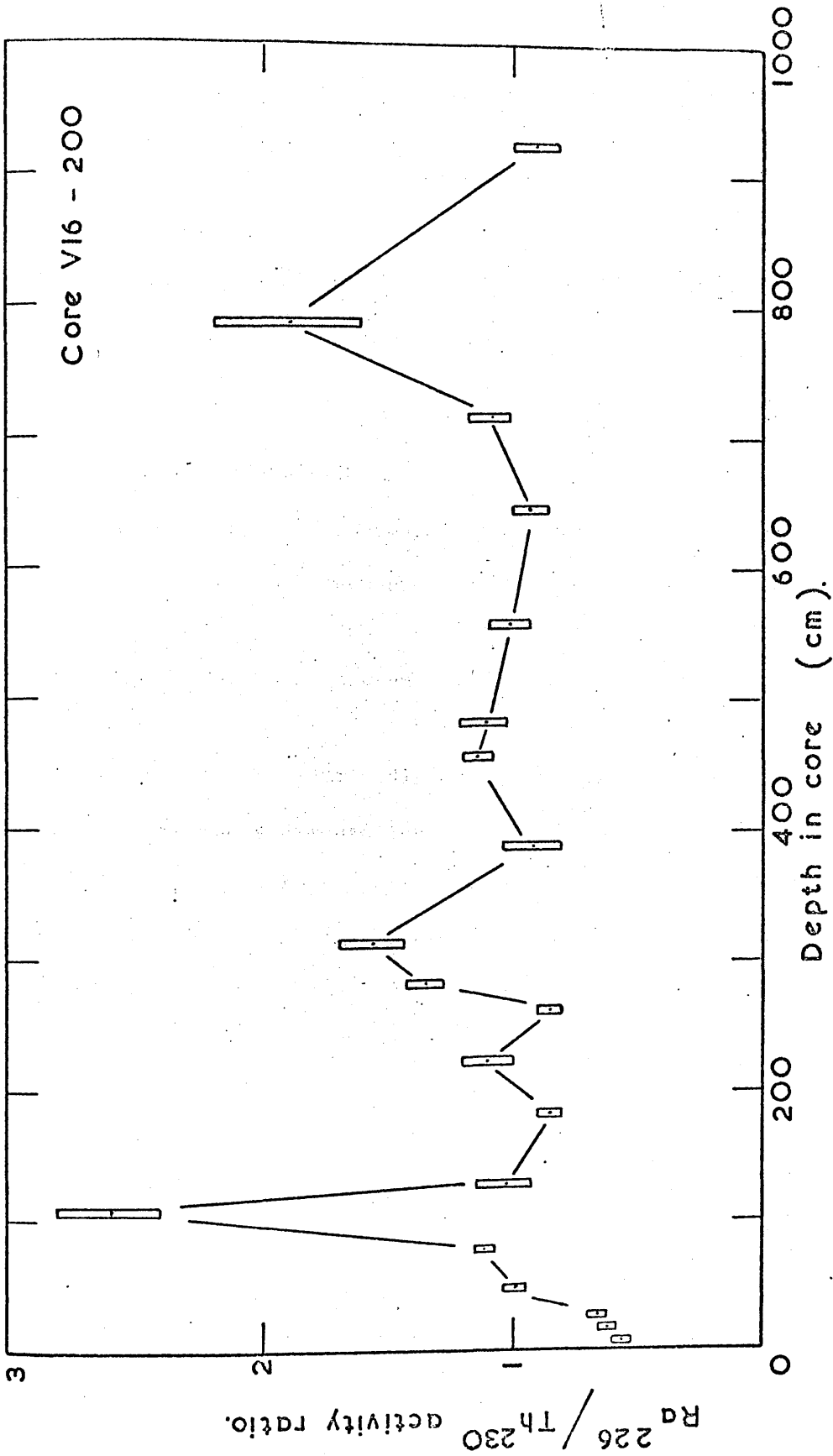


Figure 26: Ra^{226} / Th^{230} activity ratio versus depth.

The rates of production and removal of Ra²²⁶ at a given depth are equal in the steady state, So, with the above assumptions:

$$D \cdot \frac{d^2 C_x}{dx^2} - S \cdot \frac{dC_x}{dx} + \lambda_1 N_0 \cdot e^{-\lambda_1 x/S} - \lambda_2 C_0 = 0$$

where: x is the depth in the core.

C_x is the Ra²²⁶ concentration at depth x ,

C_0 is the Ra²²⁶ concentration at the sediment-water interface,

N_0 is the Th²³⁰ concentration at the sediment-water interface

D is the effective diffusion coefficient

S is the sedimentation rate

λ_1 is the disintegration constant of Th²³⁰

λ_2 is the disintegration constant of Ra²²⁶

The solution of this equation is :

$$C_x = C_0 \cdot e^{-(\sqrt{S^2/4D^2 + \lambda_2/D} - S/2D)x} + \frac{\lambda_1 N_0}{D(\lambda_1/S)^2 + \lambda_1 - \lambda_2} \left[e^{-(\sqrt{S^2/4D^2 + \lambda_2/D} - S/2D)x} - e^{-\lambda_1 x/S} \right]$$

(Steen, 1955, Ku, 1966)

This equation can be simplified with the approximations:

$$\lambda_{2/D} \gg S^2/4D^2 \quad \text{and} \quad \lambda_2 \gg \lambda_1 \quad (\text{Koczy, 1963})$$

so that:

$$C_x = C_0 e^{-\sqrt{\lambda_{2/D}} \cdot x} - \frac{\lambda_1 N_0}{\lambda_2 - D(\lambda_1/S)^2} \left[e^{-\sqrt{\lambda_{2/D}} \cdot x} - e^{-\lambda_1 x/S} \right]$$

The Th^{230} concentration at depth x , $N_x = N_0 e^{-\lambda_1 x/S}$, and on division by $(N_0 \cdot e^{-\lambda_1 x/S} \cdot \lambda_1/\lambda_2)$,

$$\begin{aligned} R_x &= R_0 e^{-\left(\sqrt{\lambda_{2/D}} - \lambda_1/S\right)x} - \frac{\lambda_2}{\lambda_2 - D(\lambda_1/S)^2} \left[\frac{e^{-\sqrt{\lambda_{2/D}} \cdot x} - e^{-\lambda_1 x/S}}{e^{-\lambda_1 x/S}} \right] \\ &= R_0 e^{-\left(\sqrt{\lambda_{2/D}} - \lambda_1/S\right)x} + \frac{\lambda_2}{\lambda_2 - D(\lambda_1/S)^2} \left[1 - e^{-\left(\sqrt{\lambda_{2/D}} - \lambda_1/S\right)x} \right] \\ &= \left[R_0 - \frac{\lambda_2}{\lambda_2 - D(\lambda_1/S)^2} \right] e^{-\left(\sqrt{\lambda_{2/D}} - \lambda_1/S\right)x} + \frac{\lambda_2}{\lambda_2 - D(\lambda_1/S)^2} \quad (1) \end{aligned}$$

where R_x is the $\text{Ra}^{226}/\text{Th}^{230}$ activity ratio at depth x

R_0 is the $\text{Ra}^{226}/\text{Th}^{230}$ activity ratio at the sediment-water interface.

R_x therefore increases exponentially from R_0 towards a steady-state value, R_s , equal to $\frac{\lambda_2}{\lambda_2 - D \cdot (\lambda_1/S)^2}$.

R_s is slightly greater than unity, and may be found from the experimental results by determining the mean $\text{Ra}^{226}/\text{Th}^{230}$ activity ratio below a certain depth. In the case of core V16-200, if this depth

is 100 cm., the error involved in R_s can not exceed 2%.

If the sedimentation rate, S , is known, it is possible to find D directly from the steady state activity ratio, since

$$R_s = \frac{\lambda_2}{\lambda_2 - D(\lambda_1/S)^2} \cdot \text{Normally } \lambda_2 \gg D. (\lambda_1/S)^2, \text{ so that a small}$$

change in R_s will have a disproportionately large effect on the value of D obtained. Another method is therefore preferable. Koczy (1963) pointed out that it is appropriate to use the lower part of a Ra^{226} profile to estimate the sedimentation rate, and the upper part to determine the diffusion coefficient. From equation (1) above,

$$\left[R_x - \frac{\lambda_2}{\lambda_2 - D(\lambda_1/S)^2} \right] = \left[R_0 - \frac{\lambda_2}{\lambda_2 - D(\lambda_1/S)^2} \right] \cdot e^{-(\sqrt{\lambda_2/D} - \lambda_1/S) x}$$

$$\text{or } (R_s - R_x) = (R_s - R_0) \cdot e^{-(\sqrt{\lambda_2/D} - \lambda_1/S) x}$$

Therefore a plot of $\ln. (R_s - R_x)$ versus x will be a straight line, with gradient $-(\sqrt{\lambda_2/D} - \lambda_1/S)$ from which D can be calculated, and intercept $\ln. (R_s - R_0)$ from which R_0 can be calculated.

The mean value of R_s for core V16-200, as calculated from the data between 105 and 927 cm., is 1.23 ± 0.12 . In Figure 27, $\ln.(R_s - R_x)$ is plotted versus depth for the top 100 cm. of the core.

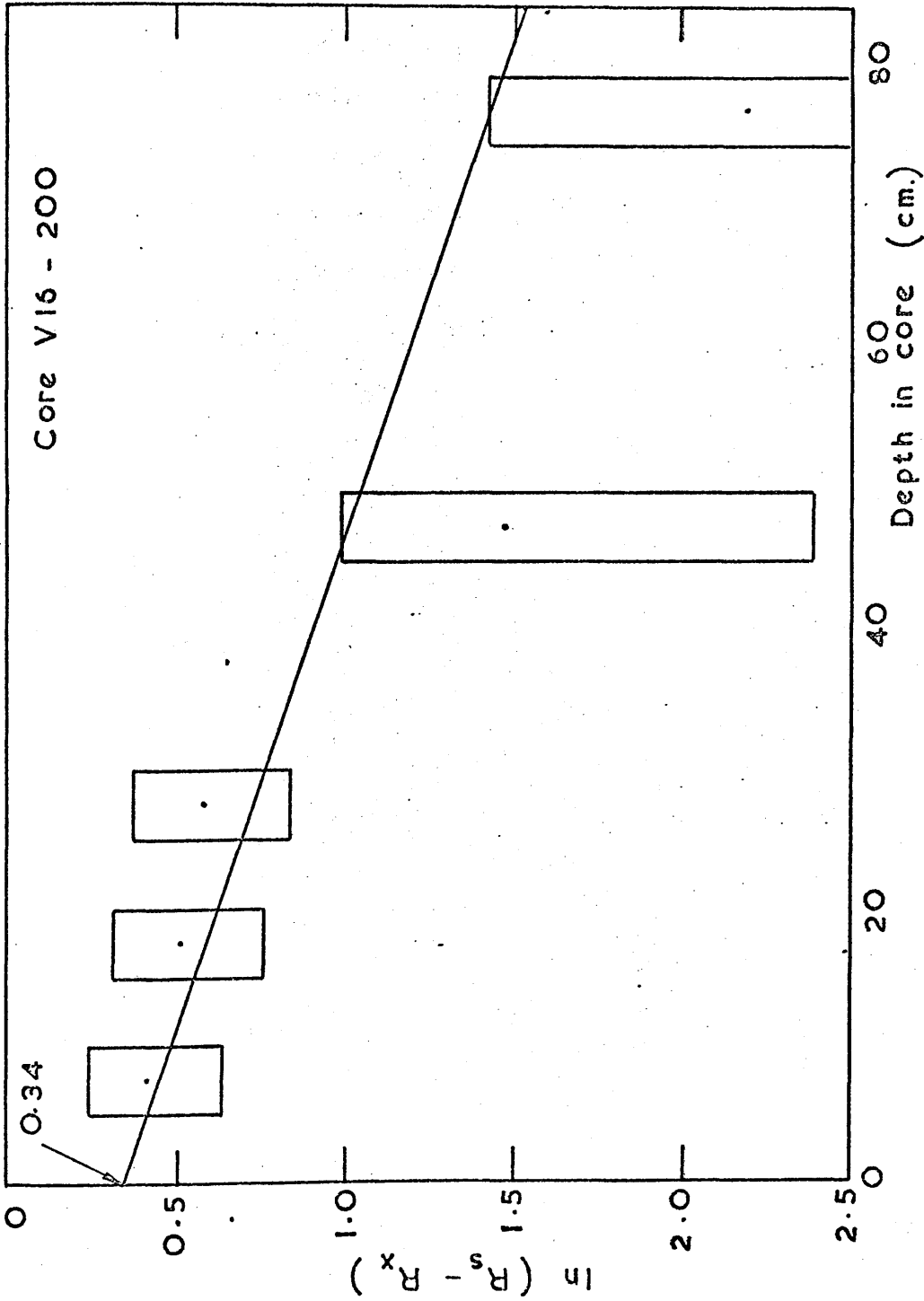


Figure 27: Radium diffusion: $\ln(R_s - R_x)$ versus depth.

The best-fit line was calculated by the least squares method: from the intercept, R_0 was calculated as 0.52, and from the gradient, D was calculated as $1.3 \text{ cm.}^2/\text{yr.}$ or $4.1 \times 10^8 \text{ cm.}^2/\text{sec.}$ This value for the effective diffusion coefficient is small compared with the diffusion coefficients of salts in water (around $10^5 \text{ cm.}^2/\text{sec.}$), implying that only a small proportion of the Ra^{226} atoms are in solution in pore water at any one time. Values on the order of 10^8 and $10^{-9} \text{ cm.}^2/\text{sec.}$ for the effective diffusion coefficients of both Ra^{226} and U^{234} have been found by other workers (Koczy, 1963; Ku, 1965).

CHAPTER 4.DATING OF CORE V16-200.4.1 Introduction.

As outlined in Section 1.3, studies of planktonic foraminifera in Atlantic deep sea cores have established two independent climatic sequences. These sequences are derived from two different approaches:

- i) Ericson and coworkers (Ericson et al., 1964; Ericson and Wollin, 1968) employ the absolute abundance of Globorotalia menardii as their indicator of surface water temperature, and
- ii) Emiliani (1955, 1966) uses oxygen isotopic analysis of specific foraminiferal types to obtain paleotemperatures.

The most complete correlation of the two climatic curves has been made by Broecker and van Donk (1970), although the absolute dating is still controversial.

Ericson's sequence in particular has been confirmed in a large number of cores taken throughout the tropical Atlantic Ocean. It is evident, therefore, that establishment of an absolute time scale in any core, whose continuity and place in the climatic sequence is

certain, allows an independent estimate to be made of the tropical Atlantic chronology.

Ericson et al. (1964) selected 26 globigerina ooze cores from the Lamont-Doherty Observatory collection (3000 cores at that time) in their construction of the Pleistocene record (Figure 1). From early radiocarbon work, it was established that if the texture of a core was uniform, then the rate of accumulation of the sediment had remained reasonably constant with time. All the cores used in the compilation fulfilled this criterion of textural uniformity, and the climatic zones were not distinguished by any physical characteristic of the sediments. Core V16-200 is one of the cores from the suite, and represents the complete sequence from the present back to the U zone.

In this study, sections for radiochemical analysis were taken from each paleontologic zone back to the beginning of zone V, usually with one sample taken just above and just below each zone boundary. Previous work on equatorial Atlantic cores has shown that changes may occur in the relative sedimentation rates of the clay and carbonate components and Th^{230} itself (Walton and Broecker 1958; Broecker et al., 1958). If this situation existed in core V16-200, the sampled sections would exhibit sharp deviations across the zone boundaries in the plot of $\log (\text{Th}_{\text{excess}}^{230})$ versus depth.

The sharpest boundaries are those which represent a change from cold to warm surface water, because the gradual decline of temperature makes warm to cold boundaries difficult to identify with accuracy. In core V16-200, three such cold to warm boundaries exist, Y/Z, W/X, and U/V, at depths of 25, 300, and 930 cm. respectively. The warm to cold boundaries, W/Y and V/X, occur at 170 to 180 cm. and 360 cm. respectively. The climatic curve from the core is included in the figures of ($\text{Th}_{\text{excess}}^{250}$) versus depth in the following section (4.2).

4.2. ($\text{Th}^{230}_{\text{excess}}$) Sedimentation Rates.

The dating approach employed here is to obtain a mean rate of sedimentation over the sampled depth interval, then to use this rate data to yield boundary ages (Sarma, 1964; Ku et al., 1968). The inherent assumptions in this method are that both sedimentation and authigenic Th^{230} precipitation have remained relatively constant over the dated interval, and that Th^{230} does not migrate in the sediment column (Section 3.2c).

With these constraints,

$$A_x = A_0 \cdot e^{-\lambda x/S}$$

$$\text{or, } \ln. A_x = \ln. A_0 - \lambda x/S$$

where A_0 is the specific activity of unsupported

Th^{230} , ($\text{Th}^{230}_{\text{excess}}$), at the sediment-water interface,

A_x is the specific activity of ($\text{Th}^{230}_{\text{excess}}$) at depth x ,

S is the mean sedimentation rate over the sampled interval,

λ is the decay constant of Th^{230}

$$(t_{\frac{1}{2}} = 75,200 \text{ yr. : Attree et al., 1961}).$$

Thus, if the assumptions of the method are fulfilled, a semilogarithmic plot of ($\text{Th}^{230}_{\text{excess}}$) in d.p.m./g. versus depth should yield a

straight line. The sedimentation rate is then calculated from the value of the gradient of an objective line of regression of $\log. (Th_{excess}^{230})$ on depth. This best-fit line, plus the standard deviation of the gradient, was determined on a KDF 9 computer using the programme reproduced in Appendix 3.

The logarithm of the unsupported Th^{230} specific activity is plotted in three different ways in Figures 28, 29, and 30. Figure 28 shows (Th_{excess}^{230}) in the total sediment, and Figure 29 shows (Th_{excess}^{230}) calculated on a "carbonate free" or "clay only" basis. Figure 30 shows the (Th_{excess}^{230}) specific activity normalised against the Th^{232} specific activity. Although the geochemistries of the thorium isotopes are dissimilar, it is felt that the homogeneity of the thorium concentration in the clay fraction (Section 3.2a) makes the normalisation valid in this case.

In all three plots, a fairly regular linear decrease is found. The apparently larger errors associated with points at greater depth is due to amplification by the logarithmic scale at low values of (Th_{excess}^{230}) . While the relative errors on these values are large, the quality of the data from which they were calculated is similar to that from lesser depths. An additional factor which may cause scatter in the low values is U^{234} migration (Sections 3.2b and 3.2c).

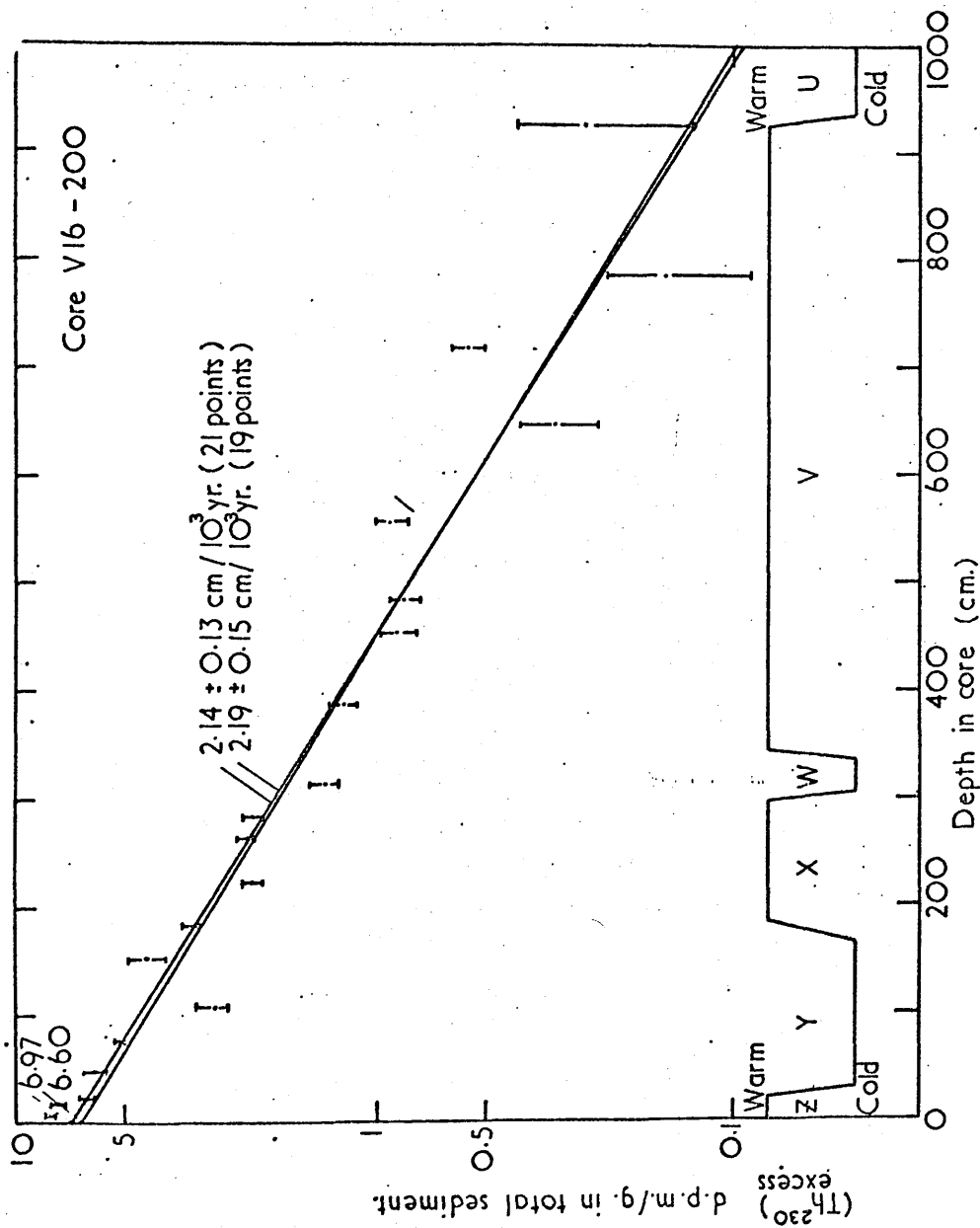


Figure 28. (Th^{230}) excess specific activity in total sediment.

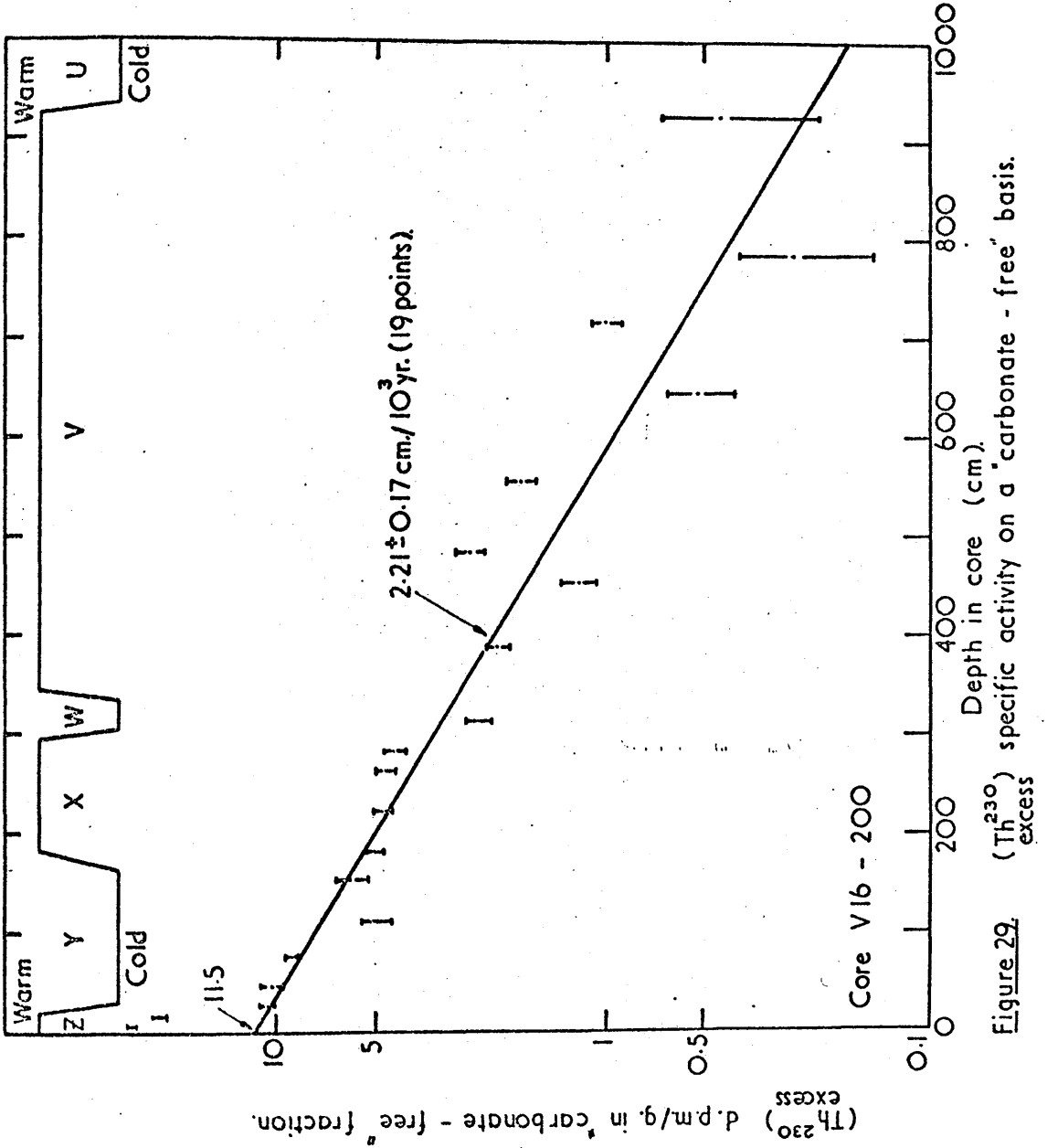


Figure 29. $(Th^{230})_{\text{excess}}$ specific activity on a 'carbonate-free' basis.

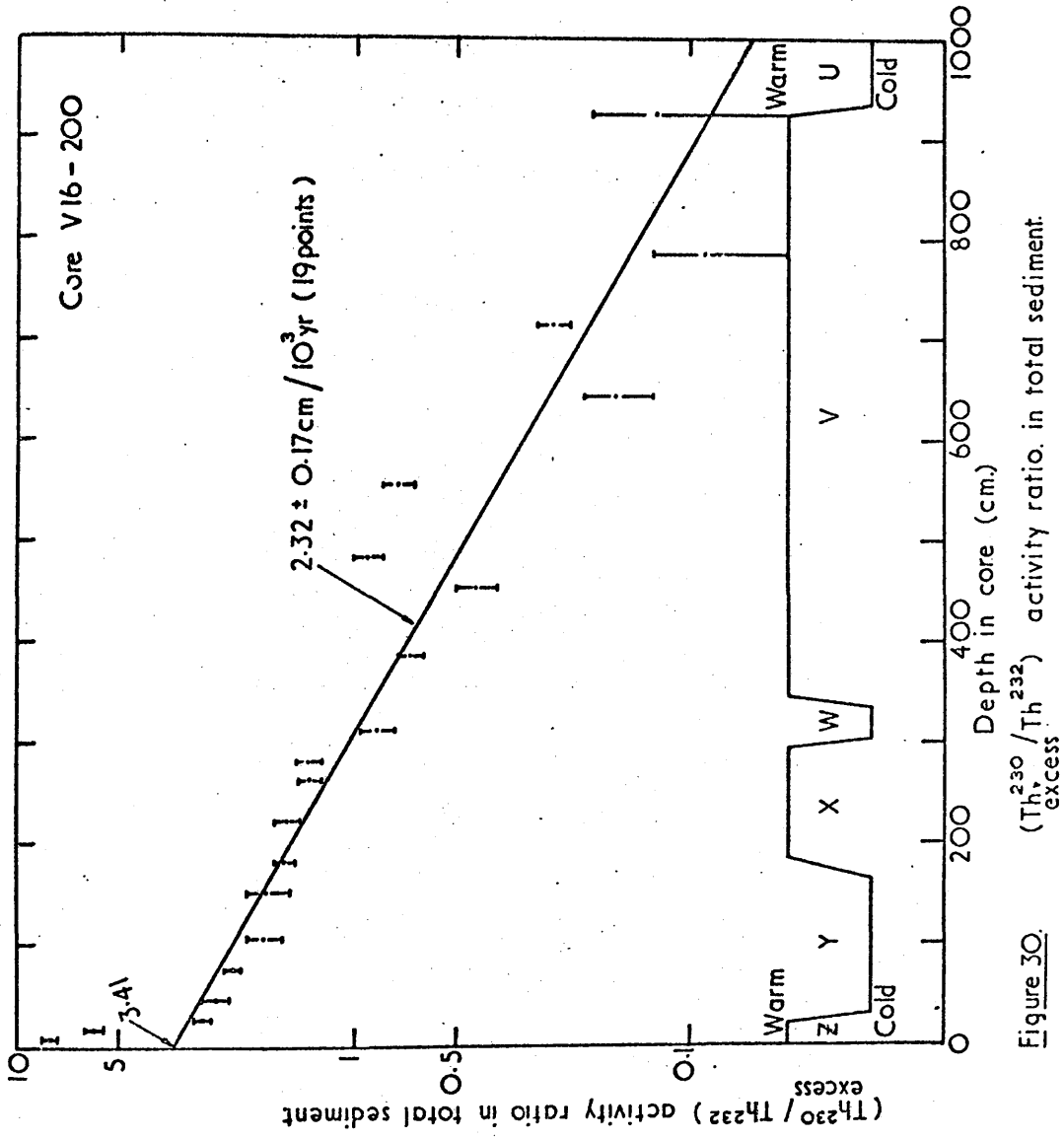


Figure 30. (Th^{230}/Th^{232}) activity ratio in total sediment.

On inspection of Figures 28, 29, and 30, it is evident that the points from the Z zone (5 to 10 cm. and 15 to 20 cm.) appear to define a line of steeper gradient (lower sedimentation rate) than the remaining 19 points. This phenomenon has been encountered previously in globigerina ooze sediments taken near the mid-Atlantic ridge (Goldberg et al., 1963) and in the equatorial Atlantic (Walton and Broecker, 1958; Broecker et al., 1958). Broecker and coworkers postulated that carbonate and non-carbonate sedimentation, and Th^{230} precipitation all changed across the Y/Z boundary in the mid-Atlantic. Goldberg et al. (1963) erroneously assigned a $\text{Th}^{230}/\text{Th}^{232}$ age of 90,000 yr. to the Y/Z boundary, conclusively dated at 11,000 yr. by the radiocarbon method (Ericson et al., 1961). If these two points from the Z zone of core V16-200 are omitted in the calculation of sedimentation rates, the remaining 19 points yield mean rates which are higher than those from 21 points by between 2.3 and 7.8%. The sedimentation rates obtained by the different approaches are tabulated in Table 8.

The two methods of plotting ($\text{Th}_{\text{excess}}^{230}$) data alone yield mean rates and standard deviations of 2.19 ± 0.15 and 2.21 ± 0.17 cm./ 10^3 yr. If the authigenic Th^{230} were associated primarily with the clay fraction, a smaller scatter of the data from linearity and a correspondingly smaller standard deviation would have been evident from the "carbonate-free" data. This is not the case. It can be seen that the

mean $(Th_{excess}^{230})/Th^{232}$ sedimentation rate, 2.32 ± 0.17 cm./ 10^3 yr., is 5% greater than the mean value from the (Th_{excess}^{230}) data, 2.20 cm./ 10^3 yr., but that all three rates agree within one standard deviation. The ages determined for the cold to warm boundaries of core VI6-200 are shown in Table 9.

0.84 ± 0.09 1.40 1.70 2.00 2.30 2.60 2.90 3.17
 0.81 ± 0.06 1.70 2.00 2.30 2.60 2.90 3.17

TABLE 9

Age boundaries for core VI6-200

| Boundary | Mean $(Th_{excess}^{230})/Th^{232}$ | Age (yr.) |
|----------|-------------------------------------|---------------|
| 100 | 1.36 | 1.7 ± 0.1 |
| 130 | 1.36 | 1.7 ± 0.1 |
| 160 | 1.36 | 1.7 ± 0.1 |

TABLE 8.

Sedimentation rates (cm./10³ yr.) determined for Core V16-200.

| Section | <u>Method.</u> | | | | |
|-------------------|--|--|--|--|--|
| | (Th ²³⁰ _{excess}) | (Th ²³⁰ _{excess}) | (Th ²³⁰ _{excess}) | (Pa ²³¹ _{excess}) | (Pa ²³¹ _{excess}) |
| Interval (cm.) | total sediment | "carbonate free" | (Th ²³²) | total sediment | "carbonate free" |
| 5-927 | 2.14 ± 0.13 | 2.05 ± 0.15 | 2.16 ± 0.15 | -- | -- |
| 25-927 | 2.19 ± 0.15 | 2.21 ± 0.17 | 2.32 ± 0.17 | -- | -- |
| 5-185 | 1.84 ± 0.45 | 1.07 ± 0.24 | 1.25 ± 0.34 | 3.11 ± 0.49 | 2.03 ± 0.95 |
| 25-185 | 2.24 ± 0.96 | 1.76 ± 0.46 | 2.58 ± 0.30 | 3.37 ± 0.86 | 2.85 ± 0.51 |

TABLE 9.

Boundary Ages determined for Core V16-200.

| Boundary | Boundary depth (cm.) | Mean (Th ²³⁰ _{excess}) rate age * (X10 ³ yr. B.P.) | (Th ²³⁰ _{excess} /Th ²³²) rate age + (X10 ³ yr. B.P.) |
|----------|-------------------------|--|--|
| Y/Z | 25 | 11.4 ± 0.8 | 10.8 ± 0.8 |
| W/X | 300 | 136 ± 10 | 129 ± 10 |
| U/V | 930 | 423 ± 30 | 401 ± 30 |

* Calculated from a rate of 2.20 ± 0.16 cm./10³ yr.+ Calculated from a rate of 2.32 ± 0.17 cm./10³ yr.

4.3. $(\text{Pa}_{\text{excess}}^{231})$ Sedimentation Rates.

Samples were analysed for Pa^{231} down to a depth of 180 to 185 cm. (in the X zone), at which point the $(\text{Pa}_{\text{excess}}^{231})$ specific activity fell below 0.1 d.p.m./g. The $(\text{Pa}_{\text{excess}}^{231})$ data are used to calculate mean sedimentation rates in an analogous fashion to $(\text{Th}_{\text{excess}}^{230})$ data (Section 4.2), with a value of 32,340 years assumed for the half life of Pa^{231} (Brown et al., 1969). Figure 31a shows the semilogarithmic plot of $(\text{Pa}_{\text{excess}}^{231})$ and $(\text{Th}_{\text{excess}}^{230})$ specific activities in the total sediment versus depth, while Figure 31b shows the semilogarithmic plot of the nuclides on a "carbonate-free" basis.

The $(\text{Pa}_{\text{excess}}^{231})$ data follow the same general pattern as the $(\text{Th}_{\text{excess}}^{230})$ data in the top 200 cm. of the core, and again the data from zone Z appear anomalously high and suggest a much lower accumulation rate in this zone. Sedimentation rates have been calculated from both the $(\text{Pa}_{\text{excess}}^{231})$ and $(\text{Th}_{\text{excess}}^{230})$ data over the common section of the core, with and without the data from the Z zone (Table 8). The rates range from 1.07 ± 24 to 3.86 ± 0.86 cm./ 10^3 yr., with those derived from $(\text{Pa}_{\text{excess}}^{231})$ results consistently higher than those from $(\text{Th}_{\text{excess}}^{230})$ results, but large standard deviations are associated with rates from both sets of data. These large uncertainties on the derived sedimentation rates arise from the deviations

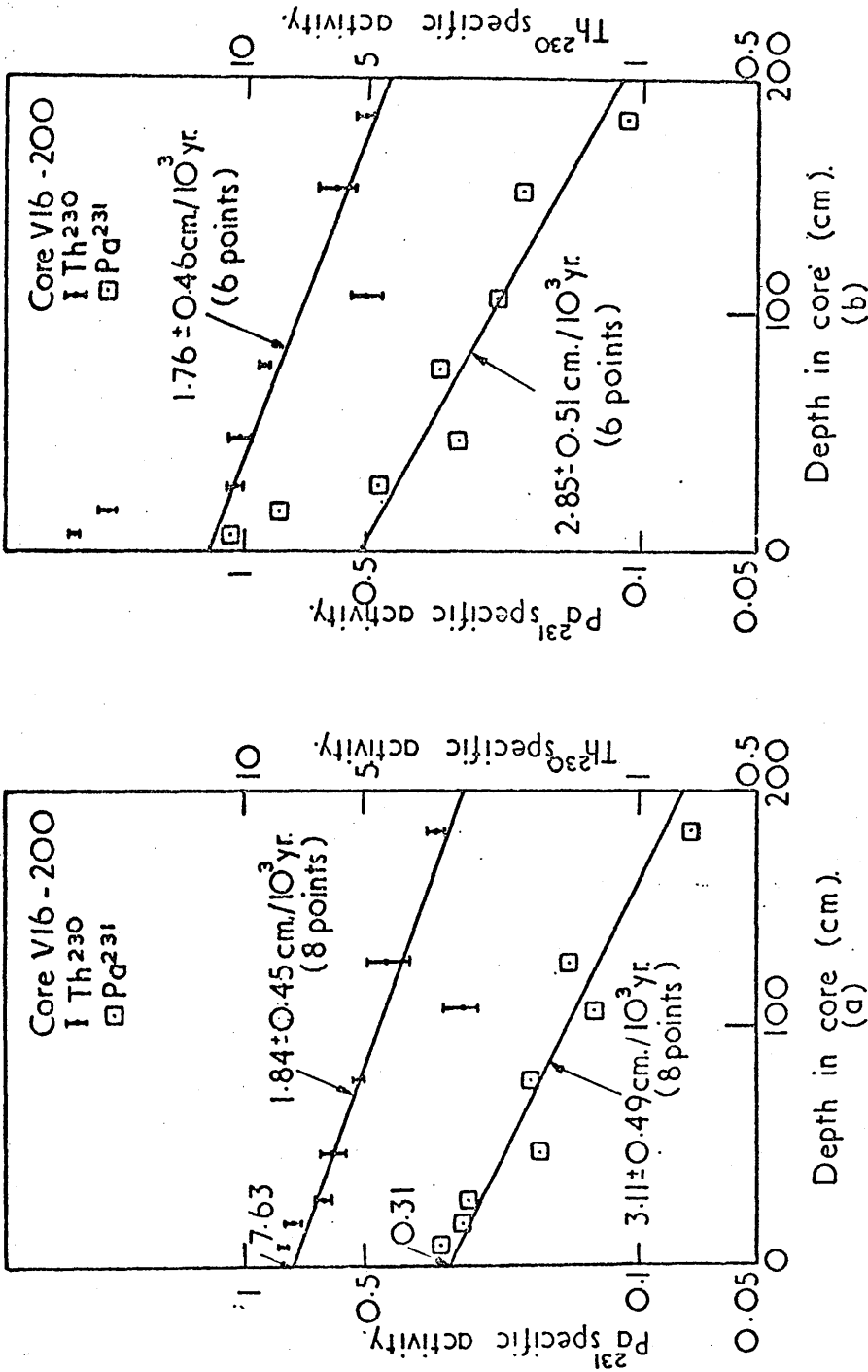


Figure 31. a) Th²³⁰ and Pa²³¹ specific activities in the total sediment
 b) Th²³⁰ and Pa²³¹ specific activities on a "carbonate-free" basis.

of the data from smooth logarithmic decreases (Figures 31a and 31b).

Over the top 200 cm. of the core, the "calcium carbonate plus salt" weight percentage decreases from 73% in the 5 to 10 cm. interval to 28% in the 150-155 cm. interval. Apart from the Z zone, only one other section of the core has a "calcium carbonate plus salt" weight percentage greater than 55%. Studies of three equatorial Atlantic cores by Turekian (1964) showed that both clay and calcium carbonate deposition rates changed from the Y to the Z zones, and that both were at least a factor of 2 higher in the Y zone.

While these variations in the sediment type may account for the deviations of the authigenic data from a smooth exponential decrease, they do not explain the systematically different sedimentation rates. In addition, the $(\text{Th}_{\text{excess}}^{230} / \text{Pa}_{\text{excess}}^{231})$ activity ratios over the Z and Y zones do not show a progressive trend. Using the expression

$$t = 8.26 \cdot \ln. (0.106 \text{Th}_{\text{excess}}^{230} / \text{Pa}_{\text{excess}}^{231}) \times 10^4 \text{ yr. (Section 1.4)}$$

the ratio from the 5-10 cm. section, 25.5, yields an age of 82,000 yr., and that from the 180-185 cm. section, 44.6, an age of 128,000 yr. It thus appears that either:

- i) the Th^{230} and Pa^{231} authigenic deposition rates have not varied sympathetically in time, or

- ii) some non-systematic error is present in either, or both, Th^{230} and Pa^{231} analyses.

In the following section, an attempt is made to compare the experimental determinations with the anticipated values, as derived from our present knowledge.

4.4 Comparison of Theoretical and Experimental ($\text{Th}^{230}_{\text{excess}}$) and ($\text{Pa}^{231}_{\text{excess}}$) Specific Activities.

The activity ratio ($\text{Th}^{230}_{\text{excess}}/\text{Pa}^{231}_{\text{excess}}$) may be calculated to have a theoretical value of 10.8 in freshly deposited sediments, and to decrease with an effective half life of 57,000 yr. (This calculation assumes only a $\text{U}^{234}/\text{U}^{238}$ activity ratio of 1.15, a $\text{U}^{238}/\text{U}^{235}$ atomic ratio of 137.8 in sea water, and deposition of Th^{230} and Pa^{231} in times short with respect to their half lives (Section 1.4).)

The value of the ($\text{Th}^{230}_{\text{excess}}/\text{Pa}^{231}_{\text{excess}}$) ratio at the sediment-water interface of core V16-200 is around 25 (Table 7b). Ku (1966) has noted that values of the ratio close to the theoretical 10.8 have been found only in cores taken from the Caribbean Sea and Antarctic Ocean, all other oceanic areas having higher values. It was suggested by Ku that this finding in the Caribbean and Antarctic might be related to the intense vertical mixing in the two areas, because this is their most obvious similarity, but this suggestion is purely speculative. From his results, Ku (1966) proposed that there existed, on average, an additional source of Th^{230} which amounted to 30% of the calculated Th^{230} production in the mean ocean depth (3800m.). Scott (1968) criticised this proposal on the following

grounds:

- i) the calculation was based on a low value for the mean oceanic uranium concentration,
- ii) the experimental ($\text{Th}_{\text{excess}}^{230}$) values were obtained from cores whose depths exceeded the mean oceanic depth by 16%, and
- iii) the value selected by Ku for the mean sediment density (lg./cm.^3) was too high,

and proposed that it was, in fact, authigenic Pa^{231} which was deficient.

With the concepts discussed in Sections 3.2a to 3.2c, it is possible to calculate the maximum unsupported specific activities of Th^{230} and Pa^{231} in the authigenic and clay fractions of core V16-200 as follows.

Unsupported Th^{230} and Pa^{231} in Terrigenous Minerals.

The necessary assumptions for this calculation are:

- i) the typical U/Th ratio of 0.285 found in igneous rocks is altered to 0.179 during transport to the sediment as clay,
- ii) no Th^{232} is weathered during transport,
- iii) the average $\text{U}^{234}/\text{U}^{238}$ activity ratio in pelagic clays is 0.925 (mean value for V16-200, 0.94 ± 0.02).

The first two assumptions imply that 37.2% of the initial uranium content in igneous-derived minerals is leached before sedimentation occurs. If the total transportation time from source to sediment is short by comparison with the half lives of Th^{230} and Pa^{231} , and no leaching of either isotope occurs, the third assumption allows calculation that the $\text{Th}^{230}/\text{U}^{238}$ and $\text{Pa}^{231}/\text{U}^{235}$ activity ratios in freshly deposited clay are 1.59, and the $\text{Th}^{230}/\text{U}^{234}$ activity ratio is 1.72. This means that the $(\text{Th}_{\text{excess}}^{230}/\text{Pa}_{\text{excess}}^{231})$ activity ratio in this component is initially 24.5. The mean uranium concentration in the clay component of core V16-200 is 2.29 p.p.m., which results in initial maximum unsupported initial activities of 1.23 and 0.05 d.p.m./g. for Th^{230} and Pa^{231} respectively. If the transportation time from source to sediment is very long, these unsupported activities will be lower, but the $(\text{Th}_{\text{excess}}^{230}/\text{Pa}_{\text{excess}}^{231})$ ratio will be greater than 24.5.

Authigenic Th^{230} and Pa^{231} Precipitated from the Ocean.

The data necessary for this calculation are:

- i) the mean uranium concentration in the world's oceans is 3.3 ug./l. (Rona and Gilpatrick, 1956; Wilson et al., 1960; Milner et al., 1961),

- ii) the U^{234}/U^{238} activity ratio in ocean water is 1.15,
- iii) the U^{238}/U^{235} isotopic ratio is 137.8
- iv) precipitation of Th^{230} and Pa^{231} occurs in a time short relative to the nuclide half-lives,
- v) the half-lives of the isotopes concerned are:

| | | | | | |
|------------|---|------|---|--------|-----|
| U^{238} | : | 4.51 | x | 10^9 | yr. |
| U^{234} | : | 2.48 | x | 10^5 | yr. |
| U^{235} | : | 7.13 | x | 10^8 | yr. |
| Th^{230} | : | 7.52 | x | 10^4 | yr. |
| Pa^{231} | : | 3.23 | x | 10^4 | yr. |

Using the above values, the activities of U^{238} , U^{234} and U^{235} in ocean water may be calculated as 2.44, 2.81, and 0.11 d.p.m./l. respectively. In the water depth of core V16-200, 4093m., this corresponds to Th^{230} and Pa^{231} production rates of 10.6 and 0.96 d.p.m./ 10^3 yr./cm.² respectively (with no allowance for decay).

Specific Activities of Th^{230} and Pa^{231} in core V16-200.

To calculate specific activities, the effective density of the sediment must be known. Ku (1966) assumed a figure of 1.0g./cm³., but values as low as 0.4 g./cm³. have been determined (Amin et al., 1966). Turekian (1965) suggests that a figure of 0.72 g./cm³. is

applicable to globigerina ooze. With the value of $2.20 \text{ cm.}/10^3 \text{ yr.}$ chosen as the mean sedimentation rate of V16-200 (Section 4.2) and values of 0.469 and 0.531 as the mean weight fractions of "calcium carbonate plus salt" and clay (Table 7a) respectively, the average clay sedimentation rate is then $0.84 \text{ g./cm}^2./10^3 \text{ yr.}$ This rate for clay sedimentation yields maximum detrital unsupported Th^{230} and Pa^{231} activities of 0.65 and 0.03 d.p.m./g. respectively, and the authigenic Th^{230} and Pa^{231} contributions will give rise to activities of 6.7 and 0.6 d.p.m./g. in the total sediment ($1.58 \text{ g./cm}^2./10^3 \text{ yr.}$).

The calculated value of the maximum initial ($\text{Th}_{\text{excess}}^{230}$) specific activity in the total sediment, 7.35 d.p.m./g., compares favourably with the experimental activity in the 5 - 10 cm. section, 8.12 d.p.m./g. and with the extrapolated surface value of the " $\text{Th}_{\text{excess}}^{230}$ total sediment" best fit line, 6.97 d.p.m./g. (Figure 28). On the other hand, the maximum calculated ($\text{Pa}_{\text{excess}}^{231}$) specific activity, 0.63 d.p.m./g., is much larger than either the activity determined in the 5 to 10 cm. section, 0.32 d.p.m./g., or the extrapolated surface value of the " $\text{Pa}_{\text{excess}}^{231}$ total sediment" best fit line, 0.31 d.p.m./g. (Figure 31a). Thus core V16-200 exhibits an expected value for the initial ($\text{Th}_{\text{excess}}^{230}$) specific activity, but the experimental value for the initial ($\text{Pa}_{\text{excess}}^{231}$) specific activity is only about 50% of the expected value.

This deficiency of authigenic Pa^{231} remains unexplained. Scott (1968) has suggested that manganese nodules may be a possible sink for authigenic Pa^{231} , because Sackett (1966) found surface values of the $(\text{Th}_{\text{excess}}^{230}/\text{Pa}_{\text{excess}}^{231})$ activity ratio lower than 10.8 in these species. However, calculation showed that around 40% of the ocean floor would have to be covered with manganese nodules to account for the low $(\text{Th}_{\text{excess}}^{230}/\text{Pa}_{\text{excess}}^{231})$ ratios in sediments (Scott, 1968). Another unexplored possibility is that specific incorporation of Pa^{231} may occur in living species.

4.5 Dating of Climatic Changes from Core V16-200.

The radiometric chronologies attached to the two climatic curves have been firmly established to around 40,000 yr. B.P. by radiocarbon dating. The two proposed extensions of the time scales (to a claimed 400,000 yr. in each case) have been established by natural series disequilibrium dating of only 4 Caribbean cores (Section 1.5). Rona and Emiliani (1969) used an acid leach analytical method to obtain ($\text{Th}_{\text{excess}}^{230} / \text{Pa}_{\text{excess}}^{231}$) ages up to 167,000 yr. B.P. for various levels of the very similar cores P6304-8 and P6304-9. One curious feature of these stratigraphic dates is that they indicate rates of sedimentation which vary by a factor of two in very homogenous cores. The extension of Emiliani's time scale to 425,000 yr. is by linear extrapolation (Emiliani, 1966). Broecker and coworkers (Broecker et al., 1968; Broecker and van Donk, 1970) have used ($\text{Th}_{\text{excess}}^{230}$) and ($\text{Pa}_{\text{excess}}^{231}$) rates of accumulation to extend the chronology of Ericson's sequence to the U/V boundary in one core, V12-122. Oxygen isotopic analysis of core V12-122 allowed the most complete intercomparison of the two sequences to date (Figure 32). This study revealed that Ericson's Y/Z and W/X boundaries are equivalent to Emiliani's 2/1 and 6/5 transitions, but that the U/V boundary occurred during the temperature decline of stage 12. Nevertheless, the U/V boundary, as defined by a re-appearance in the tropical Atlantic of Globorotalia menardii, is

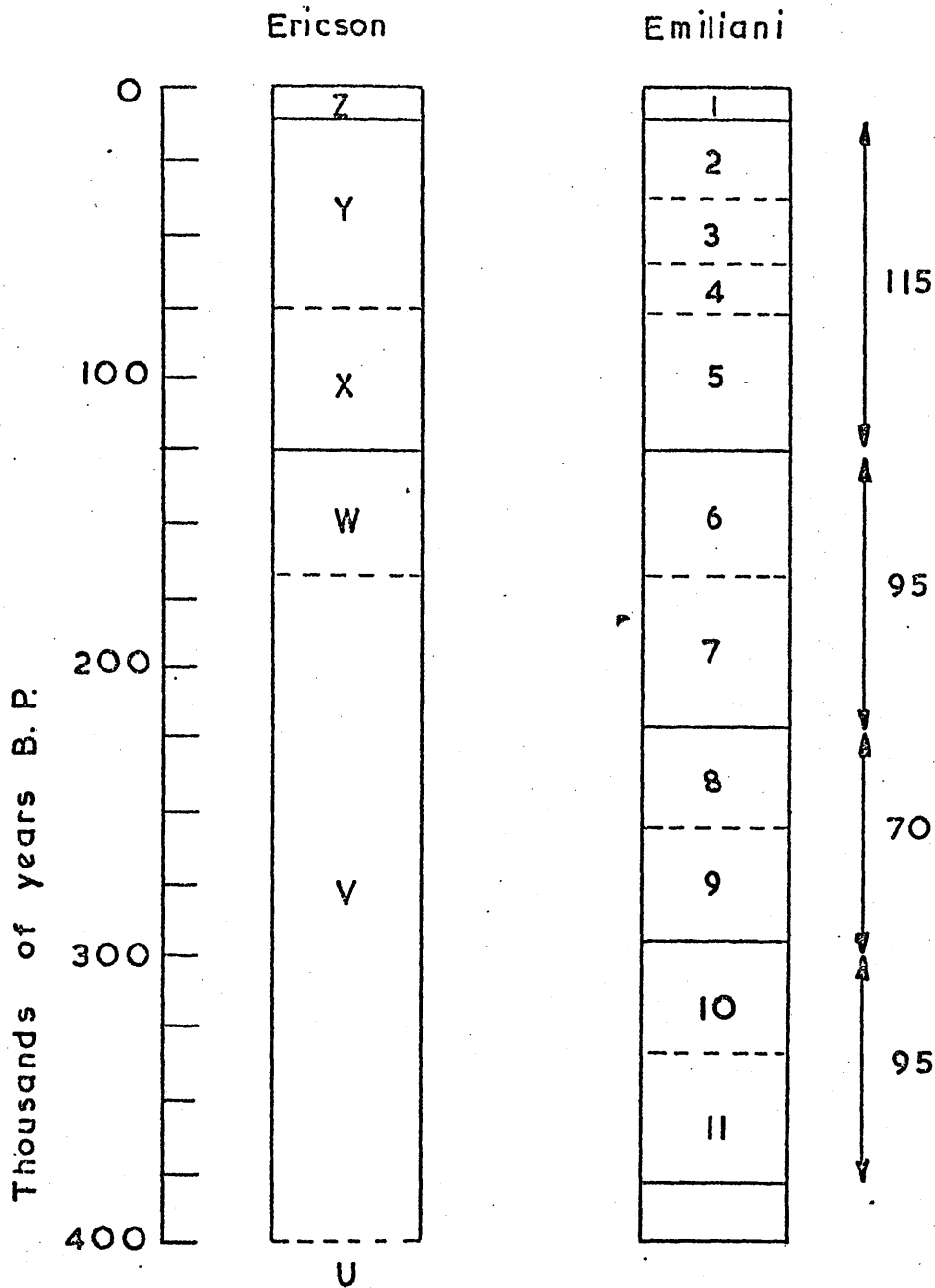


Figure 32: Comparison of Paleoclimatic Curves and Timescale
 (After Broecker and van Donk, 1970.)

very sharp. With supporting experimental evidence from dated high sea stands, paleomagnetic measurements, and a mathematical treatment of the Milankovitch Hypothesis (Section 1.5), Broecker and van Donk (1970) suggest that Emiliani's determinations of 100,000 and 290,000 yrs. B.P. for the W/X and U/V boundaries are low by at least 25%.

In effect, the approach employed by Broecker and van Donk (1970) is to fix certain points on the two climatic curves, and then use the radiometric data from core V12-122 as corroborative evidence for the resultant time scale. These points which may be fixed with confidence arise from the following evidence:

- i) precision dating of 3 coral terraces on Barbadoes Island yielded ages of 82,000, 103,000, and 122,000 yr. B.P. (Broecker et al., 1968; Ku, 1968). These terraces may be expected to represent high sea stands, and consequently warm surface ocean temperatures. Barbadoes is an island in an area which suffers tectonic uplift, and the contention is that this uplift allowed formation and preservation of coral terraces during each of the three minor paleotemperature peaks of Emiliani's stage 5

(Emiliani, 1961; Shackleton, 1969). The maximum temperature (and hence highest sea level) of stage 5 is consistently recorded near the beginning of the stage, and this first minor peak is considered synchronous with the extensively recorded 124,000 yr. B.P. coral terraces (Section 1.5). The two more recent peaks of stage 5 are considered to have been unsuitable for coral preservation in tectonically stable regions because the sea did not stand higher at that time than it does at present. Nevertheless, some evidence exists for the presence of the two terraces in uplifted localities elsewhere (Szabo and Rosholt, 1969; Veeh, 1970).

The time lapse between the 2/1 (Y/Z) boundary and the maximum temperature recorded in stage 1 is 6,000 yr. (Broecker et al., 1960, 1968). With the assumption that a similar period elapsed between the 6/5 (W/X) boundary and the maximum of stage 5, Broecker and

van Donk (1970) conclude that the age of the 6/5 (W/X) boundary is $127,000 \pm 5,000$ yr. B.P.

- ii) a paleomagnetic reversal investigation of five Atlantic cores (Glass et al., 1967; Ericson and Wollin, 1968) yielded ages for Ericson's U/V boundary ranging from 380,000 to 440,000 yr. B.P. with a mean value of $400,000 \pm 20,000$ yr. These values were obtained by linear interpolation between the core tops (zero age) and the Brunhes-Matuyama boundaries (690,000 yr. B.P.; Cox, 1969), i.e. assuming a constant rate of accumulation in the cores.

Thus, with assumed values of 11,000, 127,000 and 400,000 yr. B.P. for the Y/Z, W/X and U/V boundaries respectively, the time scale is quite rigorously fixed.

A comparison of the depths at which Ericson's zone boundaries occur in cores V12-122 and V16-200 (Table 10) shows that the sedimentation rates cannot be identical because the zones do not coincide precisely. Although the W/X boundary occurs in both cores at 300 cm. the zone thicknesses are all different. The compilation of Ericson et al. (1961) of the thicknesses of the X and Y zones in many cores

shows variability by a factor of two either way in the ratio of the thickness. While this is possibly due partly to some insensitivity in Ericson's method, the rate of sedimentation obviously varies in time at any locality besides varying from place to place. This variability in sedimentation rates illustrates that uncertainties may be anticipated to arise when authigenic isotope data are fitted to yield mean sedimentation rates.

Broecker and van Donk (1970) obtain ($\text{Th}^{230}_{\text{excess}}$) and ($\text{Pa}^{231}_{\text{excess}}$) rates of sedimentation for core V12-122 ranging from 2.03 to 2.99 cm./ 10^3 yr. by consideration of data points in analogous positions near boundaries of the same type i.e. in corresponding parts of two similar climatic cycles. The published data allow the mean rates of accumulation in Table 11 to be calculated.

The sedimentation rates of cores V12-122 and V16-200 required to yield Broecker's postulated ages for the W/X and U/V boundaries are shown in Table 12. It is evident that the required sedimentation rates for core V16-200 are more uniform between the Y/Z and W/X boundaries and between the W/X and U/V boundaries than those of core V12-122 (2.37 and 2.31 cm./ 10^3 yr. respectively for V16-200, and 2.33 and 2.16 cm./ 10^3 yr. for V12-122).

TABLE 10.

Comparison of Zone Boundaries in Cores V16-200 and V12-122

(after Ericson et al., 1964).

| Core | Boundaries | | | | |
|---------|------------|---------|-----|-----|-----|
| | Y/Z | X/Y | W/X | V/W | U/V |
| V16-200 | 25 | 170-180 | 300 | 340 | 930 |
| V12-122 | 30 | 210 | 300 | 360 | 890 |

TABLE 11.Sedimentation Rates (cm./10³ yr.) Determined for Core V12-122

(calculated from the data of Broecker and van Donk, 1970).

| Method. | | | |
|-------------------------------|-------------------------------|-------------------------------|-------------------------------|
| (Th ²³⁰ excess) | (Th ²³⁰ excess) | (Pa ²³¹ excess) | (Pa ²³¹ excess) |
| total sediment | "carbonate free" | total sediment | "carbonate free" |
| 2.52 ± 0.10 | 2.37 ± 0.10 | 2.62 ± 0.15 | 2.36 ± 0.09 |

TABLE 12.

Comparison of Mean Sedimentation Rates required from Cores V16-200
and V12-122 to fit Broecker's Time Scale. *

| | V16-200 | V12-122 |
|--|---------|---------|
| Depth to Y/Z boundary (cm.) | 25 | 30 |
| Depth between W/X and Y/Z boundaries (cm.) | 275 | 270 |
| Depth between U/V and W/X boundaries (cm.) | 630 | 590 |
| Sedimentation rate Y/Z to present (cm./10 ³ yr.) | 2.27 | 2.73 |
| Sedimentation rate, W/X to Y/Z (cm./10 ³ yr.) | 2.37 | 2.33 |
| Sedimentation rate, U/V to W/X (cm./10 ³ yr.) | 2.31 | 2.16 |
| Sedimentation rate U/V to present (cm./10 ³ yr.) | 2.33 | 2.23 |

* Based on ages

: Y/Z boundary, 11,000 yr. B.P.
W/X boundary, 127,000 yr. B.P.
U/V boundary, 400,000 yr. B.P.
(Broecker and van Donk, 1970).

The sedimentation rates derived from the ($\text{Th}_{\text{excess}}^{230}$) data of core V16-200 ($2.20 \pm 0.16 \text{ cm./10}^3 \text{ yr.}$) (Table 9) result in values of 136,000 yr. B.P. and 423,000 yr. B.P. for the W/X and U/V boundaries respectively (both 7% higher than Broecker's values of 127,000 and 400,000 yr.). The ($\text{Th}_{\text{excess}}^{230}/\text{Th}^{232}$) rate of core V16-200 ($2.32 \pm 0.17 \text{ cm./10}^3 \text{ yr.}$) yields values of 129,000 and 401,000 yr. B.P. for the two boundaries (2% and 0.2% higher than Broecker's values respectively). Since both sedimentation rates have associated standard deviations of about 7%, it is evident that the data from core V16-200 lend strong support to the time scale of Broecker and van Donk (1970). On the other hand, Emiliani's (1966) time scale would require a sedimentation rate of around $3.00 \text{ cm./10}^3 \text{ yr.}$ for core V16-200, some 33% higher than the determined rates, or over 4 standard deviations higher.

CHAPTER 5.GEOCHRONOLOGY OF ALDABRA ATOLL.5.1. Introduction.

In the past five years considerable scientific attention has been directed towards Aldabra Atoll. Because of the unusual tides round the island, the difficult terrain, and the lack of fresh water, the ecology of the island has been naturally protected, and remains relatively undisturbed. On other elevated coral atolls in the Indian Ocean, the natural ecology has been modified by commercial developments for guano and copra. Aldabra provides a unique opportunity to study evolution and biological process in its extensive and varied flora and fauna, some species and subspecies of which are peculiar to the island.

Aldabra Atoll ($9^{\circ} 24'S. 46^{\circ} 20'E.$) is a slightly elevated coral reef, 420 km. N.W. of Madagascar and 640 km. from the East African mainland. Four main islands separated by channels form a land rim enclosing the lagoon (Figure 33). The total area of the atoll is 365 km.², of which 155 km.² is land. The coral reef is inferred to overlie a submarine elevation, possibly a truncated volcanic cone (Stoddart et al., 1971). Such a basement must be circa 4000m. high, rising from a fairly flat sea floor at 4,000 to

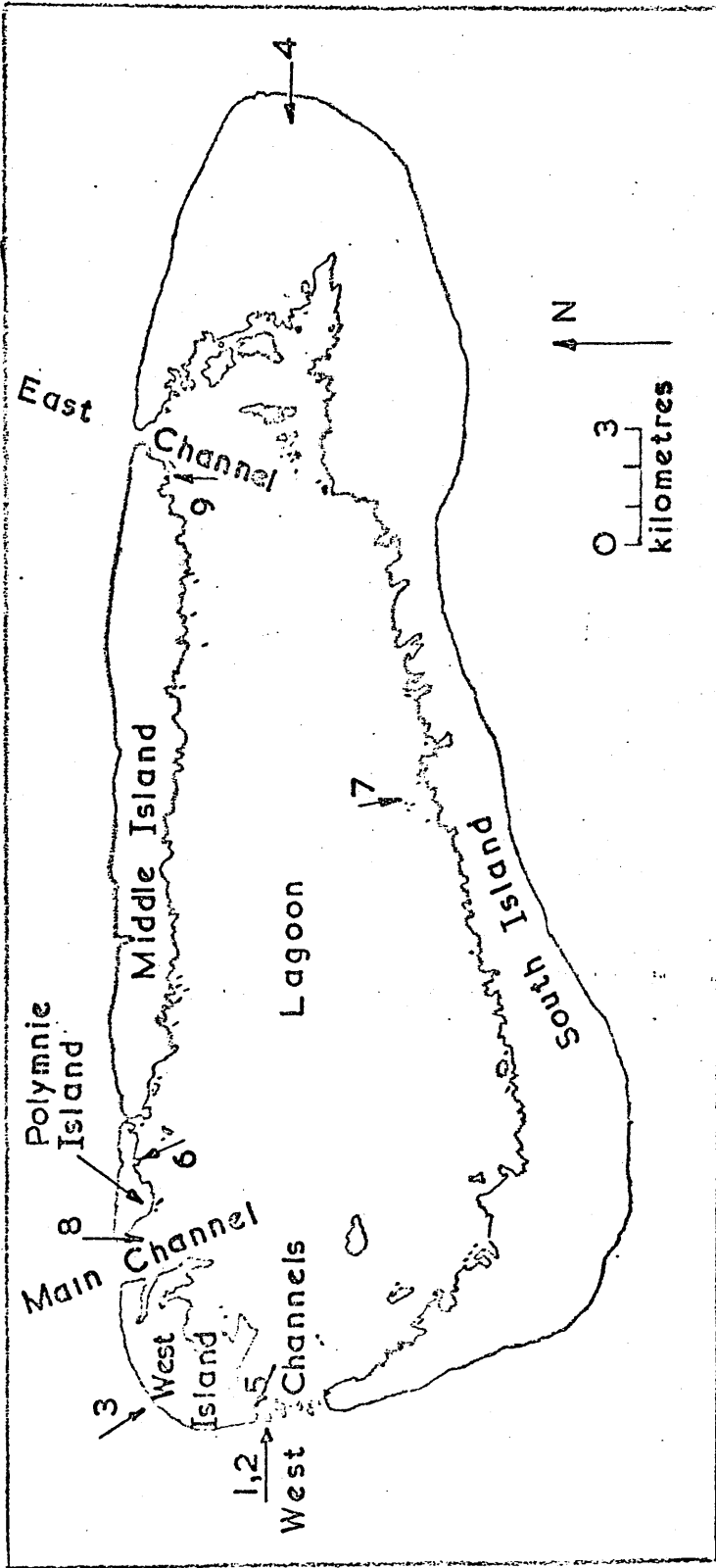


Figure 33: Map of Aldabra Atoll showing sample locations.

4,300m. depth.

The geomorphology of the atoll has been described by Stoddart et al. (1971). These workers identified two distinct coral terraces. The main limestone, the Lower Terrace, was postulated to be the foundation of all the present exposed land. It was described as a dense reef limestone with large corals, much recrystallised and tightly cemented. Two distinct levels were found in this terrace, at 8 m. and 4 m. elevation (relative to a datum at the present intertidal reef flat). A second younger reef limestone, the Upper Terrace, was recognised in some places on the seaward side of the lower reaches of the 4 m. level. This limestone was found in more protected situations such as on islands within lagoon channels. The Upper Limestone was described as much less altered, with some retained colour banding in the fossil corals. During the period of formation of this more recent terrace, much of the present land surface, possibly nine tenths, must have been submerged (Peake, 1971). Thus dating the Upper Terrace provides an important marker on the time scale of the development of Aldabra Atoll.

5.2. Results and Calculation.

The analytical results from the coral determinations are presented in Table 13, and the sample locations are included in Figure 33. All the samples but one were collected from the Upper Terrace, and apart from the Lower (Algal) Limestone sample, all are 100% aragonite within the limits of detection (Section 2.1b).

From inspection of the data, it is evident that the Upper Terrace corals satisfy the criteria quoted in Section 2.1b, i.e.

- i) the uranium concentrations fall in the range 2.6 to 3.6 p.p.m., which compares with previously determined values from 2 to 4 p.p.m.,
- ii) no Th^{232} was found in any of the samples,
- iii) the $\text{U}^{234}/\text{U}^{238}$ activity ratio, when corrected for age, lies in the range 1.15 ± 0.03 .
(Table 14).

If corals were to form with the secular equilibrium value of the $\text{U}^{234}/\text{U}^{238}$ activity ratio, 1.00, their age could be calculated directly from the buildin of Th^{230} towards equilibrium:

TABLE 13.

Analytical Data on Coral Samples.

| Sample number | U ²³⁸ d.p.m./g. (±0.03) | U ²³⁴ d.p.m./g. (±0.03) | Th ²³² d.p.m./g. | Th ²³⁰ d.p.m./g. (±0.03) | Uranium p.p.m. | Aragonite |
|------------------|--|--|--------------------------------|---|-------------------|-----------|
| 1 | 2.66 | 2.89 | n.d. | 2.01 | 3.59 | 100 |
| 2 | 2.63 | 2.91 | n.d. | 2.01 | 3.55 | 100 |
| 3 | 1.84 | 2.03 | n.d. | 1.47 | 2.48 | 100 |
| 4 | 2.51 | 2.75 | n.d. | 1.82 | 3.40 | 100 |
| 5 | 1.92 | 2.11 | n.d. | 1.54 | 2.60 | 100 |
| 6 | 2.31 | 2.56 | n.d. | 1.85 | 3.13 | 100 |
| 7 | 2.29 | 2.53 | n.d. | 1.84 | 3.09 | 100 |
| 8 | 2.09 | 2.36 | n.d. | 1.63 | 2.82 | 100 |
| 9 | 0.88 | 0.90 | n.d. | 0.94 | 1.19 | n.d. |

n.d. - not detected.

Samples 1 and 2 are duplicates.

TABLE 14.

Coral Activity Ratios and Ages.

| Sample | Species | $\frac{U^{234*}}{U^{238}}$ | $\frac{U^{234*}}{U^{238}}_0$ | $\frac{Th^{230*}}{U^{234}}$ | $\frac{Th^{230*}}{U^{238}}$ | Age ($\pm 9,000$ yr.) |
|--------|--------------|----------------------------|------------------------------|-----------------------------|-----------------------------|---------------------------|
| | | (± 0.01) | | (± 0.02) | (± 0.02) | |
| 1 | A. pallifera | 1.09 | 1.13 | 0.70 | 0.76 | 126,000 |
| 2 | A. pallifera | 1.11 | 1.15 | 0.69 | 0.76 | 123,000 |
| 3 | Goniastrea | 1.10 | 1.14 | 0.72 | 0.80 | 136,000 |
| 4 | P. nigresens | 1.09 | 1.13 | 0.66 | 0.73 | 118,000 |
| 5 | Porites | 1.10 | 1.14 | 0.73 | 0.80 | 136,000 |
| 6 | Porites | 1.11 | 1.15 | 0.72 | 0.80 | 134,000 |
| 7 | A. pallifera | 1.10 | 1.14 | 0.73 | 0.80 | 136,000 |
| 8 | Porites | 1.13 | 1.18 | 0.69 | 0.78 | 124,000 |
| 9 | Porites | 1.02 | -- | 1.04 | 1.07 | -- |

* - activity ratio.

A. pallifera - Acropora pallifera.

P. nigresens - Porites nigresens.

$(U^{234}/U^{238})_0$ - activity ratio at the time of formation,

assumed 125,000 yr. B.P.

Sample 1 and 2 are duplicates. Sample 9 is from the Lower

(Algal) Limestone.

$$t = -1 / \lambda_{\text{Th}} \cdot \ln \cdot \left[1 - (\text{Th}^{230}/\text{U}^{238})_p \right] \quad (\text{A})$$

where t is the time since formation,

λ_{Th} is the decay constant of Th^{230}

$(\text{Th}^{230}/\text{U}^{238})_p$ is the present activity ratio.

Since the actual $\text{U}^{234}/\text{U}^{238}$ initial activity ratio is 1.15, allowance must be made for the contribution of Th^{230} from the excess U^{234} , and for the decay of U^{234} towards equilibrium (Broecker, 1963):

$$\left(\frac{\text{Th}^{230}}{\text{U}^{238}} \right)_p = (1 - e^{-\lambda_{\text{Th}} t}) + \left\{ \left[\left(\frac{\text{U}^{234}}{\text{U}^{238}} \right)_o - 1 \right] \cdot \frac{\lambda_{\text{Th}}}{\lambda_{\text{Th}} - \lambda_{\text{U}}} (e^{-\lambda_{\text{U}} t} - e^{-\lambda_{\text{Th}} t}) \right\} \quad (\text{B})$$

where t is the time since formation,

λ_{Th} and λ_{U} are the decay constants of

Th^{230} and U^{234} respectively,

$(\text{Th}^{230}/\text{U}^{238})_p$ is the present activity

ratio of the nuclides,

$(\text{U}^{234}/\text{U}^{238})_o$ is the activity ratio

of the nuclides at the time of formation.

This expression yields ages somewhat lower than those obtained from (A). Preliminary calculations using expression (A) on the activity ratios obtained from the coral samples (Table 14) indicated that the true age of the Upper Terrace must lie in the range 120,000 to

130,000 yr. B.P. Accordingly, the experimental values of the U^{234}/U^{238} activity ratio were corrected to 125,000 yr. B.P. to yield the initial U^{234}/U^{238} ratio. (The alternative to this approach is to assume that all samples formed with an initial U^{234}/U^{238} ratio of 1.15. In 125,000 years this value would have decreased to 1.106. Since the determined values of the present U^{234}/U^{238} ratio range from 1.09 ± 0.01 to 1.13 ± 0.01 , it was decided to correct each separately.) Adopting the symbols R_p to represent $(Th^{230}/U^{238})_p$, R_o to represent $(U^{234}/U^{238})_o - 1$ and λ to represent $\lambda_{Th} / \lambda_{Th} - \lambda_U$, the solution of equation (B) is:

$$t = \frac{-\log. \left[\frac{1 + 0.7051 \cdot R_o \cdot \lambda - R_p}{1 + R_o} \right]}{0.43429 \cdot \lambda_{Th}}$$

The ages thus calculated for the Upper Terrace corals range from 118,000 yr. B.P. to 136,000 yr. B.P., with a maximum error, as derived from one sigma counting statistics, of $\pm 9,000$ yr., and have a mean value of 129,000 yr. B.P. (Table 14). The age assigned to this terrace is therefore $127,000 \pm 9,000$ yr. (calculated from the spread of the results). No age can be assigned to the one sample from the Lower (Algal) Limestone. This coral was

essentially calcite, with calcite inclusions evident when cut, but it was the best sample available in that it had been recently exposed and some evidence of the coralline structure remained.

Both the low value of the uranium concentration and the high $\text{Th}^{230}/\text{U}^{238}$ activity ratio indicate that uranium isotopes have been leached from the sample. This open system behaviour is typical of fossil corals which have been elevated for a prolonged period, because the aragonitic coral structure is metastable when exposed to the atmosphere (Thurber et al., 1965; MacNeil, 1968).

5.5. Implications to the development of Aldabra.

The only ages previously determined for samples from Aldabra Atoll were obtained by the radiocarbon method (Isotopes Inc., New Jersey), and formed the basis of the stratigraphic interpretation of Stoddart et al. (1971) (Section 5.1). Samples from the 8 m. level yielded ages greater than 40,000 yr., and others from the fresh Upper Terrace material at less than 4 m. ranged from 34,000 to 39,000 yr. B.P. Such ages lie at the outer limit of the radiocarbon method, and may be produced by contamination of an infinitely old sample with a few percent of natural modern carbon.

The result of this study, $127,000 \pm 9,000$ yr. B.P., agrees well with ages from other raised coral reefs. Apart from localities where tectonic uplift has balanced eustatic sea level regressions, Th²³⁰/U²³⁴ dating indicates that the last time sea level stood higher than it does today occurred circa 125,000 yr. B.P. (cf. Section 4.5). Emiliani and Rona (1969) calculate an average value of 122,000 yr. B.P. for this high sea stand from analyses in the literature, while Broecker and van Donk (1970) estimate an age of $125,000 \pm 5,000$ yr., again from published data.

Veeh (1966) analysed corals from raised coral reefs of the Indian and Pacific Oceans, and found ages ranging from $90,000 \pm 20,000$

to $160,000 \pm 40,000$ yr. (the large uncertainties arise from the analytical method employed). Geographically, the closest comparisons with the present work were samples from Mauritius and the Seychelles, which yielded ages of $160,000 \pm 40,000$ and $140,000 \pm 30,000$ yr. respectively. Elevations between 2 and 9 m. above present mean sea level were reported for the localities of samples, all of which were taken from their original positions of growth.

An alternative interpretation of the stratigraphy of Aldabra has been proposed by J.D. Taylor and W.J. Kennedy (personal communication, 1971), on the basis of field evidence collected during the 1969-70 Royal Society expedition to Aldabra, and viewed in the light of this work. Their interpretation suggests that most of the exposed limestone identified as "Lower Terrace" is in fact Upper Terrace material which has suffered subaerial diagenesis. The well-preserved corals identified as "Upper Terrace" which occur at the foot of the 4 m. terrace are considered to have been exposed recently by cliff falls. All the Upper Terrace samples analysed in this study came from such localities. An older limestone has been identified in some places, underlying the Upper Terrace, the so-called "Lower (Algal) Limestone."

Fossil giant tortoise bones have been found in both the Upper Limestone and the Algal Limestone. It is suggested that the flora

and fauna of Aldabra must have been absent during the formation of the Upper Terrace, because it formed during the last high sea stand (Veeh, 1970) and no evidence of tectonic uplift has been found. If the stratigraphic interpretation of Taylor and Kennedy is correct, the available evidence strongly suggests that the present ecology of Aldabra has been completely established in the last 120,000 years.

APPENDIX 1.V - 16 - 200.Megasconic Description of a Split Core.

| | | | |
|---------------|--------------|---------------|---------------------------|
| Latitude: | 01°58'N | Longitude: | 37°04'W |
| Corr. depth: | 4093 M | P.D.R. depth: | 2180 fms. |
| Date taken: | 12 July 1960 | Date opened: | 14 February 1963 |
| Described by: | J. Suggs | Flow-in: | 155 cm. |
| Core length: | 1050 cm. | Location: | Para Rise |
| | | Topography: | Relief of approx. 20 fms. |

Possible sub-bottom at 4-5 fms.

0-7 cm.- Gray-brown lutite. Contains approximately 40% foraminifera, particularly Globigerina in both mature and juvenile forams. A few siliceous monaxon sponge spicules. Highly calcareous; however, this results from the high foraminifera content rather than the carbonate content of the sediment. Gradational lower contact. Layer is relatively friable.

7-30 cm.- Light brown lutite. Contains approximately 30% foraminifera, as in the 0-7 cm. layer. A few inclusions of dark gray lutite. Gradational lower contact.

- 30-180 cm.- Brown lutite. Contains approximately 30% foraminifera, abundant Globigerina. Highly calcareous. Frequently dark brown lutite inclusions ranging from .5 to 2 cm. in thickness. Yield positive results when tested for manganese. Lutite becomes slightly lighter in colour toward the lower contact which is gradational.
- 180-205 cm.- Medium brown lutite. Foraminifera approximately 30%. Highly calcareous. Positive reaction for manganese. A few dark gray inclusions of lutite, approximately .5 cm. thick and contain manganese. Gradational lower contact.
- 205-286 cm.- Light brown lutite. Contains foraminifera approximately 35%. Abundant Globigerina. Calcareous. Lutite becomes very light brown toward the lower contact which is distinct. Occasional inclusions of dark gray lutite are approximately .5 cm. thick and contain manganese.
- 286-297 cm.- Dark gray lutite. Foraminifera: approximately 20%. Positive reaction for manganese. Moderately distinct lower contact. End of the gutter pipe at 288 cm.

- 297-369 cm.- Red-brown lutite. Foraminifera approximately 30%. Abundant Globigerina, both mature and juvenile forms. Dark gray inclusions of lutite, .5-1 cm. thick, throughout, containing manganese. From 306-312 cm. a zone of mixed dark gray lutite contains manganese. Moderately distinct lower contact.
- 369-425 cm.- Medium brown lutite. Foraminifera approximately 25%. Relatively common inclusions of gray lutite varying in thickness from .5-1.5 cm. and containing manganese. Lower contact is distinct.
- 425-427.5 cm.- Medium gray lutite. Foraminifera approximately 15%. Manganese. Slightly calcareous. Distinct lower contact.
- 427.5 -524 cm.- Light brown lutite. Foraminifera approximately 20%. At 429-437 cm. and at 452-460 cm. slightly darker brown lutite. Occasional inclusions of dark gray lutite approximately .5 cm. thick and containing manganese. Layer tends to grade into a reddish brown. Distinct lower contact.

- 524-538 cm.- Light gray brown lutite. Foraminifera approximately 30%. Calcareous. Colour tends to become slightly lighter toward the bottom. Gradational contact.
- 538-569 cm.- Reddish-brown lutite. Calcareous. Foraminifera approximately 25%. Piston effect at 547 cm. Red colour increases toward bottom. This layer tends to be slightly more indurated than the overlying and underlying ones. Gradational lower contact.
- 569-697 cm.- Medium brown lutite. Calcareous. Foraminifera approximately 15%. Zone from 569-590 cm. has several 1-4 cm. thick inclusions of gray lutite that contains manganese. From 670-675 cm. are dark gray lutite inclusions that are approximately 1-2 cm. thick and contain manganese. From 670-696 cm. occasional inclusions of dark brown lutite range from .5-1 cm. in thickness. At 696 cm. a .75 cm. thick discontinuous band of very light brown lutite crosses the axis of the core at approximately a 30° angle. Distinct lower contact.
- 697-715 cm.- Reddish-brown lutite. Calcareous. Foraminifera approximately 15%. Gradational lower contact.

- 715-805 cm.- Brown lutite. Calcareous. Foraminifera approximately 10%. Inclusions of gray lutite ranging in thickness from .5 to 1.5 cm. throughout. The matrix lutite tends to become lighter in colour toward the bottom while the inclusions grade from gray to brown. Moderately distinct lower contact.
- 805-820 cm.- Light brown lutite grading into a gray-white lutite from 805 to 810 cm. Foraminifera approximately 15%. Gradational contact.
- 820-841 cm.- Gray-brown lutite. Calcareous. Foraminifera approximately 20%. Slightly more indurated than the overlying and underlying layers.
- 841-863 cm.- Reddish-brown lutite. Calcareous. Foraminifera approximately 20%. Gradational lower contact.
- 863-975 cm.- Medium brown lutite. Calcareous. Foraminifera approximately 30%. Dark gray zones of lutite between 868-870 cm., 893-894 cm., and 923-925 cm. Lutite gives a positive reaction when tested for manganese. Distinct lower contact.
- 975-986 cm.- Brown lutite. Calcareous. Foraminifera: approximately 25%. Colour tends to become lighter toward the bottom. Distinct lower contact.

- 986-1141 cm.- Flow-in.
- 1141-1205 cm.- Reddish-brown lutite. Calcareous. Contains approximately 30% foraminifera. Colour tends to become lighter toward the bottom of this layer. This layer is partially disturbed.

Paleoclimatic Zonations. (D.B. Ericson, Personal Communication).

| Y/Z | X/Y | W/X | V/W | U/V |
|-----|---------|-----|-----|-----|
| 25 | 170-180 | 300 | 340 | 930 |

APPENDIX 2.Typical Sample Calculations.Core Section 150 - 155 cm.1. Analysis for Uranium, Thorium and Radium (1/7/69).

Mass of sediment used for analysis = 5.8156 g.
 Spike added (1 ml.) = 5.4 d.p.m./g. U^{232}
 Total dissolved volume = 160 ml.
 25 ml. aliquot for Ra^{226} analysis equivalent to 0.9087g.

Uranium mount. (1440 min. count period, 25 channel integration)

$$U^{238} \text{ peak sum} = 1306 \pm 36$$

$$U^{234} \text{ peak sum} = 1223 \pm 35$$

$$U^{232} \text{ peak sum} = 1023 \pm 32$$

$$\text{Corrected } U^{234} \text{ peak sum} = (1223 \pm 35) - 0.022(1023 \pm 32) = 1201 \pm 35$$

$$U^{238}/U^{232} = 1.17 \pm 0.05$$

$$\text{Total d.p.m./g. } U^{238} = 5.4 \times (1.17 \pm 0.05) = 6.89 \pm 0.29$$

$$\text{D.p.m./g. } U^{238} = (6.89 \pm 0.29)/5.8156 = 1.19 \pm 0.05$$

$$\text{Similarly, d.p.m./g. } U^{234} = 1.09 \pm 0.05$$

$$U^{234}/U^{238} = 0.92 \pm 0.04$$

Thorium mount. (1560 min. count period, 25 channel integration)

$$\text{Th}^{232} \text{ peak sum} = 1787 \pm 42$$

$$\text{Th}^{230} \text{ peak sum} = 4079 \pm 64$$

$$\text{Th}^{228} \text{ peak sum} = 2569 \pm 51$$

$$\text{Ra}^{224} \text{ peak sum} = 1344 \pm 37$$

$$\begin{aligned} \text{Corrected Th}^{228} \text{ peak sum} &= (2569 \pm 51) - (1787 \pm 42) - 0.052(1344 \pm 37) \\ &= 712 \pm 66 \end{aligned}$$

$$\text{Th}^{232} / \text{Th}^{228} = 2.51 \pm 0.24$$

$$\text{Total d.p.m. Th}^{232} = 5.4 \times 1.03 \times (2.51 \pm 0.24) = 13.96 \pm 1.33$$

$$\text{D.p.m./g. Th}^{232} = (13.96 \pm 1.33) / 5.8156 = 2.40 \pm 0.23$$

$$\text{Similarly, d.p.m./g. Th}^{230} = 5.47 \pm 0.51$$

$$(\text{Th}_{\text{excess}}^{230}) = (5.47 \pm 0.51) - (1.09 \pm 0.05) = 4.38 \pm 0.51 \text{ d.p.m./g.}$$

$$(\text{Th}_{\text{excess}}^{230} / \text{Th}^{232}) = (4.38 \pm 0.51) / (2.40 \pm 0.23) = 1.83 \pm 0.28$$

Ra²²⁶ analysis

Storage period : 8/7/69 to 11/2/70 (secular equilibrium)

Separation time : 17-22 hrs. (11/2/70).

First count : 21-02 (11/2/70) to 08 - 51 (12/2/70):

709 minutes, 4329 counts.

Count rate = 6.11 c.p.m; 5.73 c.p.m. (corrected for background,
0.38 \pm 0.09 c.p.m.)

Count rate corrected to separation time from midpoint of counting time
(9.5 hrs., 6.2% decay) = 5.73/0.938 = 6.11 c.p.m.

Similarly, second count 08-51 to 12-00 (12/2/70)

189 minutes, 1250 counts.

Count rate corrected to separation time and corrected for background = $(6.61 - 0.38) / 0.880 = 7.08$ c.p.m.

Weighted mean count rate = $(6.11 \times 709) + (7.08 \times 1.89) / 898$
 $= 6.31 \pm 0.13$ c.p.m. (standard deviation calculated from the total counts recorded and the background count rate uncertainty).

Efficiency of counting vessel used = $40.7 \pm 2.8\%$.

Therefore total corrected count rate (Rn^{222} plus 2 daughters)
 $= (6.31 \pm 0.13) / (0.407 \pm 0.028) = 15.50 \pm 1.11$ d.p.m.

Therefore Ra^{226} parent specific activity =
 $(15.50 \pm 1.11) / 3 \times 0.9087$ d.p.m./g. = 5.67 ± 0.41 d.p.m./g.

2. Pa^{231} analysis (26/8/70).

Mass of sediment used for analysis = 6.24592 g.

1 ml. Pa^{233} spike added.

Counter alpha background on stainless steel dimpled planchette
 at 1100V (15/9/70) = 0.015 ± 0.001 c.p.m.

Counter alpha efficiency at 1100V. = $50.8 \pm 0.7\%$

Pa mount. Count at 1100V (15/9/70)

| Count times | Count period (minutes) | Count | Rate (c.p.m. \pm 1 sigma) |
|------------------------------|---------------------------|-------|--------------------------------|
| 15-48 (15/9) to 16-15 (16/9) | 1467 | 578 | 0.394 \pm 0.016 |
| 16-15 (16/9) to 16-15 (17/9) | 1440 | 522 | 0.363 \pm 0.016 |
| 16-15 (17/9) to 16-15 (18/9) | 1440 | 505 | 0.351 \pm 0.015 |
| 16-15 (18/9) to 18-00 (19/9) | 1545 | 595 | 0.385 \pm 0.015 |
| 15-48 (15/9) to 18-00 (19/9) | 5892 | 2200 | 0.373 \pm 0.008 |

β^- count rates at 1800V., 20 minute counts, automatically timed (19/9/70).

Pa mount, total count 11,423; 11,457.

Mean count/20 minutes, less background (1300/20 minutes) = 10,140 \pm 76

Pa²³³ tracer discs, mean of 2 counts less background 18,470;
17,836; 18,843; 17,671.

Mean tracer count rate/20 minutes = 18,205 \pm 274.

$$\begin{aligned} \text{Total d.p.m. Pa}^{231} &= \frac{\text{C.p.m. Pa mount} - \text{C.p.m. background}}{\text{Counter efficiency} \times \text{Chemical yield}} \\ &= \frac{(0.373 \pm 0.008) - (0.015 \pm 0.001)}{(0.508 \pm 0.007) \times (10,140 \pm 76) / (18205 \pm 274)} \\ &= 1.265 \pm 0.033. \end{aligned}$$

$$\begin{aligned} \text{D.p.m./g. Pa}^{231} &= (1.265 \pm 0.033) / 6.24592 = 0.203 \pm 0.005 \\ (\text{Pa}^{231} \text{ excess}) &= (0.203 \pm 0.005) - 0.046 (1.19 \pm 0.05) \\ &= 0.148 \pm 0.005 \text{ d.p.m./g.} \end{aligned}$$

APPENDIX 3.

Best-fit Straight Line Programme.

D124--00WPU+S030555XSSP→

begin comment This programme works out m and c for the equation $y = mx + c$ by least squares from n pairs of x and y and gives the rms error $(\sqrt{[v\uparrow 2]/(n - 2)})$ plus the individual deviations in y - It has been modified by J.C.S. in March, 1971, and again slightly in May, to print out the L.S. totals ;

integer n, i, p;
real sx, sy, sxy, sx2, sy2, m, c, d;
open(20); open(70);

start: n:= read(20);

begin array x,y, e [1:n];
 sx:=sy:=sxy:=sx2:=sy2:=0.0;
for i:=1 step 1 until n do
 begin x[i]:= read(20);
 y[i]:= read(20)
 end;

for i:=1 step 1 until n do
begin sx:= sx + x[i];
 sy:= sy + y[i];
 sxy:=sxy + x[i]y[i];
 sy2 := sy2 + y[i]²;
 sx2:=sx2 + x[i]²
end;

d:= nxsx2 -sx²; m:= (n × sxy -sx × sy)/d;
 c:= (sx2 × sy - sx × sxy)/d;
 d:= sqrt((sy2 - sy × c - sxy × m)/(n - 2));

for i:= 1 step 1 until n do
begin

 e[i] := y[i];
 y[i] := y[i] - m × x[i] - c
end;

```

write text (70, [[4c] m*=*]);
write (70, format ([-d.ddddd10-nd]), m);
write text (70, [[3s] c*=*]);
write (70, format ([-d.ddddd10-nd]), c);
write text (70, [[3s] rms*error*=*]);
write (70, format ([-d.ddddd-nd]), d);
write (70, format ([2s -d.ddddd10-nd]), e[1]);
for write (70, format ([3s -d.ddddd-nd]), m × x[1] + c);
write 70, format ([3s -d.ddddd-ndc]), y[1]
d;
write text (70, [[4c] least*squares*totals*x2*x*xy*n*y*y2 [3c
write 70, format ([3s -d.ddddd-ndc]), y[1]);
end;
write text (70, [[4c] least*squares*totals*x2*x*xy*n*y*y2 [3c]);
write (70, format ([-d.ddddd10+nd]), sx2);
write (70, format ([3ss-d.ddddd+nd]), sx);
write 70, format ([3ss-d.ddddd+ndcc]), sxy);
write text (70, [[=s]);
write 70, format ([-nd]), n);
write 70, format ([4s -d.ddddd+ndcc]), sy);
write text 70, [[32s]);
write 70, format ([-d.ddddd+nd]), sy2);

```

comment if another set of data is to follow punch 1 otherwise 0;

p := read (20);

if p = 1 then goto start;

close (70);

close (20);

comment The data tape consists of n followed by n pairs of values of x and y. A 1 is punched after each set of n pairs if another set follows, and a zero after the final set;

end →

REFERENCES CITED.

- Adams, J.A.S., J.K. Osmond, J.J.W. Rogers, (1959), in "Physics and Chemistry of the Earth", Vol.3, 298, Pergamon Press.
- Almodovar, I., (1960), Ph.D. thesis, Carnegie Institute of Technology.
- Amin, B.S., D.P. Kharkar, K. Lal, (1966), Deep-Sea Res. 13, 805.
- Arrhenius, G.O.S., (1952), Reps. Swed. Deep-Sea Exped., 5, Goteborg.
- Arrhenius, G.O.S., (1963), Chapter 25, 655, in "The Sea", Vol.3, ed. M.N. Hill, Interscience.
- Arrhenius, G.O.S., E.D. Goldberg, (1955), Tellus, 7, 226.
- Arrhenius, G.O.S., E. Bonatti, (1965), Progress in Oceanography Vol.3., Pergamon Press.
- Attree, B.W., M.J. Cabell, R.L. Cushing, J.J. Pieron, (1962), Canadian Jour. Physics, 40, 194.
- Baranov, V.I., L.A. Kuzmina, (1958), Geochemistry, 2, 131.
- Barnes, J.W., E.J. Lang, H.A. Potratz, (1956), Science, 124, 175.
- Berger, W.H., G.R. Heath, (1968), J. Marine Res., 26, 134.
- Berggren, W.A., J.D. Phillips, A. Bertels, D. Wall, (1967), Nature, 216, 253.
- Berggren, W.A., J.D. Phillips, A. Bertels, D. Wall, (1968), Deep-Sea Res., 14, No.2.
- Bernat, M., E.D. Goldberg, (1969), Earth Planet. Sci. Lett., 5, 308.
- Biscaye, P.E., (1964), Ph.D. thesis, Yale University.

- Blanchard, R.L., M.H. Cheng, H.A. Portratz, (1967), J. Geophys. Res., 72, 4745.
- Bonatti, E., D.E. Fisher, O. Joensuu, H.S. Rydell, (1971), Geochim. Cosmochim. Acta, 35, 189.
- Bowles, F.A., (1970), paper 0123, Amer. Geophys. Union, Annual Meeting, April 20-24, 1970.
- Broecker, W.S., (1963), J. Geophys. Res., 68, 2817.
- Broecker, W.S., (1965), Quaternary of the U.S. Review Vol. VII, INQUA Congress, Boulder, Colo., p 737.
- Broecker, W.S., (1966), Science, 151, 299.
- Broecker, W.S., (1971), Quaternary Res., 1, 188.
- Broecker, W.S., K.K. Turekian, B.C. Heezen, (1958), Amer. J. Sci., 256, 503.
- Broecker, W.S., M. Ewing, B.C. Heezen, (1960), Amer. J. Sci., 258, 429.
- Broecker, W.S., D.L. Thurber, (1965), Science, 149, 58.
- Broecker, W.S., Y.H. Li, J. Cromwell, (1967), Science, 158, 1307.
- Broecker, W.S., D.L. Thurber, J. Goddard, T.L. Ku, R.K. Matthews, K.J. Mesolella, (1968), Science, 159, 297.
- Broecker, W.S., T.L. Ku, (1969) Science, 166, 404.
- Broecker, W.S., J. van Donk, (1970), Rev. Geophys. Space Phys. 8, 169.
- Brown, D., S.N. Dixon, K.M. Glover, F.J.G. Rogers, (1968), J. Inorg. Nucl. Chem., 30, 19.

- Burton, J.D., (1965), Chapter 22, 425, in "Chemical Oceanography" Vol. 2, eds. J.P. Riley, A. Skirrow. Academic Press.
- Cherdyntsev, V.V. et al., (1955), (Russian). Trudy 111 Sessii Komissi Opred. Absol. Vozrasta, pp. 175-233. Izd. Acad. Nauk S.S.S.R., Moscow.
- Conlan, B., P. Henderson, A. Walton, (1969), Analyst, 94, 15.
- Cox, A., (1961), U.S. Geol. Surv. Bull., 1083-E, 131.
- Cox, A., R.R. Doell, G.B. Dalrymple, (1964), Science, 144, 1537.
- Cox, A., (1969), Science, 163, 237.
- Craig, H., (1965), Consiglio Nazionale Delle Ricerche, Laboratorio di Geologia Nucleare - Pisa, Spoleto, July 26-30.
- Dearnaley G., D.C. Northrop, (1966), "Semiconductor Counters for Nuclear Radiations". 2nd Ed. Spon, London.
- di Ferrante, E.R., E. Gourski, R.R. Boulenger, (1964), in "The Natural Radiation Environment", eds. J.A.S. Adams, W.M. Lowder, Univ. of Chicago Press. Chapter 20, 353.
- Dymond, J., (1969), Earth Planet. Sci. Lett., 6, 9.
- Emery, K.O., R.S. Dietz, (1941), Bull. Geol. Soc. Amer., 62, 1685.
- Emery, K.O., J. Hulsemann, (1964), Sedimentology, 3, 144.
- Emiliani, C., (1955), J. Geol., 63, 538.
- Emiliani, C., (1958), J. Geol., 66, 264
- Emiliani, C., (1961), Ann. N.Y. Acad. Sci., 95, 521.

- Emiliani, C., (1964), Geol. Soc. Amer. Bull., 75, 129.
- Emiliani, C., (1966), J. Geol., 74, 109.
- Emiliani, C., (1969), Science, 166, 1503.
- Emiliani, C., (1970), Science, 168, 822.
- Emiliani, C., (1971), Science, 171, 571.
- Emiliani, C., R.F. Flint, (1963), Chapter 34, 888, in "The Sea"
Vol. 3, Ed. M.N. Hill, Interscience.
- Emiliani, C., E. Rona, (1969), Science, 166, 1551.
- Ericson, D.B., (1963), Chapter 31, 832, in "The Sea" Vol. 3,
Ed. M.N. Hill, Interscience.
- Ericson, D.B., G. Wollin, (1956), Micropaleontology, 2, 257.
- Ericson, D.B., W.S. Broecker, J.L. Kulp, A. Wollin, (1956),
Science, 124, 385.
- Ericson, D.B., M. Ewing, A. Wollin, B.C. Heezen, (1961), Bull.
Geol. Soc. Amer., 72, 193.
- Ericson, D.B., M. Ewing, A. Wollin, (1963), 139, 727.
- Ericson, D.B., M. Ewing, A. Wollin, (1964), Science, 146, 723.
- Ericson, D.B., A. Wollin, (1968), "The Ever-Changing Sea",
MacGibbon and Kee, London.
- Ericson, D.B., A. Wollin, (1968), Science, 162, 1227.
- Foster, J.H., N.D. Opdyke, (1970), J. Geophys. Res., 75, 4465.
- Glass, B., (1969), Earth Planet. Sci. Lett., 6, 409.
- Glass, B., D.B. Ericson, B.C. Heezen, N.D. Opdyke, J.A. Glass,
(1967), Nature, 216, 437.

- Goldberg, E.D., M. Koide, (1958), *Science*, 128, 1003.
- Goldberg, E.D., M. Koide, (1962), *Geochim. Cosmochim. Acta*, 26, 417.
- Goldberg, E.D., M. Koide, (1963), in "Earth Science and Meteoritics", John Wiley, N.Y., Chapter 5, p.90.
- Goldberg, E.D., M. Koide, J.J. Griffin, M.N.A. Peterson, (1964) Chapter 17, 211, in "Isotopic and Cosmic Chemistry", Eds. H. Craig, S.L. Miller, A.J. Wasserburg, North-Holland.
- Goldberg, E.D., M. Koide, J.J. Griffin, (1964), in "Recent Researches in the Fields of Hydrosphere, Atmosphere and Nuclear Geochemistry (Ken Sugihara Festival Volume). Tokyo.
- Goldberg, E.D. (1968), *Earth Planet. Sci. Lett.*, 4, 17.
- Griffin, J.J. E.D. Goldberg, (1963), Chapter 26, 728, in "The Sea", Vol. 3, Ed. M.N. Hill, Interscience.
- Griffin, J.J., H. Windom, E.D. Goldberg, (1968), *Deep Sea Res.*, 15, 433.
- Hamer, A.N., E.J. Robbins, (1960), *Geochim. Cosmochim. Acta*, 19, 143.
- Harrison, C.G.A., B.M. Funnell, (1964), *Nature*, 204, 566.
- Hays, J.D., N.D. Ondyke, (1967), *Science*, 158, 1001.
- Hays, J.D., T. Saito, N.D. Ondyke, L.H. Burkle, (1969), *Bull. Geol. Soc. Amer.*, 80, 1481.
- Heye, D., (1969), *Earth Planet. Sci. Lett.*, 6, 112.
- Hoffman, B.W., S.B. Camerik, (1967), *Anal. Chem.*, 39, 1198.
- Holland, H.D., J.L. Kulp, (1954), *Geochim. Cosmochim. Acta*, 5, 197.
- Holmes, C.W., J.K. Osmond, H.G. Goodell, (1968), *Earth Planet. Sci. Lett.*, 4, 368.

- Isaac, N., E. Picciotto, (1954), *Nature*, 171, 742.
- Joly, J.J., (1908), *Phil. Mag.*, 16, 190.
- Kane, J., (1953), *Micropaleontologist*, 7, 25.
- Kaufman, A., (1964), Ph.D. thesis, Columbia University.
- Kaufman, A., (1969), *Geochim. Acta.*, 33, 717.
- Kirby, H.W., (1961), *J. Inorg. Nuclear Chem.*, 18, 8.
- Koczy, F.F., (1958), *Proc. 2nd Int. Conf. Peaceful Uses of Atomic Energy*, 18, 336.
- Koczy, F.F., (1963), Chapter 30, 816, in "The Sea", Vol. 3, Ed. M.N. Hill, Interscience.
- Koczy, F.F., R. Bourret, (1958), Progress Rep. N.S.F. Grant A - 3995, Marine Lab., Univ. of Miami.
- Koide, M., E.D. Goldberg, (1965), *Geochim. Cosmochim. Acta*, 26, 417.
- Kolodny, Y., I.R. Kaplan, (1970), *Geochim. Cosmochim. Acta.*, 34, 3.
- Kolthoff, I.M., E.B. Sandell, (1956), *Textbook of Quantitative Inorganic Analysis*, 3rd. Ed., McMillan, N.Y.
- Kraus, K.A., G.E. Moore, (1950), *J. Amer. Chem. Soc.* 72, 4293.
- Kraus, K.A., G.E. Moore, F. Nelson, (1956), *J. Amer. Chem. Soc.*, 78, 2692.
- Kroll, V. St., (1953), *Nature*, 171, 742.
- Kroll, V. St., (1954), *Deep Sea Res.*, 1, 211.
- Kroll, V. St., (1955), *Rep. Swedish Deep-Sea Exped., 1947-1948*, 10, Fasc. 1.

- Ku, T.L., (1965), J. Geophys. Res., 70, 3457.
- Ku, T.L. (1966), Ph.D. thesis, Columbia University.
- Ku, T.J., (1968), J. Geophys. Res., 73, 2271.
- Ku, T.L., W.S. Broecker, (1966), Science, 151, 448.
- Ku, T.L., W.S. Broecker, N.D. Opdyke, (1968), Earth Planet. Sci. Lett. 4, 1.
- Kullenberg, B., (1947), Svenska Hydrog.-Biol. Komm. Skr., S.3, 1, 1.
- Lederer, C.M., J.M. Hollander, I. Perlman, (1967), "Table of Isotopes", 6th Ed., John Wiley, N.Y.
- Lidz, L., (1966), Science, 151, 448.
- Lucas, H.F., (1964), in "The Natural Radiation Environment", eds., J.A.S. Adams, W.M. Lowder, Univ. of Chicago Press, Chapter 17, 315.
- MacNeil, F.S., (1968), in "Encyclopaedia of Geomorphology", ed. R.W. Fairbridge, Reinhold, p. 35.
- May, I., F.S. Grimaldi, (1954), U.S. Geol. Surv. Bull., 1006, eds. F.S. Grimaldi, I. May, M.H. Fletcher, J. Titcomb.
- McCrea, J.M., (1950), J. Chem. Phys., 18, 849.
- McDougall, I., J.J. Stipp, (1968), Nature, 219, 51.
- Mesolella, K.J., R.K. Matthews, W.S. Broecker, D.L. Thurber, (1969), J. Geol. 77, 250.
- Milankovitch, M., (1938), Bull. Acad. Sci. Math. Nat. Belgrade, 4, 49.
- Milner, G.W.C., J.D. Wilson, G.A. Barnett, A.A. Smales, (1961), J. Electroanalyt. Chem., 2, 25.

- Mo, T., B.C. O'Brien, A.D. Suttle, (1971), *Earth Planet. Sci. Lett.*, 10, 175.
- Moore, W.S., W.M. Sackett, (1964), *J. Geophys. Res.*, 69, 5401.
- Murray, J.W., (1970), *Earth Planet. Sci. Lett.*, 10, 39.
- Ninkovitch, D., N. Opdyke, B.C. Heezen, J. Foster, (1966), *Earth Planet. Sci. Lett.*, 1, 476.
- Opdyke, N.D., B. Glass, J.D. Hays, J. Foster, (1966), *Science*, 154, 349.
- Peake, J.F., (1971), *Phil. Trans. Roy. Soc. Lond. B*, 260, 581.
- Pettersson, H., (1937), *Anz. Acad. Wiss., Wien*, 127.
- Pettersson, H., (1949), *Tellus*, 1, 1.
- Pettersson, H., (1951), *Nature*, 167, 942.
- Phleger, F.B., F.L. Parker, J.F. Pierson, (1953), *Reps. Swed. Deep-Sea Exped., 1947-48*, 7, No. 1.
- Picciotto, E., S. Wilgain, (1954), *Nature*, 173, 632.
- Piggott, C.S., (1933), *Amer. J. Sci.*, 25, 229.
- Piggot, C.S., W.D. Urry, (1939), *J. Wash. Acad. Sci.*, 29, 405.
- Piggot, C.S., W.D. Urry, (1941), *Amer. J. Sci.*, 239, 81.
- Piggot, C.S., W.D. Urry, (1942), *Bull. Geol. Soc. Amer.*, 53, 1187.
- Prospero, J.M., F.F. Koczy, (1967), in "*Encyclopaedia of Oceanography*", ed. R.W. Fairbridge, Elsevier. Pp. 730-748.
- Ramthun, H., (1966), *Nukleonik*, 8, 244.
- Riedel, W.R., (1959), in "*Silica in Sediments*", *Society of Economic Paleontologists and Mineralogists Spec. Publ.*, 7, 80.

- Rogers, J.J.W., J.A.S. Adams, (1969), in "Handbook of Geochemistry", Vol. 2, ed. K.H. Wedepohl, Springer-Verlag, Berlin. Sect. 92C.
- Rona, E., Gilpatrick, L.O., L.M. Jeffrey, (1956), Trans. Amer. Geophys. Union, 37, 697.
- Rona, E., C. Emiliani, (1969), Science, 163, 66.
- Ross, D.A., W.R. Riedel, (1967), Deep-Sea Res., 14, 285.
- Rosholt, J.N., (1967), Radioactive Dating and Methods of Low Level Counting, Proc. Symp. Monaco, IAEA, Publ. Sm- 87/50. p 299.
- Rosholt, J.N., C. Emiliani, J. Geiss, F.F. Koczy, P.J. Wangersky, (1961), J. Geol. 69, 162.
- Rosholt, J.N., C. Emiliani, J. Geiss, F.F. Koczy, P.J. Wangersky (1962), J. Geophys. Res., 67, 2907.
- Rosholt, J.N., B.R. Doe, M. Tatsumoto, (1966), Bull. Geol. Soc. Amer., 77, 987.
- Rubin, M., H.E. Suess, (1955), Science, 121, 481.
- Rubin, M., H.E. Suess, (1956), Science, 123, 442.
- Sackett, W.M., (1960), Science, 132, 1761.
- Sackett, W.M., (1964), Annal. N.Y. Acad. Sci., 119, 339.
- Sackett, W.M., (1965), in "Symposium on Marine Geochemistry", Eds. D.R. Schink, J.T. Corless, Univ. of Rhode Island, Occasion. Publ. No 3, p.29.
- Sackett, W.M., (1966), Science, 154, 646.
- Sackett, W.M., G.O.S. Arrhenius, (1962), Geochim. et Cosmochim. Acta, 26, 955.
- Sarma, T.P., (1964), Ph.D. thesis, Carnegie Institute of Technology.

- Schneider, R.A., K.M. Harmon, (1958), USAWC Report HW-53386. 31pp.
- Schott, W., (1935), *Wiss. Ergebn. Deut. Atlant. Exped. "Meteor"*, 1925-1927, 3, No 3, 43.
- Scott, M.R., (1968), *Earth Planet. Sci. Lett.*, 4, 245.
- Selli, R., (1967), *Progress in Oceanography*, 4, 67.
- Senftle, F.E., L. Stieff, F. Cuttitta, P.K. Kuroda, (1957), *Geochim. Cosmochim. Acta*, 11, 189.
- Shackleton, N.J., (1967), *Nature*, 215, 15.
- Shackleton, N.J., (1969), *Proc. Roy. Soc. Lond. B.*, 174, 135.
- Shackleton, N.J. C. Turner, (1967), *Nature*, 216, 1079.
- Somayajulu, B.L.K., E.D. Goldberg, (1966), *Earth Planet. Sci. Lett.*, 1, 102.
- Starik, I.E., F.E. Starik, V.A. Mikhailov, (1958), *Geochemistry*, 587.
- Steen, F.H., (1955), "Differential Equations", Ginn and Co.
- Stoddart, D.R., J.D. Taylor, F.R. Fosberg, G.E. Farrow, (1971), *Phil. Trans. Roy. Soc. Lond. B*, 260, 31.
- Strominger, D., J.M. Hollander, G.T. Seaborg, (1958), *Rev. Mod. Phys.*, 30, 585.
- Szabo, B.J., J.N. Rosholt, (1969), *J. Geophys. Res.*, 74, 3253.
- Tatsumoto, M., E.D. Goldberg, (1958), *Geochim. Cosmochim. Acta*, 17, 201.
- Thurber, D.L., (1962), *J. Geophys. Res.*, 67, 4518.
- Thurber, D.L., (1963), Ph.D. thesis, Columbia University.
- Thurber, D.L., W.S. Broecker, R.L. Blanchard., H.A. Portratz, (1965), *Science*, 149, 55.

- Turekian, K.K., (1956), Bull. Amer. Assoc. Petro. Geologists, 40, 2507.
- Turekian, K.K., (1964), Trans. N.Y. Acad. Sci., 26, 312.
- Turekian, K.K., (1965), Chapter 16, 81 in "Chemical Oceanography" Vol. 2, eds. J.P. Riley, A. Skirrow. Academic Press.
- Urey, H.C., (1947), J. Chem. Soc., 562.
- Urry, W.D., (1942), Amer. J. Sci., 240, 426.
- Urry, W.D., (1948), J. Mar. Res., 7, 618.
- Urry, W.D. (1949), Amer. J. Sci., 247, 257.
- Urry, W.D., C.S. Piggot, (1942), Amer. J. Sci., 240, 93.
- Varnekar, A.D., (1968), in "Research on the Theory of Climate", Vol. 2, Travelers Research Center, Inc., Hartford, Conn., 289 pp.
- Veeh, H. H., (1966), J. Geophys. Res., 71, 3399.
- Veeh, H.H., J. Chappell, (1970), Science, 167, 862.
- Volchok, H.L., J.L. Kulp, (1957), Geochim. Cosmochim. Acta, 11, 219.
- Walton, A., W.S. Broecker, (1959), "International Oceanographic Congress, Preprints", ed. M. Sears, AAAS, Washington, 505.
- Wilson, J.D., R.K. Webster, G.W.C. Milner, G.A. Barnet, A.A. Smales, (1960), Analyt. Chim. Acta., 23, 505.
- Yaffe, L., (1962), Ann. Rev. Nuclear Sci., 12, 153.
- Yokoyama, Y., J. Tobailem, T. Grjebino, J. Labeyrie, (1968), Geochim. Cosmochim. Acta, 32, 347.

A C K N O W L E D G E M E N T S.

I extend thanks to Dr. Alan Walton, supervisor of this thesis, for his support, constructive criticism and encouragement throughout. Thanks are also due to Dr. Murdoch Baxter for many helpful discussions and comments after Dr. Walton's departure.

Mr. John Hardy provided valuable advice for setting up the alpha spectrometer and on various other counting problems.

I am indebted to several individuals for collection and supply of samples and material. Drs. D.B. Ericson and A. Kaufman, both of Lamont-Doherty Geological Observatory, kindly supplied sections of core V16-200 and the U²³² - Th²²⁸ spike respectively. Drs. John Taylor and Jim Kennedy kindly selected coral samples collected by them on Aldabra.

I should also like to thank Mrs. Isobel Nicol for her untiring patience in typing the manuscript. Also, I appreciate the support and encouragement received from my wife, Sylvia.

Finally, the financial support of the Carnegie Trust for the Universities of Scotland (during the first two years of the work) and The University of Glasgow is gratefully acknowledged.